THE ANTI-TUMOR ACTIVITY OF UV3, AN ANTI-CD54 ANTIBODY, IN SCID MICE XENOGRAFTED WITH A VARIETY OF HUMAN TUMOR CELL LINES

APPROVED BY THE SUPORVISORY COMMITTEE

Ellen Vitetta
Ellen S. Vitetta, Ph.D., Professor of Microbiology
Director, Cancer Immunobiology Center

Pila Estess
Pila Estess, Ph.D., Assistant Professor of Pathology

John Minna
John D. Minna, M.D., Professor, Hamon Cancer Center

Jerry Niederkorn
Jerry Niederkorn, Ph.D., Professor of Ophthalmology

Dorothy Yuan
Dorothy Yuan, Ph.D., Professor of Pathology

I dedicate this work

to my husband, Roger, for your constant love and support,

to my parents, for your continued encouragement,

and to Roger Brooks, Sr., June Weston, and the many others I have lost to cancer along the way.

THE ANTI-TUMOR ACTIVITY OF UV3, AN ANTI-CD54 ANTIBODY, IN SCID MICE XENOGRAFTED WITH A VARIETY OF HUMAN TUMOR CELL LINES

By

KIMBERLY JOE BROOKS

DISSERTATION

Presented to the Faculty of the Graduate School of Biomedical Sciences

The University of Texas Southwestern Medical Center at Dallas

In Partial Fullfillment of the Requirements

For the Degree of

DOCTOR OF PHILOSOPHY

The University of Texas Southwestern Medical Center at Dallas

Dallas, Texas

August 2008

Acknowledgements

I owe thanks to many individuals for their contributions throughout my graduate work at UT Southwestern. First and foremost I would like to thank my mentor, Dr. Ellen Vitetta, for her guidance in so many aspects of research and for her early faith in my potential. She taught me to approach science critically and objectively, to overcome challenges with determination, to communicate effectively, and to take pride in work well done.

I thank my dissertation committee members, Drs. Pila Estess, John Minna, Jerry Niederkorn, and Dorothy Yuan for their time, interest, and guidance throughout my project. It has been a pleasure working with each of them.

I thank my collaborators, Dr. Elaine Coleman for her help with the lymphoma and prostate xenograft models, with the production and purification of antibodies and antibody fragments, and with the initial set-up of *in vitro* assays; Drs. Jerry Niederkorn and Shiuxan Wang for their work with UV3 in the uveal melanoma xenograft models; Dr. Maria-Ana Ghetie and Stephanie Kufert for advice associated with the lymphoma xenograft models; Dr. Camelia Spiridon for her advice associated with the breast cancer xenograft model; Dr. Victor Ghetie for his assistance with

the production and purification of F(ab')$_2$ antibody fragments; Dr. Joan Smallshaw for her technical advice; and Dr. Laurentiu Pop for his assistance with the ADCC and CDC assays and for his advice and support throughout this project. I would also like to thank Dr. Pop for his adoption of the ongoing UV3 project, which remains dear to me.

I thank Phyllis Barron for her technical support with the many, many mice involved in this project. I thank Ana Firan and Ming-Mei Liu for their patience in teaching me proper cell culture and antibody production techniques. I thank Lien Le, Kelly Mapes, Lilin Xiang, Ayesha Ahmed, Linda Trahan, and Dr. Iliodora Pop for their assistance with cell line maintenance, antibody production, and assay protocols.

I thank Karen Kazemzadeh of the Immunology Graduate Program and Erica Garza, Catherine Holloway, and especially Linda Berry of the Cancer Immunobiology Center for their excellent administrative support.

I thank Linda Berry, who has been like a mother to me at UT Southwestern, and Andrew Bitmansour, Allison Case, Pavitra Chakravarty, Dr. Elaine Coleman, Dr. Charlie Liu, Drs. Laurentiu and Iliodora Pop, Praveena Selvaduray, Lydia Tsai, and the many other friends I have worked with in the Cancer Immunobiology Center for their continued friendship and support. I already miss our daily interactions, our group happy hours, and our heartfelt conversations.

I thank all of my friends and family for their role in this accomplishment. I especially thank my parents, Joe and Kathy Sanford, for instilling in me at a young age a strong work ethic and the importance of a good education. I thank my other parents, Roger and Joyce Brooks, for their support and encouragement. I also thank my brothers and sisters and the many friends who have taken such wonderful care of me, especially when times were hardest. Without all of their continuous support, this long journey would not have been possible.

Finally, I thank my husband, Roger, for his constant patience, encouragement, understanding, and love.

THE ANTI-TUMOR ACTIVITY OF UV3, AN ANTI-CD54 ANTIBODY, IN SCID MICE XENOGRAFTED WITH A VARIETY OF HUMAN TUMOR CELL LINES

Kimberly Joe Brooks

The University of Texas Southwestern Medical Center at Dallas, 2008

Supervising professor: Ellen S. Vitettta, Ph.D.

UV3, a monoclonal antibody that specifically recognizes human CD54, also known as intercellular adhesion molecule-1 (ICAM-1) was previously developed for the treatment of multiple myeloma. Even at low doses UV3 was highly effective at prolonging the survival of SCID mice with advanced multiple myeloma. Since CD54 is expressed on many

different cancer types, we have now investigated the anti-tumor activity of UV3 in several other $CD54^+$ tumors. A panel of 28 human non-Hodgkin's lymphoma, breast, prostate, non-small cell lung, pancreatic, and melanoma tumor cell lines was examined for reactivity with UV3, and 24 were strongly positive. A representative $CD54^+$ cell line from each cancer type was then grown in SCID mice, and UV3 was administered using different dose regimens. UV3 prolonged survival and/or slowed tumor growth in all of the investigated tumor models, although it was not curative. When UV3 or gemcitabine were administered to SCID mice xenografted with non-small cell lung or pancreatic tumor cell lines, UV3 was as effective as the chemotherapy alone. However, the best anti-tumor responses were observed when gemcitabine and UV3 were administered together.

In order to better understand how UV3 mediates its anti-tumor activity, some mechanisms of action were also investigated. Previous studies in multiple myeloma cells indicated that UV3 did not directly inhibit tumor cell growth or cell adhesion and that the Fc portion of UV3 was required for activity in mice. Similarly, in this study, UV3 did not induce cell cycle arrest or apoptosis in any of the tumor cell lines evaluated, and UV3 did mediate Fc effector mechanisms. However, the involvement of both

Fc-dependent and Fc-independent mechanisms is suggested by the results, although the specific Fc-independent mechanisms are unknown.

UV3 has already been chimerized (cUV3), and both toxicology studies and clinical trials are in the planning stage to assess the safety and activity of cUV3 in patients with one or more of these tumors.

Table of Contents

Chapter 2: Materials and Methods

Chapter 3: Results

Prior Publications

Wang, S., E.J. Coleman, L.M. Pop, K.J. Brooks, E.S. Vitetta, and J.Y. Niederkorn. 2006. Effect of an anti-CD54 (ICAM-1) monoclonal antibody (UV3) on the growth of human uveal melanoma cells transplanted heterotopically and orthotopically in SCID mice. *Int J Cancer* 118:932-941.

Coleman, E.J., K.J. Brooks, J.E. Smallshaw, and E.S. Vitetta. 2006. The Fc portion of UV3, an anti-CD54 monoclonal antibody, is critical for its antitumor activity in SCID mice with human multiple myeloma or lymphoma cell lines. *J Immunother (1997)* 29:489-498.

Brooks, K.J., E.J. Coleman, and E.S. Vitetta. 2008. An anti-CD54 antibody has anti-tumor activity in SCID mice with human breast, prostate, non-small cell lung, and pancreatic tumor cell lines. *Submitted*.

List of Figures

List of Tables

List of Abbreviations

5-FU	5-fluorouracil
ADCC	Antibody-dependent cell cytotoxicity
AR	Androgen receptor
ATCC	American Type Culture Collection
B-CLL	B cell chronic lymphocytic leukemia
CDC	Complement-dependent cytotoxicity
CDR	Complementarity-determining region
CPM	Counts per minute
cUV3	Chimerized UV3 antibody
dCTP	Deoxycytidine triphosphate
dFdC	2',2'-difluorodeoxycytidine (gemcitabine)
dFdCDP	Gemcitabine diphosphate
dFdCTP	Gemcitabine triphosphate
DMEM	Dulbeco's modified Eagle medium
EDTA	Ethylene diamine tetraacetic acid
EGFR	Epidermal growth factor receptor
ELISA	Enzyme-linked immunosorbent assay
ER	Estrogen receptor
E:T	Effector cell to target cell ratio
FACS	Fluorescently activated cell sorting

FBS	Fetal bovine serum
FcγR	Fc-gamma receptors
FDA	U.S. Food and Drug Administration
FITC	Fluorescein-isothiocyanate
HBSS	Hank's balanced salt solution
HEPES	4-(2-Hydroxyethyl)piperazine-1-ethanesulfonic acid
HER-2	Human epidermal receptor-2
HPLC	High-performance liquid chromatography
IC_{50}	Drug dose that reduces cellular proliferation by 50%
ICAM-1	Intercellular adhesion molecule-1; CD54
IFN	Interferon
IL	Interleukin
i.p.	Intraperitoneal
i.v.	Intravenous
LD_{50}	Dose of drug which is 50% lethal
MEM	Minimal essential medium
MFI	Mean fluorescence intensity
NHL	Non-Hodgkin's lymphoma
NK	Natural killer cells
NSC	Non-small cell (lung cancer)
OD_{280}	Absorbance reading at 280λ
PBS	Phosphate-buffered saline, pH 7.4

PBS/EDTA/FBS	PBS containing 2 mM EDTA and 2% FBS
PR	Progesterone receptor
PSA	Prostate specific antigen
s.c.	Subcutaneous
sCD54	Soluble CD54 protein
SCID	Severe combined immunodeficiency
SDS	Sodium dodecyl sulfate
TNF	Tumor necrosis factor
UTSW	University of Texas Southwestern Medical Center
VEGF	Vascular endothelial growth factor

Chapter 1: Introduction

A. Cancer as a Disease.

Cancer is a general term referring to a group of diseases in which abnormal cells grow and spread without control. Cancer can arise from almost any cell in the body, resulting in significant diversity among cancers from different organs and cell types. Moreover, cancer is a major health concern. In 2004, cancer was the second leading cause of death in the U.S., accounting for nearly one in four deaths (23.1%). American men and women have approximately a 1 in 2 or a 1 in 3 lifetime risk of developing cancer, respectively. It is estimated that in 2007 over 1.4 million new cases of cancer were diagnosed in the U.S., and that cancer was the underlying cause of death for over half a million Americans. In addition to the physical and emotional tolls that cancer has on patients and their loved ones, cancer is estimated to cost Americans over $200 billion per year in direct and indirect costs[4, 101]. Despite significant advances in the development of more sensitive detection methods and more effective treatment options, cancer remains a serious health problem both in the U.S. and worldwide.

Common Cancer Therapies.

Although the specific therapeutic regimens indicated for each cancer type vary, they typically consist of some combination of surgery, radiation, chemotherapy, and biologic therapies depending upon the specific pathology, location, metastatic status, and gene expression pattern of the tumor.

Surgical Options.

Surgical resection of the primary tumor is still considered the mainstay for cancer treatment, especially if tumor growth is localized. Surgery is used to remove primary or metastatic tumors, to reduce the size of the primary tumors, or to provide palliation of symptoms. For hematopoietic cancers, surgical options may include autologous stem cell transplants to replenish normal blood cells following depletion with chemotherapy. Operative risk is related to the general health of the patient, the degree to which surgery would disrupt normal physiological functions, the type of anesthesia required, and the complexity of the surgical procedure. Therefore, surgery is not an option for patients in poor health or with tumors that are too large or too difficult to remove[8, 164, 195].

Radiation Therapy.

Ionizing radiation therapy works primarily by causing DNA damage through the direct or indirect creation of intracellular ions, resulting in cell cycle arrest and apoptosis of rapidly dividing cells, such as tumor cells. Ionizing radiation has been used as a cancer treatment for decades and is available in several different forms. The most commonly used form is high energy photon radiation, while electron beam radiation is used for tumors close to the body surface; particle radiation (i.e. proton and neutron radiation) is also used for some cancers[17, 53].

Radiation therapy is targeted locally, either to the site of primary tumors or of large, well-defined metastases. While radiation is capable of eliminating some tumors on its own, it is also often used in combination with chemotherapy to shrink tumors prior to surgical resection or to provide palliation. However, the effectiveness of ionizing radiation therapy can be limited by the hypoxic environment present within tumors, since molecular oxygen is a major facilitator of intracellular ionization. Investigations into the use of high-pressure oxygen with ionization radiation have generated mixed results depending upon the dose of radiation and the type and location of the tumor, and this technique is cumbersome to administer. The use of inhaled carbogen, an unpressurized mixture of 95% oxygen and 5% carbon dioxide, is also

under investigation[53]. Additionally, radiation therapy is most often targeted to tumors using an external beam source, and therefore must pass through normal tissues to reach the tumor site[17]. Therefore, radiation is associated with a variety of acute adverse effects, such as skin irritation and loss of stem cells, as well as with chronic adverse effects that occur months to years later, such as nerve injury, renal failure, fibrosis, and an increased risk of developing other cancers due to damage to the DNA of normal tissues surrounding the tumor[53]. Depending upon the type and location of the tumor, some high-dose, short-distance radiation therapy can be administered internally (brachytherapy) to minimize damage to normal tissues[17]. Other advances in the development of better radiation therapy techniques include better tumor mapping, more precise delivery of radiation to tumors via proton radiation, and combination with chemotherapeutic drugs that act as chemosensitizers[17].

Chemotherapy.

Chemotherapy refers to a large group of drugs that have anti-tumor activity by killing rapidly dividing cancer cells. Chemotherapy is a commonly used treatment option, both alone and in combined with radiation, surgery, or other anti-cancer agents depending upon the type

and stage of cancer. Since chemotherapy is typically used as a systemic therapy, it kills both primary and metastatic tumor cells, making it a valuable therapeutic option for patients with metastatic cancers. There are several common classes of chemotherapeutic drugs approved by the U.S. Food and Drug Administration (FDA) for the therapy of various cancers, including DNA alkylating agents, platinum compounds, anti-metabolites, topoisomerase interactive agents, and anti-microtubule agents. Most chemotherapeutic drugs target rapidly growing cancer cells by interfering with DNA replication or cell division. Unfortunately, because these agents typically affect all rapidly proliferating cells, they are associated with a variety of minor and severe side effects, including myelosuppression, hair loss, nausea/vomiting, and irritation of the skin, mouth, and throat. Myelosuppression is the greatest concern because it can lead to immunosuppression and subsequent infections, anemia, and deficient wound healing[46, 47]. Newer chemotherapeutic drugs are less toxic than traditional chemotherapeutic regimens because they are specifically targeted to receptors involved in cellular processes known to be altered or up-regulated in tumor cells. For exaple, gefitinib is a tyrosine kinase inhibitor that reversibly targets the epidermal growth factor receptor (EGFR) [46, 54].

Gemcitabine (2',2'-difluorodeoxycytidine, dFdC) is a deoxycytidine analog and a newer member of the anti-metabolite class of chemotherapeutic drugs[88]. After crossing the plasma membrane gemcitabine is metabolized within the cell into a diphosphate form (dFdCDP) and a triphosphate form (dFdCTP), both of which inhibit DNA synthesis. Gemcitabine dFdCTP competes with the natural nucleotide deoxycytidine triphosphate (dCTP) for incorporation into the "C" sites of growing DNA strands. Once dFdCTP is incorporated, only one more deoxynucleotide is added before DNA synthesis stalls[73, 92]. Further, once incorporated, the dFdCTP nucleotide analog is difficult to excise. Meanwhile, gemcitabine dFdCDP decreases the pool of available dCTP through the inhibition of ribonucleotide reductase, a key enzyme involved in the *de novo* synthesis of dCTP. The resulting depletion of available dCTP allows the gemcitabine dFdCTP metabolite to better compete for incorporation into new DNA strands[28, 86]. This inhibition of DNA synthesis subsequently activates intracellular signaling which leads to apoptotic cell death. The ability of gemcitabine to inhibit DNA repair mechanisms has led to synergistic activity in combination with other chemotherapeutic drugs and with radiation therapy[105, 120].

Gemcitabine targets rapidly dividing cells, which are actively undergoing DNA synthesis, including tumor cells as well as some normal

cell populations. Adverse effects due to the interaction of gemcitabine with normal cells include nausea/vomiting, immunosuppression, liver toxicity, renal toxicity, and flu-like symptoms, all of which are typically mild to moderate and are less severe than most chemotherapeutic drugs[81]. Despite these adverse effects, gemcitabine anti-tumor activity has led to FDA approval for some patients with breast, non-small cell (NSC) lung, pancreatic, and ovarian cancers[16]. Clinical trials have also demonstrated a role for gemcitabine therapy in renal and bladder cancers, uveal melanoma, colorectal cancer, and head and neck cancers[64, 116, 135, 173, 174, 215, 219].

Hormonal Therapy.

For cancers of the male and female reproductive systems, the modification of hormone levels can inhibit tumor growth. In these cancers, testosterone in men binds to androgen receptors (ARs), while in women estrogen and progesterone bind to the estrogen and progesterone receptors (ERs and PRs), providing a necessary stimulus for the continued growth of tumor cells. Therefore, in women with ER^+ and PR^+ breast cancer and in men with AR^+ prostate cancer, the production and signaling activity of hormones are targeted. Surgery can be used to remove the source of hormone, such as orchiectomy (removal of testicles)

in men and ovarian ablation in women. However, many patients prefer the administration of agents that inhibit hormone receptor binding and signaling or reduce hormone production *via* upstream inhibition[63, 141].

Targeted Biologic Therapies.

In addition to the traditional therapies of surgery, chemotherapy, and radiation, several therapies targeted to the immune system and to tumor-specific antigens have been developed in the last few years. Tumor-specific vaccines that can prevent infection with tumor-related viruses have been developed. Increased activation of anti-tumor T cells has been accomplished in patients by the administration of cytokines such as interferon (IFN)-α, interleukin (IL)-2, and IL-15 or by pulsing antigen presenting cells with highly immunogenic peptides that mimic tumor antigens. In addition, some monoclonal antibodies (MAbs) have been used to bind to and inhibit immunosuppressive receptors, such as CTLA-4, or to stimulate immune-activating receptors[132, 152, 209].

In addition to agents intended to increase the immune response against tumor cells, several other therapies have been developed that mediate anti-tumor activity *via* binding to tumor-associated antigens. Most agents bind to growth factor receptors, such as epidermal growth factor receptor (EGFR) or human epidermal receptor-2 (HER-2), to factors

involved in the metastatic process, such as matrix metalloproteinase proteins, or to antigens and receptors involved in the process of angiogenesis, such as vascular endothelial growth factor (VEGF)[59, 99, 140, 166]. Angiogenesis is the formation of new blood vessels from pre-existing ones, which is important for the continued delivery of oxygen and other nutrients to cells within the growing tumor mass[70]. These novel targeted agents include MAbs, conjugated antibodies, small molecule tyrosine kinase inhibitors, proteinase inhibitors, and antisense messenger RNA inhibitors. While the inhibitors typically induce cell cycle arrest or apoptosis, passively administered MAbs directed against tumor-selective antigens can activate or inhibit antigen-specific intracellular signaling pathways and can mediate tumor cell lysis *via* Fc effector functions[99, 166].

Cancer is a Heterogeneous Disease.

Although cancers of different origins share many properties, such as sustained proliferation, evasion of programmed cell death, evasion of the immune system, stimulation of angiogenesis, and the ability to metastasize to other tissues, many cancers also have unique features depending upon their cell of origin[27]. Thus, treatment strategies have varying degrees of efficacy depending upon the specific properties and

pathology of the tumor. The cancers selected for investigation in this study were chosen to include those most commonly diagnosed in the U.S.[101] and those of several origins, including hematopoietic, breast, prostate, respiratory, digestive, skin, and ocular cancers.

B Cell Non-Hodgkin's Lymphoma.

Lymphoma is a heterogeneous group of cancers that develop from the uncontrolled proliferation of B cell or T cells, which are normally a part of the adaptive immune system. There are two main types of lymphoma—Hodgkin's lymphoma, which develops from Reed-Sternberg B cells, and non-Hodgkin's lymphoma (NHL), which includes all other lymphomas. Approximately 4% of all cancers diagnosed are NHLs, and there were an estimated 63,000 new cases in the U.S. in 2007. Since the early 1970s the incidence of lymphoma has nearly doubled, and it continues to climb. It is also estimated that 18-19,000 individuals died in 2007 from NHL. Although NHLs can be of either T cell or B cell origin, fewer than 15% of diagnosed lymphomas are of T cell origin. While some subtypes of NHL are relatively common in children, over 95% of NHLs occur in adults. The risk of developing NHL also increases in individuals who are immunosuppressed due to organ transplant, have an autoimmune disease, or have been infected with certain viruses, such as human

immunodeficiency virus, hepatitis C virus, or Epstein-Barr virus. However, the specific risk associations and epidemiology vary according to the subtype of NHL[4, 9, 101, 162].

Depending on the tumor location, patients can present with varying symptoms. In lymph nodes just under the skin, patients identify palpable, tender lumps. When the disease grows in the abdomen, chest, or brain, the nodes cause painful swelling that compresses the intestinal tract, trachea, and veins, or that causes alterations in mood and results in seizures. B cell-associated symptoms such as fever, chills, and weight loss occur in patients with advanced disease. Unfortunately, there are no early diagnostic tests, so patients must develop symptoms accompanied by enlarged nodes to be diagnosed. However, despite the continued increase in incidence and the lack of early diagnostic tests, the mortality rate of patients with NHL is steadily decreasing. Although the mortality rate varies greatly depending upon the originating cell type and the stage of disease, the average five-year and ten-year survival rates are currently 63% and 49%, respectively[4, 9, 162].

The observed decrease in the mortality rate over the last decade is thought to be due to improvements in the therapeutic options for patients with NHL. Surgery is occasionally used to remove easily accessible nodes, but radiation is preferred for the treatment of localized and/or slow-

growing tumors. More advanced, aggressive, or disseminated NHLs are often treated with a combination of cyclophosphamide, doxorubicin, vincristine, prednisone or dexamethasone chemotherapy along with Rituxan™, an anti-CD20 MAb. Other biological therapies effective in the treatment of some NHL types include the anti-CD52 MAb Campath™, the radiolabeled anti-CD20 antibodies Bexxar™ and Zevalin™, and IFN-α cytokine therapy. Autologous stem cell transplants are also used to treat patients with chemotherapy-refractory or relapsing disease. However, the preferred combination of treatment options depends upon the disease stage and historic knowledge of effective therapies for the particular NHL subtype[9, 127, 159, 195].

Breast Cancer.

Breast cancer has been the most commonly diagnosed cancer in American women since before 1975 and the second-leading cause of cancer-related mortality in American women since approximately 1955. It is estimated that in 2007 over 175,000 women and 2,000 men were diagnosed with breast cancer in the U.S., and that over 40,000 individuals died due to breast cancer. Gender and age are the two most significant risk factors for developing breast cancer, but there are many other factors that also contribute to an individual's risk, including genetic mutations in

the BRCA1 and BRCA2 genes, familial predisposition, menstrual history, obesity, use of menopausal or contraceptive hormone therapy, child birth history, and radiation exposure[4, 101, 214].

In the last 15 years the mortality rate associated with breast cancer has been on the decline due to a combination of better early stage detection and more effective treatment options. Mammography has improved, and it is estimated that 80-90% of early stage breast cancers can be detected in asymptomatic women. The most common symptom experienced is the development of a palpable, painless mass, but some individuals experience thickening, swelling, distortion, skin irritation, or tenderness of the breast or develop nipple abnormalities. Once diagnosed, tumors are evaluated for the expression of ER, PR, and HER-2, since their expression is considered to be predictive of outcome and of potential therapeutic options. ER and/or PR are present on approximately 70% of invasive breast tumors, and their expression is associated with better survival rates due to hormone-dependence. In contrast, HER-2 is over-expressed in 20-30% of breast cancers, and amplification of HER-2 is associated with a poorer prognosis[4, 80, 214].

Depending upon the size and stage of the breast cancer, lumpectomy (removal of tumor mass) or mastectomy (removal of the whole breast) and removal of regional lymph nodes may be indicated to

remove all cancerous tissue. In addition to surgery, treatment often incudes radiation, chemotherapy, hormone therapy, or targeted biologic agents to reduce or eliminate metastatic growth. The addition of radiation to surgery reduces the ten-year localized recurrence rate from 39.2% to 14.3%. Several classes of chemotherapeutic drugs have activity against breast cancer, with anthracyclines (doxorubicin and epirubicin) and taxanes (paclitaxel and docetaxel) the most commonly used to eliminate metastases or provide palliation. Hormone therapy involves the inhibition or down-regulation of estrogen to prevent its binding to ER^+ breast cells, since its binding provides a necessary signal for the growth of hormone-dependent tumor cells. Estrogen reduction can be accomplished with surgical ovarian ablation, but most patients prefer the administration of aromatase inhibitors or selective estrogen response modulators, namely tamoxifen, which mediate their effects *via* the ER. The most successful targeted biologic therapy for breast cancer is Herceptin™, a MAb that specifically binds to the HER-2/neu growth factor receptor. Other biologic agents demonstrating therapeutic efficacy in clinical trials include small molecule inhibitors and MAbs that target HER-2, EGFR, or angiogenic factors, such as VEGF[4, 16, 80, 141, 214].

Prostate Cancer.

Prostate cancer has remained the most diagnosed cancer in U.S. men since 1975, with over 215,000 new cases estimated in 2007. Prostate cancer has also been the second-leading cause of cancer-related deaths in American men for over two decades, although the mortality rate has been sharply decreasing since the early 1990s. There are few known risk factors for the development of prostate cancer, though age and genetic predisposition have shown significant correlations[4].

The marked decline in mortality is attributed in part to the development of better diagnostic techniques, since 90% of patients are now diagnosed with early local or regional disease. The most important diagnostic development is the screening for prostate-specific antigen (PSA) *via* noninvasive blood test, which is now used routinely in addition to digital rectal exams. PSA induces seminal fluid liquification and the release of mobile spermatozoa. When growing prostate tumors disrupt the epithelial basement membrane, PSA enters the circulation. In general, higher serum PSA amounts correlate with larger tumor volumes and more advanced stages of differentiation. Aside from elevated amounts of circulating PSA, patients with early prostate cancer are often asymptomatic, while those with metastatic disease present with symptoms related to bladder outlet obstruction, such as weak flow, hesitancy, pain,

and increased frequency of urination, which are common to a variety of pathologic conditions[4, 172].

Early disease is treated successfully with surgical resection and radiation, occasionally in combination with chemotherapy or hormonal therapy to eliminate micrometastases. The therapy of metastatic disease has also traditionally relied on a combination of chemotherapy, radiation, and hormonal therapy, such as anti-androgens that inhibit testosterone activity and hormone analogs that reduce testosterone production. However, advanced disease is difficult to treat because prostate cancer becomes hormone-refractory through the down-regulation or inactivation of the AR and because prostate cancer cells preferentially metastasize to bone. For these reasons metastatic disease is associated with only a 33% five-year survival rate[4, 63, 172]. In recent years researchers have developed a variety of new therapeutic agents, including more effective chemotherapeutic agents and small molecule inhibitors or MAbs targeted against soluble factors and receptors involved in angiogenesis, metastasis (matrix metalloproteinase family), and growth factor signaling, especially EGFR and HER-2, or against receptors specifically up-regulated in prostate cancer, such as prostate-specific membrane antigen. Other agents, such as calcitrol, the main metabolite of Vitamin D, can enhance chemotherapy efficacy in androgen-resistant disease[83, 84, 140, 172].

Non-Small Cell Lung Cancer.

Lung cancer ranks second-highest in cancer incidence, accounting for about 15% of all cancer diagnoses, and leads cancer-related deaths (29%) for both men and women in the U.S. Both incidence and mortality have been declining in men for the past two decades, while they are just reaching a plateau in women after years of steady increase. Cigarette smoking remains the most important risk factor, as at least 40 of the 300 chemicals in cigarette smoke are known carcinogens. Other risk factors include genetic susceptibility and environmental or occupational exposure to air pollution, second-hand smoke, asbestos, ionizing radiation, and certain metals. For therapeutic purposes, lung cancers are labeled as either small cell (about 13%) or non-small cell (NSC) lung cancers (about 87%) based on cell morphology[4, 101, 176].

Mortality rates for NSC lung cancer remain high due to a combination of ineffective therapies for the treatment of advanced disease and a lack of early detection methods—the five-year survival rate jumps from 16% for all lung cancers to 49% for localized lung cancers, but only 16% of lung cancer are diagnosed in an early, localized stage[4]. Symptoms present at diagnosis commonly include persistent coughing, wheezing, blood-streaked sputum, chest pain, and recurrent pneumonia and/or bronchitis. While some patients are diagnosed with asymptomatic

lesions *via* chest x-rays, most symptomatic patients have tumors that have already metastasized to the regional lymph nodes or beyond, typically to the bones, liver, adrenal glands, and/or brain[176].

Early stage NSC lung cancer is typically treated with a combination of surgical resection and either radiation therapy or chemotherapy. Advanced metastatic NSC lung cancer remains more difficult to treat, since neither surgery nor radiation therapy can eliminate micrometastases. Patients with metastatic disease are typically treated with chemotherapy, often including one of the platinum-based drugs, such as cisplatin or carboplatin, in combination with gemcitabine, vinorelbine, irinotecan, docetaxel, or paclitaxel. A few targeted agents have recently demonstrated efficacy in patients with NSC lung cancer, especially tyrosine kinase inhibitors and MAbs that specifically target EGFR, HER-2, and VEGF, and many other agents are being evaluated in clinical trials. Despite these advances, for most patients with advanced disease the goal is to modestly extend life and to provide palliation[16, 55, 155, 176].

Pancreatic Cancer.

Although pancreatic cancer is not one of the most prevalent cancers in the U.S., with an estimated 37,000 diagnoses in 2007, it is associated with a five-year overall survival rate of only 5% and is the

fourth-leading cause of cancer-related deaths in both men and women. Cigarette smoking is considered the main risk factor for pancreatic cancer; other associated risk factors include obesity, a diet high in fat and cholesterol, chronic pancreatitis, genetic predisposition, diabetes, cirrhosis, and exposure to environmental carcinogens[4, 101, 216].

Currently there are no reliable methods for the early detection of pancreatic cancer since its early growth is often asymptomatic, contributing to the low survival rate associated with this cancer. However, the five-year survival rate is below 20% even in patients that are diagnosed with local disease. Weight loss, jaundice, and abdominal or back pain are the most common symptoms reported at the time of diagnosis, although glucose intolerance and pancreatitis are also occasionally reported[4, 216].

When possible, surgical resection to remove localized tumor bulk followed by radiation therapy and chemotherapy is the only curative option. A combination of radiation therapy and radio-sensitizing chemotherapeutic drugs, such as gemcitabine and 5-fluorouracil (5-FU), is the preferred treatment strategy for increasing survival in patients with locally advanced pancreatic cancer. Patients presenting with metastatic or recurring disease are typically treated with a chemotherapy regimen including gemcitabine, but their poor health status, weight loss, and

reduced liver function severely limit the tolerated dose of chemotherapy. Since the effectiveness of chemotherapy in pancreatic cancer has reached a plateau, MAbs and small molecule inhibitors targeted at angiogenesis factors, the EGFR family of receptors, and the Ras oncogene are currently being evaluated. While it is hoped that curative agents will eventually be discovered, at this time even an improvement in median survival or the palliation of side effects is significant[4, 16, 182, 216].

Cutanteous Melanoma.

About 4% of cancers diagnosed in U.S. men and women are skin cancers. An estimated 60,000 diagnoses and 8,000 deaths were attributed to melanoma in the U.S. in 2007. Although other types of skin cancer exist, the most serious are melanomas, which originate from melanocyte cells responsible for skin pigmentation. While the death rate associated with melanoma has recently reached a plateau, its incidence is rising faster than any other cancer, partly because melanoma is increasingly affecting a younger population. The main risk factors for melanoma include family history and the presence of moles, but sun sensitivity/skin pigmentation and excessive sun exposure also confer an increased risk of

developing melanoma. Thus, limitation of direct sun exposure is the best known preventative measure[4, 29, 101].

The development of melanoma is often identified visually as the appearance of an unusual skin growth or a progressive change in the size, shape, or color of an existing skin feature. These are also typically the only symptoms, since melanoma is diagnosed at the localized stage in approximately 80% of patients. For localized melanoma, surgical removal of the lesion and sometimes the regional lymph nodes is typically curative, with a 99% five-year survival rate. In some cases radiation therapy may also be used. For patients with regionally or distantly metastatic melanoma, systemic chemotherapy or immunotherapy must be administered in addition to surgical resection to eliminate metastases. However, the five-year survival rate for patients with metastatic melanoma is only 65% for regionally advanced disease and 15% for distantly advanced disease, since melanoma metastasizes to many sites, including the brain, bones, liver, and kidneys. Chemotherapeutic drugs, including temozolomide, the most used agent, have been disappointing even when used in combination with other agents. Immunotherapy has also demonstrated some efficacy and currently consists of the administration of immune activating cytokines, such as IFN-α or IL-2, which are associated with an abundance of adverse effects. Other treatment strategies are

under investigation, and include adoptive transfer of T cells, anti-angiogenic therapies, melanoma vaccines, prevention of tumor-induced immunosuppression *via* blockade of the CTLA-4 receptor on T cells, and MAbs directed against integrins and gangliosides[4, 29, 152, 203, 213].

Uveal Melanoma.

While most melanomas arise from cutaneous melanocytes, approximately 5% are intraocular melanomas, and the majority of intraocular melanomas are uveal in origin. Despite their low incidence, uveal melanomas account for about 13% of all melanoma-related deaths in the U.S., with five-year survival rates of 6-53%. While risk factors are difficult to identify, sun sensitivity/skin and eye pigmentation are thought to be the main risk factors; the risks associated with sunlight and occupational exposures are controversial[183, 184].

Uveal melanoma can be accurately diagnosed through clinical examination of the eyes; however it is estimated that 50% of patients already have micrometastases at the time of presentation, regardless of whether they are detectable. The mortality rate of patients with uveal melanoma has remained unchanged in the U.S. over the 25-year period from 1973 to 1997, despite advances in diagnostic techniques. Prognostic factors include the location, size, and configuration of the tumor, the

expression of HLA, and the presence of abnormalities on chromosomes 1, 3, 6, or 8. Due to the slow growth of some primary uveal melanomas, older patients with small tumors are occasionally only monitored, without therapeutic intervention. For patients in whom therapy is indicated, surgical enucleation and brachytherapy plaque radiation are the most common therapeutic strategies to remove the primary tumor. Although small primary melanomas may take years to progress, patients diagnosed with metastatic uveal melanoma have a median survival of less than 6 months due to liver metastases. Patients with metastatic disease are typically treated with various systemic or intra-arterial hepatic chemotherapeutic drugs, with or without IL-2 and IFN-α therapy. However, these therapies are associated with low response rates since uveal melanomas are relatively chemoresistant. There are a number of agents being developed or evaluated for metastatic uveal melanoma that target novel aspects of uveal melanoma biology, including anti-angiogenic agents and other forms of immunotherapy[26, 58, 183, 184].

B. Monoclonal Antibodies in Cancer.

In 1975 Kohler and Milstien pioneered the development of MAbs that recognize specific antigens[113]. Their technique involved the immortalization of MAb-secreting cells from mice immunized against desired antigens and the subsequent screening of the hybridoma cells for reactivity with the target antigen. In the last 33 years, numerous advances in antibody technology have been developed to enhance the properties of MAbs. As of 2008, six MAbs and three immunoconjugates have been approved by the FDA for the treatment of cancer, and many others are currently being evaluated in clinical trials[16, 104, 198].

Specificity.

MAbs make ideal therapies because they can be developed to specifically recognize almost any antigen. Appropriate targets are tumor selective, including over-expressed antigens, unique carbohydrate antigens, differentiation antigens, oncofetal antigens, and antigens limited to one cell type or lineage, since tumor-specific antigens are rare. Although these MAbs may also react with a few normal cells, their relatively selective activity provides therapeutic efficacy with relatively few side effects. Unfortunately, the heterogeneity of antigen expression on

tumors makes the identification of MAb targets with broad anti-tumor activity difficult[69, 104, 209].

Mechanisms of Action.

MAbs mediate their activities through a variety of different mechanisms. The best characterized are Fc-dependent mechanisms, such as antibody-dependent cell cytotoxicity (ADCC) and complement-dependent cytotoxicity (CDC). In ADCC, the exposed Fc portions of IgG MAbs bound to tumor cells bind to activating receptors ($Fc_{\gamma}R$) on effector cells, such as natural killer (NK) cells. This binding then stimulates the effector cells to release cytotoxic granules that kill tumor cells. In CDC, tumor cell lysis occurs following the binding of the C1q complement component to the Fc portion of MAbs bound to tumor cells and the subsequent activation of the complement cascade, ultimately creating holes in the tumor cell membrane. Although all IgG MAbs are though to mediate these mechanisms to some extent, some are more effective than others. The mouse IgG_{2a} and human IgG_1 and IgG_3 subclasses are the most effective at mediating ADCC, while mouse IgG_3 and human IgG_3 are the most effective at mediating CDC[49, 69, 198, 208, 218].

Some MAbs mediate their activity by blocking normal receptor-ligand binding. This interference can affect tumor cell growth by blocking

the adhesion of tumor cells to each other and can prevent effective homing of tumor cells to preferred sites of growth by blocking the adhesion of tumor cells to stromal cells. MAbs can also interfere with normal signaling mechanisms by neutralizing the pool of free ligands or by blocking signaling receptors on tumor cells and tumor-associated cells. Inhibited signaling may either directly or indirectly (i.e. angiogenesis) down-regulate tumor cell proliferation and growth. In addition, some MAbs have the ability to induce cell cycle arrest or apoptosis once bound to their target antigen[69, 104, 198, 208, 218].

Advances in Monoclonal Antibody Engineering.

Although MAb therapies have been successful, they have also encountered a number of obstacles, most notably immunogenicity and tumor penetration. Most early therapeutic MAb were of mouse origin, and were therefore immunogenic in humans. To circumvent this problem, researchers developed techniques to make murine MAbs more human. Chimeric antibodies are created by joining the mouse V_L and V_H regions to human C_L and C_H regions, so that only the light and heavy chain variable regions of the MAb are of mouse origin. Humanized MAbs are mostly of human antibody domains, but with murine complementarity-determining regions(CDRs). Since the CDRs of the light and heavy chain variable

regions confer antigen specificity, antibody binding is largely unaffected while the remainder of the Mab is of human origin and is hence less immunogenic[42, 104, 198].

Other properties can also be improved by antibody engineering. The association and dissociation of a MAb with its target cell can be improved by altering its antigen-binding regions or by increasing the number of antigen binding sites[126, 134, 209]. Some laboratories have created bi-specific antibodies, capable of binding two different antigens on different cells and thereby bringing an effector cell in close proximity to the tumor cell[42, 218]. Several techniques are available for producing smaller antibody-like proteins with the antigen binding properties of MAbs and improved tumor localization due to their smaller size. However, they are also associated with a shorter half-life *in vivo*. While the rapid clearance of these smaller MAb constructs is ideal for limiting the toxicity of conjugated antibodies, a shorter half-life requires higher or more frequent dosing, which may be prohibitory for naked MAbs due to an increase in side effects and cost[69, 104]. The half-lives of MAbs can also be increased or decreased by altering the antibody's affinity for the neonatal Fc receptor (FcRn), which is involved in antibody catabolism. Additionally, engineering techniques can modify some mechanisms of action, most notably enhancement of the Fc effector mechanisms ADCC and CDC[42, 209].

Antibodies as Cancer Therapies.

Six MAbs have already been FDA-approved for the treatment of various cancers, and they mediate their activity through a variety of different mechanisms. Other MAbs are currently under development or in pre-clinical and clinical studies. Three MAbs conjugated to cytotoxic drugs or radioisotopes have also been approved for cancer therapy.

Avastin™.

Avastin™, also known as bevacizumab, is a humanized IgG_1 MAb that binds to VEGF. Avastin™ is thought to starve tumor cells by preventing the binding of VEGF to its receptor and thus inhibiting new vasculature formation. MAbs against VEGF may also improve the delivery of drugs by normalizing existing tumor blood vessels[1], which are poorly organized with excessive branching, uneven diameters, and turbulent blood flow[59, 138]. Avastin™ was first FDA-approved in 2004 for the treatment of patients with metastatic colon and rectal cancer after clinical trials of Avasin™ in combination with the chemotherapy drugs irinotecan, 5-FU, and leucovorin resulted in an increase in median survival from 15.6 months to 20.3 months as compared with patients receiving chemotherapy alone. In 2006 Avastin™ was approved for the first-line treatment of patients with unresectable, locally advanced, recurrent, or metastatic NSC

lung cancer in combination with carboplatin and paclitaxel after clinical trials demonstrated that the combination resulted in a 25% improvement in overall survival and an increase in median survival from 10.2 months to 12.3 months as compared to chemotherapy alone[1, 59]. However, clinical trials are currently investigating the efficacy of Avastin™ in over 20 tumor types, and activity has been demonstrated in metastatic breast, prostate, pancreatic, melanoma, ovarian, and hepatic cancers[1, 83, 104, 198]. The most severe adverse effects associated with Avastin™ therapy are gastrointestinal tract perforation, complications in wound healing, hemorrhaging, and hypertension[1].

Campath™.

Campath™, also known as alemtuzumab, is a humanized $IgG_{1\kappa}$ MAb that recognizes CD52. The CD52 antigen is expressed on many leukocytes, including B cells and T cells, although its physiological functions are not yet clear. Likewise, the mechanism of action for Campath™ has not yet been elucidated, although several mechanism are implicated, including ADCC, CDC, and the induction of apoptosis through several pathways. In 2001 Campath™ was FDA-approved for the treatment of patients with B cell chronic lymphocytic leukemia (B-CLL), a cancer typically developed in patients over 50 years of age and

characterized by the clonal proliferation of mature B cells in the blood, bone marrow, lymph nodes, and spleen. Campath™ has demonstrated 21-33% complete response rates in three separate studies[3, 22]. Although (B-CLL) is the only cancer for which Campath™ is currently approved, it is being evaluated in clinical trials of patients with a variety of other lymphoid malignancies[60, 156]. The most common adverse effects associated with Campath™ therapy are cytopenias, infusion reactions, and immunosuppression-related infection[3]. Due to its immunosuppressive activity, Campath™ is also being investigated for the treatment of autoimmune diseases and the prevention of graft *vs* host disease[79, 156].

Erbitux™.

Erbitux™, also known as cetuximab, is a chimeric IgG_1 MAb that specifically binds to EGFR on both tumor and normal cells. Erbitux™ is thought to slow tumor growth both through tumor cell lysis *via* ADCC and by blocking epidermal growth factor from binding to its receptor, resulting in the inhibition of tumor cell growth and proliferation, angiogenesis, and metastasis. Erbitux™ was first FDA-approved in 2004 for the treatment of metastatic colorectal cancer either in combination with irinotecan or alone (in irinotecan-resistant cancer). Administered alone Erbitux™ increased

the overall response rate from 0% to 8.0% and the overall survival from 4.6 months to 6.1 months as compared to best supportive care, and in another study the addition of irinotecan to Erbitux™ therapy improved the overall survival rate from 10.8% to 22.9% and the overall survival from 6.9 months to 8.6 months. Erbitux™ was later approved for the treatment of locally and regionally advanced head and neck cancers in combination with radiation therapy, and the combination improved the median survival of these patients from 29.3 months to 49.0 months as compared to radiation therapy alone[13, 34, 72]. Erbitux™ has additionally demonstrated anti-tumor activity in pre-clinical and clinical studies of bladder cancer, breast cancer, and prostate cancers[104, 198]. Severe adverse effects, such as infusion reactions, heart attacks and lung disease, are rare and the most common side effects include skin irritations, headaches, diarrhea, and infections[13, 72].

Herceptin™.

Herceptin™, also known as trastuzumab, is a humanized IgG_1 MAb that specifically recognizes the HER-2/neu antigen. HER-2/neu, a member of the EGFR family, forms homodimers as well as heterodimers with other HER family members and thereby mediates a variety of intracellular signals. HER-2/neu is overexpressed in approximately 25-30% of breast

cancers as well as cancers of the ovary, lung, prostate, and gastrointestinal tract, and the expression of HER-2/neu in breast cancer is a marker for poor prognosis[104]. In addition to the mediation of tumor cell lysis through Fc-dependent mechanisms, the binding of Herceptin™ to HER-2/neu has been shown to block cell cycle progression through the G_1 phase, thereby inhibiting tumor cell growth[142, 198]. Herceptin™ was first FDA-approved in 1998, and is currently approved both as an adjuvant therapy in combination with a chemotherapy regimen of doxorubicin, cyclophosphamide, and paclitaxel as well as alone or in combination with paclitaxel for metastatic breast cancer[14]. The combination of doxorubicin, cyclophosphamide, and Herceptin™ increased the overall response rate from 32% to 50% and the median overall survival from 20.3 months to 25.1 months in patients with metastatic breast cancer as compared to chemotherapy alone. Herceptin™ has also demonstrated synergistic activity with other chemotherapy regimens, radiation therapy, and biologic therapies targeting EGFR or VEGF in clinical trials, suggesting the potential for a multi-modality approach[104]. The most common adverse effects of treatment with Herceptin™ are related to infusion reaction, but incidences of severe cardiac diseases have also been reported, particularly in patients who received anthracycline[14].

Rituxan™.

In 1997 Rituxan™, also known as rituximab, became the first MAb therapy approved by the FDA for the treatment of cancer. Rituxan™ is a chimeric IgG_1 MAb that recognizes CD20 on most normal and malignant B cells. Rituxan™ is believed to mediate its activity primarily by ADCC and CDC of $CD20^+$ lymphoma cells, although other potential mechanisms of action have been demonstrated in pre-clinical studies[50, 198]. Rituxan™ is approved for the treatment of various B cell NHLs either alone or in combination with specified chemotherapy regimens[18]. As a single agent Rituxan™ induced remission in 48% of patients, and in combination with chemotherapy (cyclophosphamide, doxorubicin, vincristine, and prednisone) Rituxan™ induced remission in 95% of patients. Several studies have demonstrated synergistic effects of Rituxan™ with a variety of different chemotherapy drugs in patients with NHL[50]. In addition, Rituxan™ has also been FDA-approved for the treatment of patients with rheumatoid arthritis in combination with methotrexate, and it may hold promise for the treatment of other autoimmune diseases as well. The most common side effects associated with Rituxan™ are those related to infusion reactions and immunosuppression-related infections due to a reduction in the number of B cells and other immune cells[18].

Vectibix™.

Vectibix™, also known as panitumumab, is a fully human IgG_2 MAb approved by the FDA in 2006 for the treatment of metastatic colorectal cancer. Victibix™ specifically recognizes EGFR, and its activity is thought to be mediated through mechanisms similar to those of Erbitux. Vectibix™ alone improved the percentage of patients without disease progression from 30% to 49% and the mean time to disease progression from 60 days to 96 days as compared to best supportive care. In combination with chemotherapy Vectibix™ has demonstrated further improvements in efficacy. Vectibix™ has also demonstrated some anti-tumor activity in pre-clinical models of breast, prostate, pancreatic, ovarian, and renal cancer, and is currently being further evaluated in these and other cancers. The side effects of Vectibix™ therapy are generally related to skin irritation and infusion reactions[19, 41].

Immunoconjugates.

In addition to the “naked” MAbs, three immunoconjugates—Mylotarg™, Bexxar™, and Zevalin™—have also been FDA-approved for the treatment of cancer. Immunoconjugates represent a method of specifically delivering cytotoxic agents or radiotherapy to tumor cells *via* antibody-antigen interactions, thus reducing systemic toxicity[42, 69, 104,

209]. Mylotarg™ is an immunoconjugate consisting of a humanized $IgG_{4\kappa}$ antibody with specificity for CD33 on hematopoietic cells and the cytotoxic antibiotic calicheamicin. Mylotarg™ is used for the treatment patients with myelogenous leukemia[15]. Bexxar™ and Zevalin™ are both radioconjugates that target CD20 on certain types of B cell NHL. Bexxar™ is a murine $IgG_{2\lambda}$ antibody labeled with ^{131}I, and Zevalin™ is a murine $IgG_{1\kappa}$ antibody labeled with ^{90}Y[2, 20]. Other immunotoxins and radioconjugates are currently under evaluation in clinical trials[218].

C. UV3 as an Anti-Tumor Agent.

The Development of UV3.

Since MAbs represent an effective and potentially less toxic alternative to traditional chemotherapy, a MAb therapy was developed for the treatment of patients with multiple myeloma. Multiple myeloma is characterized as the uncontrolled proliferation of a single clone of plasma cells or plasma cell progenitors in the bone marrow. Multiple myeloma was chosen as the therapeutic target because the 5-year survival rate for this cancer remains low (about 33%) despite advances in therapeutic options[8].

UV3 was developed by immunizing BALB/c mice with alternating monthly intraperitoneal (i.p.) injections of two human multiple myeloma cell lines, RPMI-8226 and U-266. Three days after the last injection, spleens were removed from the immunized mice and the splenocytes were fused with SP2/0 mouse myeloma cells to produce immortal hybridomas capable of secreting myeloma-specific MAbs. Supernatants from the hybridomas were screened by enzyme-linked immunosorbent assay (ELISA) and flow cytometry for reactivity against multiple myeloma cells. A hybridoma clone was identified that produced antibodies with high reactivity against multiple myeloma and B cell lymphoma cells and low

reactivity against most normal cell types. The antibody, UV3, was affinity purified using Sepharose-G, and its isotype was determined to be IgG_{2a} using ELISA[94].

The purified MAb was then used to immunoprecipitate its antigen, an 83 kDa protein corresponding to CD54, also known as common intercellular adhesion molecule-1 (ICAM-1). The specificity of UV3 was confirmed using flow cytometry. UV3 bound to a known $CD54^+$ endothelial cell line and to Chinese hamster ovary cells (CHO) transfected with human CD54, but not to non-transfected CHO cells or to a known $CD54^-$ endothelial cell line. It was also determined that UV3 specifically recognizes human CD54, but not mouse CD54[94, 177].

UV3 Therapy of SCID/Multiple Myeloma Mice.

To evaluate the anti-tumor activity of UV3, a mouse model of multiple myeloma was created by irradiating severe combined immunodeficient (SCID) mice and then injecting them intravenously (i.v.) with the human ARH-77 multiple myeloma cell line. Tumor cells grew in a disseminated manner in the mice, infiltrating the vertebrae and causing compression on the spinal cord, culminating in hind-leg paralysis at about 30 to 40 days later[95]. Following tumor cell inoculation, the mice were then treated i.v. with 0.8 μg/g mouse of UV3 or an isotype-matched control

antibody on each of days 1, 2, 3, and 4 (early disease) or received 4 μg/g of antibody on days 15, 16, 17, and 18 (advanced disease). Mice receiving either phosphate buffered saline (PBS) or the control antibody developed hind-leg paralysis by day 35 following tumor cell injection. Mice receiving UV3 at an early disease stage survived for 150 days, at which point the experiment was terminated. Mice treated with UV3 at an advanced stage of disease stage survived for over 124 days, at which point the experiment was terminated[96]. UV3 was high effective at prolonging the survival of mice with multiple myeloma, even when administered at very low doses.

Chimeric UV3.

Due to its demonstrated anti-tumor activity in SCID mice with multiple myeloma, UV3 has been chimerized (cUV3) to reduce its immunogenicity in humans[187]. The heavy and light chain variable domains of UV3 were genetically spliced to human IgG_1 and κ constant domains, respectively, and the engineered chimeric light and heavy chains were co-expressed to produce cUV3. Using flow cytometry, it was shown that cUV3 and murine UV3 bind similarly to the ARH-77 and KM-3 human myeloma cell lines, and cUV3 demonstrated equivalent anti-tumor activity to UV3 in SCID/multiple myeloma mice. Clinical trials to evaluate cUV3 in patients with multiple myeloma are currently in the planning stage[187].

D. CD54.

Structure.

CD54, also known as ICAM-1, is an immunoglobulin-like cell adhesion molecule and a member of the immunoglobulin supergene family. Structurally, it is a transmembrane glycoprotein containing five serial extracellular Ig-like domains connected to a transmembrane domain and a short charged cytoplasmic tail[192, 193, 205, 210]. Of note, human CD54 shares only 50% protein homology with murine CD54[185], which may account for the difference in antibody binding observed between the two[94]. Depending upon its cellular expression, CD54 is differentially glycosylated, resulting in a molecular weight between 80 and 114 kDa. The distribution of CD54 on the cell surface is thought to be regulated by the cytoskeleton *via* association with the cytoskeleton-binding protein α-actinin[205, 210].

Expression on Normal Cells.

CD54 is constitutively expressed on a variety of different cell types, including endothelial cells, epithelial cells, macrophages, fibroblasts, and leukocytes. CD54 can also be induced on many other cell types, and its expression can be up- or down-regulated by a number of cytokines,

steroid hormones, and physical factors. Although CD54 is regulated differently by each cell type, tumor necrosis factor (TNF)-α, IFN-γ, and IL-1 are the most well known inducers of CD54 expression, while glucocorticoids are the most important inhibitors. Most regulation of CD54 expression occurs at the transcriptional level and is dependent on the availability of transcription factors and receptors for extracellular signals and on the activity of signal transduction pathways of the expressing cells, but variations in post-translational machinery and the activity of glycosylation enzymes can also regulate CD54 expression[161, 167, 205].

Since CD54 is expressed on normal cells, UV3 may bind to and elicit effects on these normal cells in patients, a possibility that raises concerns about potentially serious side effects in humans. Although clinical studies with UV3 have not yet been initiated, several studies examining the safety of another anti-CD54 MAb have been published. BIRR1 was a murine IgG_{2a} anti-CD54 antibody investigated in Phase I/II clinical trials for the treatment of patients with rheumatoid arthritis. Side effects observed were typical of antibodies in general and consisted of headache, fever, nausea/vomiting, pruritus, light-headedness, and urticaria. They were mild to moderate in severity and typically abated after the second day of therapy. However, therapy was immunosuppressive, which is why it was investigated for the treatment of rheumatoid

arthritis[106-108]. It is likely that UV3 will also be immunosuppressive, which could be problematic in cancer patients already immunosuppressed due to their cancer or to the other anti-tumor therapies they are receiving. However, its efficacy may offset this problem. The usefulness of cUV3 will not be known until its safety and efficacy have been evaluated in patients.

Functions.

CD54 binds several ligands, including the β_2 integrins lymphocyte function-associated antigen (LFA-1; CD11a/CD18) and macrophage-1 (Mac-1; CD11b/CD18) on leukocytes, sialophorin (CD43) on leukocytes and platelets, and soluble fibrinogen. CD54 is also binds to rhinoviruses and the coaxsackie A13 virus. Depending on the cell type and the bound ligand, CD54 can mediate a variety of effects. CD54 primarily functions as an adhesion molecule, facilitating specific and reversible cell-cell adhesion between cells expressing CD54 and its ligands. These intercellular adhesions are important for T cell and NK cell activation and for leukocytes migration[35, 167, 205, 206]. Some studies have also implicated CD54 ligation in immunologic cell signaling[89, 168].

Pathophysiology.

In addition to its role in normal immunologic processes, CD54 has also been implicated in various diseases. CD54 is a receptor for rhinoviruses, and therefore likely plays a role in these upper respiratory infections[205]. Since CD54 is up-regulated during inflammation, it has also been implicated in a number of different diseases characterized by either local or systemic inflammation[32, 65, 74, 136, 205]. There also appears to be a role for CD54 in the pathology of some cancers. As compared with their corresponding normal tissues, CD54 is over-expressed on many tumor types, such as multiple myeloma, some lymphomas, melanoma, NSC lung, pancreatic, gastric, and renal cancers[102, 115, 130, 133, 181, 191, 200, 202], but is sometimes expressed in lower amounts on breast tumors[38, 147]. CD54 expression has further been related to tumor metastasis and/or poor prognosis in some cancers [25, 102, 115, 125, 130].

Soluble CD54.

In addition to the traditional membrane-bound form of CD54, the expression and secretion of a soluble form of CD54 (sCD54) has been reported. sCD54 consists of the extracellular domains of CD54 and is present in circulation both as monomers and as complexes consisting of

two or more monomers. sCD54 is known to be expressed by mononuclear cells, endothelial cells, keratinocytes, hepatocytes, and some tumor cells, but the regulation of its expression is not yet well understood. The amount of sCD54 in circulation does not necessarily correlate with the expression of membrane-bound CD54, probably because sCD54 is produced both through alternative splicing and through membrane shedding *via* proteolytic cleavage[205, 212].

sCD54 induces angiogenesis, the formation of new blood vessels from pre-existing ones, and has been implicated in the pathology of a number of diseases, including cancer, rheumatoid arthritis, cardiovascular disease, some neurological disorders, and viral infections[212]. The expression of sCD54 has also been associated with the pathology of several cancers, including lymphoma, breast, prostate, renal and NSC lung cancers[23, 31, 85, 121, 128, 190, 200]. Although the mechanisms through which sCD54 mediates its effects are not well known, sCD54 is able to compete with membrane-bound CD54 for ligand binding[212].

E. Investigations into the Mechanisms of Action of UV3.

Although it is not essential to understand UV3's mechanisms of action in order to appreciate its anti-tumor activity, understanding its mechanisms of action might better predict the therapeutic outcome of UV3 in patients. How a MAb mediates its activity determines the tumor types in which it is effective, the adverse effects most likely to be problematic, and the other anti-tumor agents that would be best in combination therapies. Therefore, potential mechanisms of action for UV3 were investigated in multiple myeloma.

Since CD54 primarily functions as an adhesion molecule, several potential mechanisms of action of UV3 related to this function were examined in multiple myeloma cells. However, UV3 did not interfere with homotypic tumor cell adhesion or with the adhesion of tumor cells to murine stromal cells *in vitro*[96]. Other studies have demonstrated a role for CD54 in post-homing events in metastatic lymphoma, although the mechanism is not well understood[25, 118].

Most MAbs mediate their activity at least in part through Fc-dependent effector functions. Therefore, the involvement of ADCC and CDC were investigated. *In vitro*, UV3 mediated both ADCC and CDC of the ARH-77 and KM-3 myeloma cell lines, indicating a role for Fc effector

functions[96, 187]. However, initial experiments indicated that $F(ab')_2$ fragments of UV3, which lack the Fc portion of the antibody, still had potent anti-tumor activity in SCID mice xenografted with human multiple myeloma cell lines[96]. It was later discovered that part of this activity was due to the presence of minute amounts of contaminating IgG, and "ultrapure" $F(ab')_2$ fragments later demonstrated no anti-tumor activity in this model. Together these data indicate that the Fc effector mechanisms ADCC and CDC are essential to the activity of UV3 in multiple myeloma[52].

Fc-independent signaling mechanisms were further investigated for UV3 in multiple myeloma. It was found that UV3 did not directly induce apoptosis or cell cycle arrest of multiple myeloma cell lines *in vitro*[96]. However, although other signaling mechanisms have been suggested by studies using UV3 or an anti-murine CD54 MAb, the pathways are difficult to identify[52, 89]. Due to the involvement of CD54 in adhesion and inflammation, processes related to angiogenesis[205], and the ability of sCD54 to induce angiogenesis[212], attention focused on the potential of UV3 to prevent tumor growth by inhibiting tumor angiogenesis. The development of new blood vessels through the process of angiogenesis is critical to tumor expansion in order to provide tumor cells with the oxygen and nutrients they need to grow and divide. By inhibiting tumor

angiogenesis, the tumor cells starve and die[110]. The effect of UV3 on the secretion of several angiogenic factors *in vitro* was examined by gene array, quantitative PCR, ELISA, and the migration and invasion of human endothelial cells. Although UV3 treatment down-regulated the secretion of some pro-angiogenic cytokines by ARH-77 human myeloma cells, many factors were unaffected. Also, UV3 did not affect the migration or invasion of human endothelial cells responding to angiogenic factors secreted by ARH-77 cells into the serum. Together, these data were inconclusive on the effect of UV3 treatment on tumor angiogenesis[51].

Despite these investigations, the mechanisms of UV3 in multiple myeloma are not well understood. In addition, the mechanisms of action for UV3 may be different in other tumors since the tumor biology can vary greatly according to the tumor cell type.

F. Study Objectives.

The goal of this study was to evaluate the anti-tumor activity of UV3 in a variety of human tumor cell lines in order to identify cancers appropriate for treatment. The specific objectives of this study were: 1) to examine a panel of human tumor cell lines for the expression of CD54, 2) to establish xenograft models of selected CD54+ human tumor cell lines in SCID mice, 3) to evaluate the anti-tumor activity of UV3 in those xenograft models, 4) to confirm the specificity of UV3 therapy *in vivo*, 5) to compare the anti-tumor activity of murine UV3 and cUV3, 6) to evaluate the benefit of combining UV3 with chemotherapy *in vivo*, 7) to determine whether UV3 inhibited the proliferation of CD54+ tumor cells *in vitro*, and 8) to investigate the contribution of ADCC and CDC Fc-dependent effector mechanisms to the activity of UV3 *in vitro* and *in vivo* among a variety of tumor types.

Chapter 2: Materials and Methods

A. Culture of Human Tumor Cell Lines.

Established human tumor cell lines were cultured at 37°C in 5% CO_2/95% air in complete culture medium consisting of fetal bovine serum (FBS; Hyclone, Logan, UT) heat-inactivated at 52°C for 30 minutes and other medium components (Gibco-Invitrogen, Carlsbad, CA), as described in **Table 1**. Tumor cell lines grown in suspension were maintained at 5 x 10^5 cells/mL. Adherent cell lines were cultured to 70% confluency. The flask was then rinsed with sterile, serum-free medium and incubated with 5 mL of warm trypsin- ethylene diamine tetraacetic acid (EDTA) solution (Gibco-Invitrogen) at 37°C until the cells detached, no more than 5 minutes. Following cell detachment, 10 mL of complete culture medium was added to each flask to neutralize the trypsin solution. The cell suspension was centrifuged at 300 x g for 10 minutes in a refrigerated Sorvall RC3B centrifuge at 4°C (DuPont, Wilmington, DE). The cell pellet was re-suspended in a few milliliters of appropriate complete medium and either used in assays or placed inside a clean flask for continued culture.

For freezing, cells were washed in complete culture medium, and then re-suspended in a solution of 10% dimethyl sulphoxide (DMSO;

Sigma-Aldrich, St. Louis, MO) and 90 % FBS to a concentration of 1 x 10^7 cells/mL. Aliquots of 1 mL were frozen in cryovials (Corning Inc., Corning, NJ) and stored in a Harris Cryostar -140°C freezer (Kendro Laboratory Products, Asheville, NC).

Table 1. Cell Lines, Sources, and Media.

Cancer Type	Cell Line	Ref.	Complete Culture Media	Source
Breast Cancer	BT-474	[119]	Minimal essential media 2 mM L-glutamine 10 mM HEPES buffer 1 mM sodium pyruvate 1X MEM non-essential amino acids 1X MEM vitamins solution 100 U/mL penicillin 0.1 mg/mL streptomycin 10% FBS	American Type Culture Collection, HTB-20
	MCF-7	[188]	Minimal essential media 2 mM L-glutamine 100 U/mL penicillin 0.1 mg/mL streptomycin 10% FBS	American Type Culture Collection, HTB-22
	MDA-MB-231	[39]	Minimal essential media 2 mM L-glutamine 100 U/mL penicillin 0.1 mg/mL streptomycin 10% FBS	Dr. Janet Price, MD Anderson Cancer Center, Houston, TX
	MDA-MB-435	[39]	Minimal essential media 2 mM L-glutamine 100 U/mL penicillin 0.1 mg/mL streptomycin 10% FBS	Dr. Janet Price, MD Anderson Cancer Center, Houston, TX
Lung Cancer (Non-Small Cell)	HCC-78		RPMI-1640 media 2 mM L-glutamine 100 U/mL penicillin 0.1 mg/mL streptomycin 7% FBS	Dr. John Minna, UT Southwestern Medical Center, Dallas, TX
	HCC-827		RPMI-1640 media 2 mM L-glutamine 100 U/mL penicillin 0.1 mg/mL streptomycin 7% FBS	Dr. John Minna, UT Southwestern Medical Center, Dallas, TX

Cancer Type	Cell Line	Ref.	Complete Culture Media	Source
Lung Cancer (Non-Small Cell)	NCI-H157	[44, 45]	RPMI-1640 media 2 mM L-glutamine 100 U/mL penicillin 0.1 mg/mL streptomycin 5% FBS	Dr. John Minna, UT Southwestern Medical Center, Dallas, TX
	NCI-H1993	[148, 154]	RPMI-1640 media 2 mM L-glutamine 100 U/mL penicillin 0.1 mg/mL streptomycin 7% FBS	Dr. John Minna, UT Southwestern Medical Center, Dallas, TX
	NCI-H2347	[148, 154]	RPMI-1640 media 2 mM L-glutamine 100 U/mL penicillin 0.1 mg/mL streptomycin 7% FBS	Dr. John Minna, UT Southwestern Medical Center, Dallas, TX
Lymphoma (Non-Hodgkin's B cell)	Daudi	[112]	RPMI-1640 media 2 mM L-glutamine 100 U/mL penicillin 0.1 mg/mL streptomycin 5% FBS	American Type Culture Collection, CCL-213
	DHL-4		RPMI-1640 media 2 mM L-glutamine 100 U/mL penicillin 0.1 mg/mL streptomycin 10% FBS	Dr. Ronald Levy, Stanford University School of Medicine, Stanford, CA
	Nalm-6		RPMI-1640 media 2 mM L-glutamine 100 U/mL penicillin 0.1 mg/mL streptomycin 10% FBS	Dr. Graham Smith, UT Southwestern Medical Center, Dallas, TX
	Ramos	[144]	RPMI-1640 media 2 mM L-glutamine 100 U/mL penicillin 0.1 mg/mL streptomycin 10% FBS	American Type Culture Collection, CRL-1596

Cancer Type	Cell Line	Ref.	Complete Culture Media	Source
Melanoma	397		RPMI-1640 media 2 mM L-glutamine 100 U/mL penicillin 0.1 mg/mL streptomycin 7% FBS	Dr. Michael Nishimura, Medical University of South Carolina, Charleston, SC
	501		RPMI-1640 media 2 mM L-glutamine 100 U/mL penicillin 0.1 mg/mL streptomycin 7% FBS	Dr. Michael Nishimura, Medical University of South Carolina, Charleston, SC
	586		RPMI-1640 media 2 mM L-glutamine 100 U/mL penicillin 0.1 mg/mL streptomycin 7% FBS	Dr. Michael Nishimura, Medical University of South Carolina, Charleston, SC
	624		RPMI-1640 media 2 mM L-glutamine 100 U/mL penicillin 0.1 mg/mL streptomycin 7% FBS	Dr. Michael Nishimura, Medical University of South Carolina, Charleston, SC
	1088		RPMI-1640 media 2 mM L-glutamine 100 U/mL penicillin 0.1 mg/mL streptomycin 7% FBS	Dr. Michael Nishimura, Medical University of South Carolina, Charleston, SC
	1278		RPMI-1640 media 2 mM L-glutamine 100 U/mL penicillin 0.1 mg/mL streptomycin 7% FBS	Dr. Michael Nishimura, Medical University of South Carolina, Charleston, SC
Melanoma (Uveal)	MEL-290	[157]	RPMI-1640 media 2 mM L-glutamine 10 mM HEPES buffer 1 mM sodium pyruvate 100 U/mL penicillin 0.1 mg/mL streptomycin 10% FBS	Dr. B. Ksander, Schepens Eye Research Institute, Boston, MA

Cancer Type	Cell Line	Ref.	Complete Culture Media	Source
Melanoma (Uveal)	OCM-3	[93]	RPMI-1640 media 2 mM L-glutamine 10 mM HEPES buffer 1 mM sodium pyruvate 1X MEM non-essential amino acids 1X MEM vitamins solution 100 U/mL penicillin 0.1 mg/mL streptomycin 10% FBS	Dr. J. Kan-Mitchell, University of California, San Diego, CA
Multiple Myloma	KM3	[175]	RPMI-1640 media 2 mM L-glutamine 100 U/mL penicillin 0.1 mg/mL streptomycin 10% FBS	American Type Culture Collection,
Pancreatic Cancer	BxPC-3	[201]	RPMI-1640 media 2 mM L-glutamine 10 mM HEPES buffer 1 mM sodium pyruvate 1X MEM non-essential amino acids 1X MEM vitamins solution 100 U/mL penicillin 0.1 mg/mL streptomycin 10% FBS	American Type Culture Collection, CRL-1687
	PANC-1	[124]	Dulbecco's modified Eagle media 2 mM L-glutamine 100 U/mL penicillin 0.1 mg/mL streptomycin 10% FBS	American Type Culture Collection, CRL-1469
Prostate Cancer	1532-CP2TX	[37]	Minimal essential media 2 mM L-glutamine 100 U/mL penicillin 0.1 mg/mL streptomycin 10% FBS	Dr. Suzanne Topalian, NIH/NCI, Bethesda, MD
	1542-CP3TX	[37]	Minimal essential media 2 mM L-glutamine 100 U/mL penicillin 0.1 mg/mL streptomycin 10% FBS	Dr. Suzanne Topalian, NIH/NCI, Bethesda, MD

Cancer Type	Cell Line	Ref.	Complete Culture Media	Source
Prostate Cancer	DU-145	[197]	Minimal essential media 2 mM L-glutamine 100 U/mL penicillin 0.1 mg/mL streptomycin 10% FBS	Dr. Niel Bander, Weill Cornell Medical College, New York, NY
	LNCaP	[90]	RPMI-1640 media 2 mM L-glutamine 10 mM HEPES buffer 1 mM sodium pyruvate 100 U/mL penicillin 0.1 mg/mL streptomycin 10% FBS	Dr. Owen Witte, HHMI/UCLA, Los Angeles, CA
	PC-3	[103]	Minimal essential media 2 mM L-glutamine 10 mM HEPES buffer 100 U/mL penicillin 0.1 mg/mL streptomycin 10% FBS	Dr. Niel Bander, Weill Cornell Medical College, New York, NY

B. Production and Purification of Antibody.

Production of UV3.

UV3 hybridoma cells were produced in our laboratory by fusing Sp2/0 mouse multiple myeloma cells with antibody-secreting splenocytes isolated from BALB/c mice that had been immunized with alternating monthly injections of two human multiple myeloma cell lines (RPMI-8226 and U-266)[94].

UV3 antibody was produced and purified as described previously[94]. The hybridoma cells were cultured in complete Dulbecco's modified Eagle medium (DMEM; Gibco-Invitrogen) with 7% FBS at approximately 5 x 10^6 cells/mL in a 37°C, 5% CO_2/95% air incubator. The hybridoma cells were maintained in culture for no more than two months before use. Two-liter capacity roller bottles (BD Falcon, Bedford, MA and Corning) were set up with 50 mL of stable hybridoma cell suspension and 450 mL of complete DMEM media. The roller bottles were gassed overnight with loose caps at 37°C, 5% CO_2/95% air, then the roller bottles were tightly capped and moved to a roller cabinet (Bellco Biotechnology, Vineland, NJ) at 1 rpm, 37°C for seven days.

Purification of UV3.

When the viability of the hybidoma cells was decreased to 70% (approximately 7 days), the cell suspension was centrifuged at 4°C, 1850 x g for 30 minutes to separate the hybridoma cells from the supernatant containing the antibody. Sodium azide (Sigma-Aldrich) in phosphate buffered saline, pH 7.4 (PBS) [from 10X stock: 175.3 g NaCl, 21 g Na_2HPO_4, 6.4 g NaH_2PO_4 , brought up to 2 L in deionized H_2O] was added to the hybridoma supernatant at a final concentration of 0.01% to prevent growth of contaminants, and the supernatant was then stored at 4°C until purified.

Hybridoma supernatant was filtered though an empty 2.5 cm x 10 cm chromatography column (BioRad, Hercules, CA) to remove any remaining cells or debris. The filtered supernatant was then run through a similar column containing 25 mL of protein-G sepharose (Amersham Biosciences, Piscataway, NJ) at 4°C at a rate of 3 mL/minute. The column flow through was collected and run over a second protein G column, again at 3 mL/minute at 4°C at a later time. Approximately 10 L of hybridoma supernatant were passed over each 25 mL column. Once loaded with antibody from 10 L of supernatant, the column was washed with 300 mL of filtered PBS. The antibody was then eluted with filtered 1.0 M glycine-HCl, pH 2.8 (Sigma-Aldrich) until all antibodies had been eluted. The eluate

was collected in 3 mL fractions in 12 x 75 mm borosilicate glass tubes (Kimble Glass Inc., Vineland, NJ) filled with 0.5 mL of 1.0 M Tris-HCl, pH 8.0 (Sigma-Aldrich) to neutralize the acidity of the antibody solution. A fraction collector was connected to a recorder and ultraviolet sensor (LKB Bromma, Bromma, Sweden) used to monitor antibody elution. Based on the recorder chart, selected fractions were further analyzed by measuring their absorbance in a separate Beckman-Coulter DU-640 spectrophotometer (Fullerton, CA), and elution was stopped when the OD_{280} was less than 0.05. Fractions with an OD_{280} absorbance reading greater than 0.05 were pooled, and the antibody solution was adjusted to pH 7.4 with 1.0 M Tris-HCl, pH 8.0 and stored at 4°C, if necessary.

UV3 was dialyzed against a ten-fold volume of PBS for at least 20 hours at 4°C in regenerated cellulose tubing with pores for a 12-14000 Da molecular weight cut off (Spectrum Laboratories Inc., Rancho Dominguez, CA). Three changes to fresh PBS were made during the dialysis time. The antibody was concentrated using an Amicon Ultra 30,000 Da molecular weight cut off centrifugal filter device (Millipore, Bedford, MA), sterile filtered through a 150 mL, 0.22 µm Stericup filter (Millipore), and evaluated for concentration. Aliquoted antibody was stored at -20°C.

Electrophoresis on PhastGels.

The purity of antibody was analyzed by gel electrophoresis using the PhastGel system (Amersham Biosciences). Antibody samples (≥ 5 mg/mL) were combined 1:1 with either reducing buffer [1.25 mL 1.0 M Tris-HCl at pH 6.8, 4 mL 10% sodium dodecyl sulfate (SDS), 1 mL 2-mercaptoethanol, 2 mL glycerol, 1.25 mL distilled water, 0.5 mL 0.1% Bromophenol Blue] or non-reducing buffer [reducing buffer without 2-mercaptoethanol], and the samples were then placed in a heat block (Lab-Line Instruments, Dubuque, IA) at 100°C for 3 minutes. Sample (3 µL) was loaded by capillary action into the teeth of the loading comb and transferred to the comb slot in the gel holder. Samples were electrophoresed on a continuous 4-15% gradient PhastGel (Amersham Biosciences) with SDS buffer strips (Amersham Biosciences) inside the separation unit for approximately 30 minutes, until the voltage reached 65V. The gel was then stained by Commassie Blue [50% prepared Blue R dye (Amersham Biosciences) and 10% acetic acid] and de-stained with a solution of 10% acetic acid and 30% methanol in distilled water according to set developer programming (5 minutes, 8 minutes, and 10 minute washes).

Production of cUV3.

UV3 has previously been chimerized (cUV3) by Dr. Joan Smallshaw (University of Texas Southwestern Medical Center (UTSW), Dallas, TX) [187]. In brief, the sequences of the heavy and light variable domains of the murine UV3 antibody were inserted into human γ1 heavy and κ light chain expression vectors. The two constructs were then co-transfected into SP2/0 non-secreting murine myeloma cells. Ig-secreting cells were selected and subcloned. A master cell bank was generated and vials were sent to the National Cancer Institute. Under the aegis of the RAID program, cUV3 was then produced and purified by the Biological Resources Branch of the Division of Cancer Treatment and Diagnosis at the National Cancer Institute.

Isotype Control Antibodies.

13G10 hybridoma cells, which secrete a murine IgG2a antibody against the bacterium *Treponema pallidum*, were a gift from Dr. M. Norgard (UTSW Medical Center, Dallas, TX) [160]. IgG2a-secreting RPC-5.4 myeloma cells were purchased from the American Type Culture Collection (ATCC; TIB-12) [139]. Antibody from both cell lines was produced and purified as described above for UV3 antibody. The UPC-10 murine IgG2a kappa antibody was purchased from Sigma-Aldrich.

FITC-Goat Anti-Mouse IgG Antibody.

Goat anti-mouse IgG was purified from hybridoma cells as described above for UV3 antibody. Purified antibody was dialyzed overnight at 4°C against 0.1 M carbonate-bicarbonate buffer at pH 9.0. An OD_{280} was obtained to determine the total amount of antibody protein. Fluorescein-isothiocyanate (FITC; Pierce Biotechnology Inc., Rockford, IL) in carbonate-bicarbonate buffer was added at 20% the total mass of goat anti-mouse IgG protein (2 to 5 mg/mL) and incubated in the dark at room temperature for 2 hours with periodic mixing. The sample was then run through a 25 cm chromatography column containing Sephadex G-25 (Amersham Biosciences) equilibrated in PBS. The column was eluted with PBS and the first yellow-tinted fraction was collected. The labeled antibody was analyzed for protein concentration [Concentration = $(OD_{280} – (0.3 \times OD_{495})) \div 1.4$] and for the ratio of fluorochrome to protein [F:P Ratio = $(OD_{495} \times 150{,}000) \div (\text{Concentration} \times 68{,}000)$] using a DU-640 spectrophotometer. The FITC-goat anti-mouse IgG antibody was further characterized by titration and flow cytometric analysis on Daudi lymphoma cells to determine an appropriate working dilution (see below).

C. Production and Purification of UV3 F(ab')2 Fragments.

Production of UV3 $F(ab')_2$ Fragments.

Purified $F(ab')_2$ fragments of UV3 were prepared as described [96, 151], with modifications. Previously produced and characterized UV3 antibody was dialyzed overnight at 4°C against acetate buffer, pH 3.7 [1760 mL 0.2 M acetic acid and 240 mL 0.2 M sodium acetate], until completely equilibrated. The dialyzed UV3 was collected in a 50 mL centrifuge tube.

The sample was read on a spectrophotometer to obtain an OD_{280} to determine the total amount of UV3 protein. Pepsin-agarose (Sigma-Aldrich) was added at 25% of the total mass of UV3 and incubated on a Labquake Shaker (Barnstead Int., Dubuque, IA) at 37°C for approximately 16 hours. The time of incubation was initially determined by collecting samples periodically over the first 24 hours, and then processing them to determine the time point at which maximum digestion into $F(ab')_2$ fragments, but not F(ab)' fragments, occurred. Following digestion, a 50 µL sample was collected, centrifuged at 10,000 rpm for 2 minutes, and then mixed with reducing or non-reducing buffers to run on a PhastGel to determine the purity of the $F(ab')_2$ fragments.

The digested UV3 (not the small samples collected for PhastGel analysis) was centrifuged at 2500 x g for 10 minutes at 4°C to remove the pepsin-agarose. The supernatant was collected and the pH of the sample was adjusted to 7.0-8.0 with 1.0 M Tris-HCl, pH 8.0 to stop the digestion reaction. The sample was then dialyzed overnight at 4°C against PBS.

Purification of UV3 $F(ab')_2$ Fragments.

The UV3 digest, at 100 mg or less, was then run through a 1 mL (100 mg packed volume) HiTrap Protein-A column (Amersham Biosciences) at a rate of 1 mL/min to eliminate any remaining IgG. The column capacity was 20 mg of IgG. The flow through, which contained the $F(ab')_2$ fragments, was collected. The column was washed with 10 mL of PBS, and the first 5 mL of column wash was combined with the column flow through and stored at 4°C. A sample (≥ 5 mg/mL) was electrophoresed on a PhastGel to ensure all of the IgG had been removed from the $F(ab')_2$ fragments (IgG less than 1% of the sample, which was the limit of detection on the gel). The remaining IgG, bound to the column, was eluted with 0.1 M glycine-HCl, pH 2.8 as 0.5 mL fractions in 12 x 75 mm borosilicate glass tubes filled with 0.1 mL of 1.0 M Tris-HCl, pH 8.0. An OD_{280} of the pooled eluate was determined to estimate the amount of undigested UV3 IgG.

The UV3 $F(ab')_2$ fragments were concentrated to 15-20 mg/mL using an Amicon Ultra centrifugal filter device with a 30,000 Da molecular weight cut off and filtered. A sample of no more than 10 mL was run over a high-performance liquid chromatography column (HPLC; LKB Bromma) at a flow rate of 5 mL/min to separate out any contaminating F(ab)' fragments. Fractions in a volume of 3 mL were collected in 12 x 75 mm borosilicate glass tubes. OD_{280} values were determined using a Beckman-640 spectrophotometer for fractions corresponding to recorded protein peaks. Samples were electrophoresed on a PhastGel to identify tubes containing high amounts of $F(ab')_2$ fragments and minimal amounts of F(ab)' fragments. These fractions were pooled and concentrated using an Amicon Ultra 30,000 Da molecular weight cut off centrifugal filter device. A small sample was concentrated to over 10 mg/mL and electrophoresed on a PhastGel, which was subsequently subjected to densitometric analysis (LKB UltraScan XL, Pharmacia/Pfizer, New York, NY) to detect trace amounts of IgG and F(ab)' fragments in the sample. GelScan-XL (Pharmacia/Pfizer) was used to calculate the area under the peaks corresponding to the number and size of the bands in the gel. The calculated area values represented relative amounts of UV3 IgG, $F(ab')_2$, and F(ab)'. UV3 $F(ab')_2$ fragments were considered to be ultra pure when the F(ab)' fragments constituted no more than 5% of the total sample and

IgG constituted no more than 1% of the sample. The final sample of UV3 $F(ab')_2$ fragments was sterile filtered, aliquoted, and stored at -20°C. The binding ability of $F(ab')_2$ fragments was examined through flow cytometry of FITC-labeled fragments bound to ARH-77 myeloma cells and was found to be identical to the binding of the IgG[51].

D. Cell Surface Staining and Flow Cytometry.

Cell Surface Staining of Tumor Cell Lines.

Human tumor cell lines were washed twice in cold PBS, and then diluted to 1 x 10^6 cells/mL in PBS after the last wash. For each condition to be investigated, 1 mL of cell suspension in PBS was pipetted into a separate 12 x 75 mm polystyrene tube (BD Falcon). The tubes were centrifuged at 300 x g for 5 minutes at 4°C, and the supernatant was removed by aspiration. The tubes were vortexed to re-suspend the pellet in 1 mL of cold PBS. Antibody was diluted to 0.2 mg/mL, and serial 1:2 dilutions were then prepared. Each tube then received 5 µL of primary antibody (UV3 or control antibodies), to give a 1:200 dilution. The cells were incubated with primary antibody at 4°C for 30 minutes.

Following the incubation period, the cells were washed twice in cold PBS as described, leaving 100 µL of supernatant in which to re-suspend the cells. FITC-labeled goat-anti mouse IgG secondary antibody was added at an appropriate concentration, as determined previously by titration, and the samples were mixed. The cells were again incubated for 30 minutes at 4°C in the dark. After the incubation, the cells were again washed twice in cold PBS as described. The supernatant was removed, and 200 µL of 1% paraformaldehyde (Sigma-Aldrich) was added to each

tube to fix the cells for storage until analysis. The tubes were mixed well, capped, and stored for no more than one week at 4°C in the dark.

Data were acquired using a FACScan (BD Biosciences, Bedford, MA) and analyzed using CellQuest software (BD Biosciences). Only live cells were analyzed, and the positive cut-off line for the FITC channel was set so that no more than 5% of the negative control cells were considered positive.

Cell Surface Staining of Fresh Xenografted Tumor Tissue.

For staining of fresh tumor samples, human tumors grown subcutaneously in SCID mice were excised and placed in cold PBS containing 2 mM EDTA and 2% FBS (PBS/EDTA/FBS) on ice. The tumors were cut into sections, and a single cell suspension was prepared by gently mashing tissue pieces inside a 100 μm cell strainer (BD Falcon) with the plunger of a sterile 10 mL syringe. The cells were washed through the strainer with cold PBS/EDTA/FBS. The cell suspension was centrifuged at 300 x g for 8 minutes at 4°C. The supernatant was discarded and the cells were re-suspended in 6 mL of M-lyse buffer from the Mouse Erythrocyte Lysing Kit (R & D Systems, Minneapolis, MN). The cell suspension was incubated for 10 minutes on ice. At the end of the incubation, the volume was diluted to approximately 35 mL with

PBS/EDTA/FBS to stop the lysis reaction, and the cells were then centrifuged at 300 x g for 8 minutes at 4°C. The supernatant was discarded and the cells were re-suspended in approximately 30 mL of PBS/EDTA/FCS. The cell suspension was passed first through a 100 μm cell strainer and then through a 40 μm cell strainer (BD Falcon) to remove any cell debris present in the suspension.

The cells were counted and distributed into 12 x 75 mm polystyrene tubes at 1 x 10^6 cells per tube. The tubes were centrifuged at 300 x g for 5 minutes at 4°C, and the supernatant was removed by aspiration. The cell pellet was re-suspended in 1 mL of cold PBS/EDTA/FBS, and 5 μL of primary antibody (UV3 or control antibodies) at 0.2 mg/mL were added to each tube, to achieve a 1:200 dilution. The cells were incubated with primary antibody at 4°C for 30 minutes. Following the incubation period, the cells were washed twice in cold PBS/EDTA/FBS as described, leaving 100 μL of supernatant in which to re-suspend the cells. FITC-labeled goat-anti mouse IgG secondary antibody was added at a concentration previously determined to be optimal by titration, and the samples were mixed. The cells were incubated for 30 minutes at 4°C in the dark. After the incubation, the cells were again washed twice in cold PBS as described. After the last wash following secondary antibody incubation,

the cells were re-suspended in 400 µL of PBS/EDTA/FBS containing a 1:1000 dilution of propidium iodide (Sigma-Aldrich).

Data were acquired immediately using a FACSCalibur (BD Biosciences) and then analyzed using FlowJo 8.5 Software (Tree Star, Inc., Stanford, CA). For analysis, live cells were identified either by size on forward and side scatter plots, or as negative for propidium iodide stain. The positive cut-off line for the FITC channel was then set so that no more than 5% of the negative control cells were considered positive.

E. Cell Proliferation.

Incorporation of ^{3}H-Thymidine.

Cultured tumor cell lines were centrifuged for 10 minutes at 300 x g at 4°C, then washed in fresh culture medium and centrifuged again. The cells were counted using trypan blue exclusion, and the cells were diluted to a concentration that would be 80% confluent in the well of a 96-well culture plate 72 hours later, as previously determined. Each well of a sterile, flat-bottomed 96-well culture plate (Corning), received 100 µL of cell suspension, with all treatment groups plated in triplicate. The plate was incubated at 37°C, 5% CO_2/95% air for 4 hours to allow for attachment of adherent cells.

UV3 and negative control antibodies were dialyzed in serum-free medium. Dialyzed antibody at 2 mg/mL or sodium azide at 10 mg/mL in serum-free medium (positive control) were added to each well in a volume of 100 µL, bringing the total volume to 200 µL. The plate was covered and placed in an incubator at 37°C, 5% CO_2/95% air for 24, 48, or 72 hours. Six hours prior to the end of plate incubation, the plate was removed and 10 µL of 1 mCi/mL ^{3}H-thymidine (Amersham Biosciences) diluted 1:10 in complete culture medium was added to each well. The plate was returned to the incubator for the remaining 6 hours, and then the cells were

collected onto FilterMAT harvester paper (Skatron Instruments, Sterling, VA) using a cell harvester (Skatron Instruments). For adherent cells, the liquid contents of the wells were harvested first, and then the plate was incubated with trypsin-EDTA solution for 10 minutes at 37°C and harvested a second time. The filter paper was air dried and the perforated circles on the filter paper were placed into individual scintillation vials (Research Products International Corp., Mount Prospect, IL). If a double harvest was carried out for adherent cells, both pieces of filter paper associated with each well were placed in the same scintillation vial. CytoScint scintillation fluid (MP Biomedicals, Solon, OH) was added to each vial in a volume of 2 mL and allowed to saturate the filter paper for about 30 minutes. The radioactivity in the vials was determined using a Wallac 1410 beta counter (Turku, Finland) set to measure single counts of 0.1 minute. Radioactivity in counts per minute (CPM) of the triplicate wells for each treatment group were averaged and represented as proliferation relative to that of untreated cells.

Cellular Metabolism of a Tetrazolium Compound.

Human tumor cell lines were centrifuged for 10 minutes at 300 x g at 4°C. The cell pellet was re-suspended in a small amount of appropriate complete culture medium, and a cell count and viability were obtained by

trypan blue exclusion. The cells were then diluted to a concentration that would give 80% confluency 72 hours later.

Each well of a sterile, flat-bottomed 96-well culture plate received 100 μL of cell suspension, and the culture plate was incubated at 37°C, 5% CO_2/95% air for 4 hours to allow the adherent tumor cells to attach. The test and control agents at 2X the desired final concentrations were added in quadruplicate to the appropriate wells in a volume of 100 μL. The plate was then covered, wrapped with plastic, and incubated at 37°C, 5% CO_2/95% air for 72 hours.

After 72 hours, 20μl of CellTiter 96 AQueous One solution (Promega, Madison, WI) was added to each well using a multi-channel pipette to create a more consistent initiation time point. The plate was tapped lightly to mix the contents of the wells and returned to the incubator for another 4 hours. The AQueous One reagent contains a tetrazolium compound and an electron coupling agent, which helped to facilitate metabolism of the tetrazolium compound to a formazan product in healthy cells. The production of formazan product was measured colorimetrically, and these measurements corresponded to the relative number of viable cells present. Data were obtained by scanning the plate with a Tecan Spectafluor Plus plate reader (Maennedorf, Switzerland) set at a wavelength of 492 nm. The data was analyzed with Magellan 2 software

(Tecan). The four individual counts for each experimental condition were averaged and the amount of proliferation was presented as proliferation relative to that of untreated cells. The concentration of gemcitabine at which tumor cell proliferation was reduced by 50% (IC_{50}) was determined by plotting concentration against relative proliferation.

F. Antibody-Dependent Cellular Cytotoxicity (ADCC).

Isolation and Activation of Splenocytes.

Two female 10-14 week-old BALB/c mice (Taconic Farms, Germantown, NY) were sacrificed by CO_2 asphyxiation according to UTSW institutional policy. The spleens were removed and placed into 30 mL of sterile Hank's balanced salt solution (HBSS; Sigma-Aldrich). The spleens were sliced into sections using sterile procedure and homogenized between two frosted glass slides. The cell suspension was passed through a sterile 70 μm cell strainer to remove tissue debris and then centrifuged at room temperature at 200 x g for 10 minutes. The supernatant was discarded, and the cell pellet was re-suspended in 4 mL of M-lyse buffer and incubated at room temperature for 10 minutes. The lysis reaction was stopped with 25 mL of PBS containing 2% FBS, and the cells were centrifuged at 200 x g for 10 minutes at room temperature. The cells were re-suspended in DMEM with 2 mM L-glutamine, 10 mM HEPES buffer, 1 mM sodium pyruvate, 1X non-essential amino acids solution, 1X vitamins solution, 100 U/mL penicillin, 0.1 mg/mL streptomycin, and 10% FBS to a concentration of 3×10^6 cells/mL. 25 mL of the cell suspension was removed to a clean tube, and 100 μL of a 20,000 IU/mL stock of recombinant IL-2 (Chemicon, Temecula, CA), 125 μL of diluted 2-

mercaptoethanol (Sigma-Aldrich) [4.41 µL of 12.7 M 2-mercaptoethanol diluted in 10 mL of complete DMEM], and 12.5 µL of a 1 mg/mL stock of crystalline indomethacin (Sigma-Aldrich) in 100% ethanol. The cell suspension was mixed and transferred at 2 mL/well to a 24-well culture plate (Corning). The plate was incubated at 37°C, 10% CO_2/90% air for 5 days.

Preparation of Target Cells.

Tumor cells in culture were centrifuged at 300 x g for 10 minutes at 4˚C. The supernatant was discarded, the cell pellet was re-suspended in complete culture medium, and the percentage of viable cells was determined by trypan blue exclusion. The cells were centrifuged as before and re-suspended in complete culture medium to a concentration of 1 x 10^7 cells/mL. A cell suspension volume of 500 µL was combined with 100-150 µL ^{51}Chromium stock (1 mCi/mL; Amersham Biosciences) and incubated for 1 hour at 37˚C in the dark with mixing every 15 minutes to enhance labeling. After an hour, the cells were washed in complete medium, and the supernatant was discarded. The cell pellet was re-suspended in 3 mL of complete medium and incubated again at 37˚C for 30 minutes in the dark with mixing after 15 minutes. The cells were washed twice in complete medium as described.

The cell pellet was re-suspended in 400 µL of serum-free culture medium, and 100 µL of cell suspension was transferred to each of four tubes. Three of the tubes received 5 µg of UV3 or control antibodies; the fourth tube was left untreated. The cells were incubated in the dark on ice for 30 minutes with mixing after 15 minutes. The cells were washed twice in serum-free media. After the last wash, the cell pellets were re-suspended in complete culture media to a final concentration of 5×10^4 cells/mL.

^{51}Chromium-Release Assay.

The activated splenocytes (effector cells) were collected into a cell suspension and centrifuged at 300 x g for 10 minutes at 4˚C. The cells were washed twice in complete culture medium, and the cell pellet was re-suspended in 5 mL of complete medium for a viable cell count determined by trypan blue exclusion. The cell suspension was brought to a final concentration of 5×10^6 cells/mL in complete culture medium. This concentration of cells was used for an effector cell to target cell ratio (E:T) of 100:1, and the suspension was further diluted for the smaller E:T ratios of 50:1 (2.5×10^6 cells/mL) and 10:1 (5×10^5 cells/mL).

5×10^3 of ^{51}Chromium- and antibody-labeled target cells were added in triplicate in a volume of 100 µL to each appropriate well in a

sterile 96-well culture plate. 100 µL of effector cell suspension at desired concentrations were added to appropriate wells, bringing the total volume to 200 µL. The amount of spontaneous ^{51}Chromium release was determined from wells containing target cells in 200 µL of complete culture medium. Maximal ^{51}Chromium release was determined in wells containing 100 µL of prepared target cells and 100 µL of 2% Triton X-100 (Sigma-Aldrich). The plate was incubated for 4 hours at 37°C, 5% CO_2/95% air.

After the incubation, the culture plates were centrifuged at 300 x g for 5 minutes at room temperature. One hundred microliters of supernatant were transferred from each well into a borosilicate glass 12 x 75 mm tube, and the amount of ^{51}Chromium released from the target cells was measured using a gamma counter (PerkinElmer, Waltham, MA). The percentage of specific target cell lysis by the effector cells in the presence of bound antibody was calculated using the formula:

$$\% \text{ specific lysis} = 100 \times \left(\frac{\text{experimental } ^{51}\text{Cr released} - \text{spontaneous } ^{51}\text{Cr released.}}{\text{maximum } ^{51}\text{Cr released} - \text{spontaneous } ^{51}\text{Cr released}} \right)$$

G. Complement-Dependent Cytotoxicity (CDC).

Preparation of Target Cells.

Target cells were prepared by labeling tumor cell lines with ^{51}Chromium and then incubating them with antibody, as described above.

^{51}Chromium-Release Assay.

The amount of tumor cell lysis by complement proteins in the presence of antibody was determined using a ^{51}Chromium-release assay similar to the one used for determining ADCC above. Target cells were added at 5 x 10^3 cells/well in a volume of 100 µL to triplicate wells of a sterile 96-well culture plate. Rabbit serum (Chemicon) was used as the source of complement. The rabbit serum was diluted into serum-free culture medium at 1:2.5, 1:5, and 1:12.5, and 100 µL of the desired diluted serum was added to the target cells, resulting in final well volumes of 200 µL and final serum dilutions of 1:5, 1:10, and 1:25. Spontaneous ^{51}Chromium release from target cells was determined without rabbit serum, and maximal ^{51}Chromium release was determined from target cells combined with 100 µL of 2% Triton X-100. The culture plate was incubated for 4 hours at 37°C, 5% CO_2/95% air. The plate was centrifuged for 5 minutes at 300 x g at room temperature, and 100 µL of supernatant

was harvested from each well. Tubes containing sample supernatants were analyzed in a gamma counter (PerkinElmer). The percentage of specific lysis of labeled target cells in the presence of complement was calculated using the formula:

$$\% \text{ specific lysis} = 100 \times \left(\frac{\text{experimental } {}^{51}\text{Cr released} - \text{spontaneous } {}^{51}\text{Cr released.}}{\text{maximum } {}^{51}\text{Cr released} - \text{spontaneous } {}^{51}\text{Cr released}} \right)$$

H. Determination of the LD_{50} of Gemcitabine in SCID Mice.

Female inbred CB.17 SCID mice, 6-8 weeks of age, were purchased from Taconic Farms (Germantown, NY) and acclimated for seven days in the UTSW animal facility. The mice were weighed twice on different days to establish baseline weights. The mice were separated into groups of four, and gemcitabine (Gemzar™; Eli Lily, Indianapolis, IN) was then administered in a single intraperitoneal injection (i.p.) at doses of 100 to 1000 mg/kg of mouse in 200 µL. The mice were weighed daily and sacrificed when they either lost 20% of their body weight or showed signs of ill health, including but not limited to weight loss, scratches/irritation marks, bite marks, poor leg movement, shaking/shivering, extended abdomens, and neurological/behavioral problems, such as habitual circular movement. The mice were followed for a minimum of two weeks after the administration of gemcitabine, which was enough time for the weights to return to their pre-treatment measurements for all mice receiving sub-lethal doses. The LD_{50} was defined by the dose at which half the mice were sacrificed.

I. Xenograft Tumor Models and Therapy.

SCID Mice.

For the xenograft experiments, inbred CB.17 severe combined immunodeficient mice (SCID) were purchased from Taconic Farms. Female mice were used in the xenograft experiments except in the prostate mouse model, where male inbred CB.17 SCID mice were used. All mice were housed in sterilized cages with filter tops in accordance with institutional animal care policy. Mice were allowed to stabilize in the facility for a minimum of seven days prior to handling. All protocols were approved by our institutional protocol review committee. The mice were 7-8 weeks of age at the time of tumor cell inoculation. Following tumor inoculation the mice were monitored for tumor development as well as any signs of ill health.

B Cell Non-Hodgkin's Lymphoma Models.

A disseminated model of human B cell NHL in SCID mice has previously been described [76-78]. For this model, SCID mice were weighed twice on separate days to establish a baseline weight. The mice were then injected intravenously (i.v.) in the lateral tail vein with 1×10^7 Daudi human NHL cells in sterile PBS in a volume of 100 µL. After tumor

inoculation the mice were weighed three times per week and checked daily for adverse signs of health. The tumor cells grew systemically and eventually infiltrated the spinal canal, resulting in hind-leg paralysis. The mice were sacrificed when they appeared in ill health, when they developed hind-leg paralysis, or when their weight dropped to 20% less than the established baseline.

A solid tumor model of NHL was generated by injecting 1×10^7 Daudi cells in 200 µL of sterile PBS subcutaneously (s.c.) into SCID mice. The mice were followed for the development of palpable tumors, and the tumors were measured 2-3 times each week using calipers. Tumor volume was calculated using the formula Volume = $W^2 \times L \div 2$, where L was the longest diameter and W was its perpendicular width. Mice were sacrificed when the tumors reached 2000 mm^3 or the mice appeared in ill health.

Antibody therapies for treatment of disseminated or solid tumors were administered i.v. or i.p., respectively, in a volume of 100 µL. For both models, therapy began one day after tumor cell inoculation and continued for four consecutive days. Mice received 0.8 mg/kg of mouse of UV3, cUV3, or isotype control antibody on each day, or they received 8 mg/kg of mouse of UV3 $F(ab')_2$ on each day. The $F(ab')_2$ fragments were given at a 10-fold higher dose than IgG to offset their faster clearance rate.

Breast Tumor Models.

Two solid tumor models of cultured human breast cancer cells in SCID mice were used, as previously described [48, 189]. SCID mice were irradiated with 150 rads of gamma irradiation using a Mark I Irradiator (J.L. Shepherd and Associates, San Fernando, CA). 24 hours later BT-474 cells (CD54-) or MDA-MB-435 cells (CD54+) were mixed 1:1 with ice cold matrigel (BD Biosciences), and injected s.c. in a volume of 200 µL into the pre-irradiated SCID mice at 5 x 10^6 cells per mouse. The growing tumors were measured using calipers as described above. When the tumors reached 100 to 200 mm^3, therapy was initiated by i.p. injection of UV3 or control antibody at a dose of either 0.3 mg or 0.75 mg in a 100 µL volume; $F(ab')_2$ fragments of UV3 were similarly administered at a dose of 1.5 mg. Injections were repeated once every 10 days for a total of four injections. The mice were sacrificed when the tumors reached 2000 mm^3 or if they appeared in ill health.

Prostate Tumor Model.

The prostate solid tumor model of cultured human PC-3 cells in male SCID mice has been described[143]. SCID mice were irradiated with 150 rads of gamma irradiation, and 24 hours later PC-3 cells in sterile PBS were injected s.c. into the pre-irradiated SCID mice at 5 x 10^6 cells

per mouse in a volume of 200 µL. The mice were followed for tumor formation, and the tumors were measured using calipers as described above. When the tumors reached 200 mm^3, therapy was initiated by i.p. injection of UV3 or control antibody at a dose of 0.3 mg in a volume of 100 µL; $F(ab')_2$ fragments of UV3 were similarly administered at a dose of 1.5 mg. Therapy injections were repeated once every 10 days for a total of four injections. The mice were sacrificed when the tumors reached 2000 mm^3 or if they appeared in ill health.

Non-Small Cell Lung Tumor Model.

NCI-H157 human NSC lung cancer cells in sterile PBS were injected s.c. into SCID mice at a dose of 1×10^6 cells in 200 µL per mouse to generate a solid tumor xenograft model. The mice were followed for the formation of palpable tumors, and developing tumors were measured 2-3 times per week using calipers. The volume of the tumors was calculated as described above. Therapy was initiated when the tumors reached 50 to 200 mm^3, as desired. UV3 or control antibodies in sterile PBS were administered i.p. in a volume of 100 µL at doses of 0.3, 0.75, or 1.5 mg per injection once a week for a total of four weeks, or at doses of 0.1, 0.25, or 0.5 mg per injection three times per week for a total of four weeks. $F(ab')_2$ fragments of UV3 were administered i.p. at a dose of 1.5 mg (and

compared to a dose of 0.3 mg IgG) in a volume of 100 µL once a week for no more than four weeks. Gemcitabine was administered i.p. in a volume of 100 µL at doses of 50, 100, 150, or 300 mg/kg mouse once a week for four weeks. Combination therapies were accomplished by separate i.p. injections of each agent. The mice were sacrificed when the tumors reached 2000 mm^3 or if they appeared in ill health.

Pancreatic Tumor Model.

BxPC-3 cells in sterile PBS were used to generate a solid tumor model of pancreatic cancer in SCID mice. The SCID mice were irradiated with 150 rads of gamma irradiation, then 24 hours later were injected s.c. with 1 x 10^6 cells in 100 µL of sterile PBS. The mice were followed for tumor formation, and the tumors were measured using calipers as described above. When the tumors reached 50 to 200 mm^3, therapy was initiated. UV3 or control antibodies in sterile PBS were administered i.p. in a volume of 100 µL at doses of 0.3, 0.75, or 1.5 mg per injection once every 10 days for a total of four injections, or at doses of 0.1, 0.25, or 0.5 mg per injection once every 3 days (3 injections per 10-day period) for a total of twelve injections. $F(ab')_2$ fragments of UV3 were administered i.p. in a volume of 100 µL at a dose of 1.5 mg (and compared to a dose of 0.3 mg IgG) once every 10 days for no more than four injections. The

chemotherapeutic drug gemcitabine was administered i.p. at doses of 50, 100, 150, or 300 mg/kg mouse in a volume of 100 µL once a week for four weeks. Combination therapies were accomplished by the administration of separate i.p. injections of the desired therapeutic doses of each agent. The mice were sacrificed when the tumors reached 2000 mm^3 or if they appeared in ill health.

Uveal Melanoma Models.

Two xenograft models of human uveal melanoma in SCID mice were developed as described previously[211]. For subcutaneous solid tumors, 6 to 8 week-old female SCID/beige mice (Taconic Farms) were injected s.c. with 1 x 10^7 cells of the OCM3 human uveal melanoma cell line in a volume of 200 µL. One day after tumor cell inoculation, therapy of UV3 or control antibody was initiated. The mice received 20 µg of antibody in 100 µL i.p. on each of four consecutive days. The mice were followed for tumor formation, and the tumors were measured twice a week using calipers. The mice were sacrificed when the tumors reached 2000 mm^3 or if they appeared in ill health.

UV3 was also tested in an orthotopic model of human uveal melanoma cells in mice in the laboratory of Dr. Jerry Niederkorn (UTSW) as described[211]. Briefly, 3 x 10^5 OCM3 cells were injected in a volume of

5 μL into the anterior chamber of anesthetized SCID/beige mice, and the mice were examined 3 times per week for the percentage of anterior chamber occupied by tumor. Therapy was begun either on the day of tumor inoculation or when the tumors reached a visible size. The mice received 20 μg of either UV3 or isotype control antibody or 100 μg of UV3 $F(ab')_2$ fragments subconjunctivally in a volume of 50 μL distributed across four injection sites 90° apart every other day for four injections (i.e. on days 0, 2, 4, and 6 post tumor cell inoculation).

J. Statistical Analysis.

Values for *in vitro* experiments were analyzed using a two-tailed t test comparing UV3-treated samples with isotype control-treated samples, unless otherwise noted. Samples were considered to be significantly different when $p < 0.05$. For *in vivo* therapy data, tumor growth curves were compared using the Wilcoxon matched-pairs signed-ranks test. Daily tumor measurements were also compared between therapy groups using a two-tailed t test. Growth curves were considered to be significantly different when $p < 0.05$ for the Wilcoxon test and $p < 0.05$ for the t test.

Chapter 3: Results

A. CD54 is Expressed on Many Human Tumor Cell Lines.

A panel of human tumor cell lines was examined for surface expression of CD54, the antigen recognized by UV3. The tumor cell lines chosen represented a variety of different cell types, including those of the immunologic, respiratory, gastrointestinal, and reproductive systems. In total, 28 cell lines were examined. The cell lines were incubated with UV3 or an isotype-matched control antibody, stained with FITC-labeled goat anti-mouse IgG, and analyzed by flow cytometry. The results are summarized in **Table 2.** With several exceptions, greater than 85% of the cells from each cell line expressed CD54 ($p < 0.001$) and fewer than 5% of the cells stained with the control antibody. Only a portion of MEL-290 uveal melanoma cells ($30.90 \pm 8.62\%$; $p < 0.001$) and MCF-7 breast cancer cells ($64.44 \pm 16.82\%$; $p < 0.001$) were $CD54^+$, indicating that cell lines were heterogeneous with respect to CD54 expression. The BT-474 breast cancer, NCI-H1993 NSC lung cancer, and LNCaP prostate cancer cell lines did not express CD54 ($p > 0.3$). These data demonstrate that CD54 is expressed on the surface of the majority, but not all, of the cell lines in the panel examined.

Table 2. CD54 is Expressed on Many Human Tumor Cell Lines.

Cancer Type	Cell Line	% of CD54$^+$ Cells	MFI
Breast Cancer	BT-474	4.69 ± 3.17	106.31 ± 45.12
	MCF-7	64.44 ± 16.82	127.10 ± 76.86
	MDA-MB-231	98.87 ± 1.25	283.21 ± 138.39
	MDA-MB-435	98.90 ± 1.30	282.59 ± 141.35
Lung Cancer	HCC-78	97.40 ± 1.46	514.40 ± 387.35
(Non-Small Cell)	HCC-827	92.97 ± 5.05	172.86 ± 94.74
	NCI-H157	95.24 ± 7.79	205.25 ± 164.73
	NCI-H1993	5.67 ± 0.80	224.58 ± 112.48
	NCI-H2347	97.20 ± 3.23	234.49 ± 157.00
Lymphoma	Daudi	94.02 ± 11.88	148.89 ± 101.83
(Non-Hodgkin's)	DHL-4	96.59 ± 4.31	129.71 ± 45.09
	Nalm-6	95.29 ± 2.27	66.06 ± 23.49
	Ramos	99.32 ± 0.92	225.29 ± 2.79
Melanoma	397	95.82 ± 4.92	100.51 ± 17.98
	501	84.23 ± 12.41	61.66 ± 13.02
	586	97.26 ± 2.36	41.01 ± 5.25
	624	91.46 ± 10.75	75.12 ± 20.73
	1088	95.93 ± 2.01	46.88 ± 11.05
	1278	97.49 ± 2.02	70.49 ± 10.79
Melanoma (Uveal)	MEL-290	30.90 ± 8.62	86.73 ± 16.68
	OCM-3	85.96 ± 3.83	175.48 ± 35.24
Pancreatic Cancer	BxPC-3	88.08 ± 13.50	144.60 ± 96.89
	PANC-1	87.32 ± 8.86	308.51 ± 190.22
Prostate Cancer	1532-CP2TX	87.41 ± 15.43	801.97 ± 259.16
	1542-CP3TX	89.92 ± 11.53	601.09 ± 203.17
	DU-145	99.40 ± 0.68	667.14 ± 193.10
	LNCaP	6.89 ± 3.16	84.18 ± 57.18
	PC-3	96.45 ± 3.50	278.71 ± 133.17

Tumor cells were stained with UV3 or isotype control antibody, followed by FITC-GAMIG. The presence of tumor cells expressing surface CD54 and their mean fluorescence intensity (MFI) were determined using flow cytometry. There are a significantly higher percentage of CD54+ cells in all cell lines except BT-474, NCI-H1993, and LNCaP ($p > 0.001$). The values represent the average of at least three separate experiments with corresponding standard deviations.

B. UV3 Slows the Growth of CD54^{+} Human Tumors in SCID Mice.

B Cell Non-Hodgkin's Lymphomas.

Female SCID mice with disseminated (i.v.) Daudi human Burkitt's NHL tumor cells received 0.8 mg/kg of UV3, cUV3, or an isotype-matched control antibody i.v. on days 1-4 following tumor cell inoculation. Untreated and control-treated mice had average survival times of 31 and 32 days, while UV3- and cUV3-treated mice had average survival times of 68 and 74 days, respectively (**Figure 1**). Both UV3 and cUV3 prolonged survival as compared with the control mice ($p < 0.005$ for both) and were not different from each other.

UV3 was also investigated in SCID mice injected s.c. with the Daudi cell line. The mice received 0.8 mg/kg mouse of UV3 or control antibody i.p. on days 1-4 following s.c inoculation with Daudi tumor cells. UV3 prevented tumor growth in 3 of 6 mice. In the other 3 mice, UV3 delayed the detection of palpable tumors from 16 days to 27 days and slowed the time required for palpable tumors to reach 2000 mm^3 from 12 days to 19 days, as compared to the control ($p < 0.005$; data not shown). Together these data indicate that UV3 therapy extended the survival of SCID/Daudi mice by two-fold, and that UV3 and cUV3 had similar *in vivo* activity.

CD54^{+} Versus CD54^{-} Breast Tumors.

The anti-tumor activity of UV3 was evaluated in female SCID mice with s.c. MDA-MB-435 (CD54+) human breast tumor cells. Mice with 100 mm3 tumors received 0.75 mg i.p. of UV3 or an isotype-matched control antibody, and therapy was repeated once every 10 days for a total of four injections. As shown in **Figure 2**, it took approximately 40 days longer for tumors in UV3-treated mice to reach 1500 mm^3 than in control-treated mice ($p < 0.005$). Although therapy was not curative, UV3 did significantly slow the growth of MDA-MB-435 breast tumors in SCID mice.

Since UV3 had anti-tumor activity in CD54^{+} tumors, the specificity of UV3 *in vivo* was investigated by injecting 0.75 mg of UV3 or control antibody into female SCID mice with 100 mm^3 CD54^{-} BT-474 or CD54^{+} MDA-MB-435 breast tumors (**Figure 2**). As compared to the CD54^{+} breast tumors, UV3 had no effect on the growth of the CD54^{-} tumors.

Prostate Tumors.

The activity of UV3 in prostate tumors was investigated by s.c. injection of male SCID mice with PC-3 human prostate tumor cells. Animals with 200 mm^3 tumors were treated with 0.3 mg UV3, cUV3, or an isotype-matched control antibody once every 10 days for a total of four injections. Both UV3 and cUV3 significantly slowed tumor growth as

compared to the control ($p < 0.005$), with tumors taking 15 to 20 days longer to reach 1000 mm^3 (**Figure 3**). The data demonstrate that UV3 and cUV3 were equally effective in SCID/PC-3 mice.

Non-Small Cell Lung Tumors.

To assess UV3 therapy in NSC lung tumors, female SCID mice with 100 mm^3 NCI-H157 human tumors were injected with 0.3 mg UV3 or an isotype-matched control antibody once every 7 days for a total of three injections. UV3 slowed tumor growth, with UV3 therapy more than doubling the time required for the tumors to reach 2000 mm^3 ($p < 0.05$; **Figure 4**). These data show that UV3 does slow the growth of $CD54^+$ NSC lung tumors in SCID mice.

Although UV3 was effective in this tumor model, it was possible that improvements in the dose regimen could further slow or stop tumor growth. To this end, multiple doses, injection schedules, and times of treatment initiation were investigated. Three doses of UV3 were investigated in SCID/NCI-H157 NSC lung cancer mice. These included 0.3, 0.75, and 1.5 mg per 10 day period. All three doses significantly slowed tumor growth as compared to the control. However, the 0.75 and 1.5 mg doses of UV3 were consistently more effective than the 0.3 mg dose, and they were also similar to each other regardless of tumor size at

the time of treatment initiation or the schedule of UV3 injections (**Figure 5** and data not shown).

Two different injection schedules were investigated to determine whether the frequency of UV3 administration would affect its *in vivo* efficacy. UV3 was administered either in a single i.p. injection of 0.3, 0.75, or 1.5 mg once every 10 days, or in three i.p. injections of 0.1, 0.25, or 0.5 once every three days. For both schedules the total amount of UV3 over each 10-day period was 0.3, 0.75, or 1.5 mg, respectively. When therapy was initiated at 50 mm^3, there was no difference in therapeutic efficacy between the two injection schedules at any of the doses investigated (data not shown). When UV3 was administered to mice with 200 mm^3 tumors, therapy was more effective when injected once every 10 days for the 0.3 and 0.75 mg doses (**Figure 6** and data not shown). There was no difference in efficacy between the injection schedules for the 1.5 mg dose (data not shown). In general, there was little difference between the two injection schedules investigated. However, in some cases less frequent injections of larger amounts of UV3 were more effective.

When mice with tumors of two different sizes were treated, it was found that therapy was more effective in mice with 50 mm^3 tumors than in mice with 200 mm^3 tumors, regardless of the dose (**Figure 7** and data not shown). The efficacy of UV3 in mice with smaller tumors could not be

investigated, since 50 mm^3 was near the limit for accurate tumor measurements. These data that indicate UV3 was effective in treating these tumors, and that therapy was improved with higher doses and smaller tumor sizes at the time of initiation.

Pancreatic Tumors.

To investigate UV3 therapy in pancreatic tumors, female SCID mice with 100 mm^3 BxPC-3 tumors were injected i.p. with 0.3 mg of UV3 or an isotype-matched control antibody once every 10 days for a total of four injections. As shown in **Figure 8**, UV3 modestly slowed tumor growth, extending the time for tumors to reach 1500 mm^3 by about 7 days ($p < 0.05$). These data demonstrate that UV3 was effective at slowing the growth of pancreatic tumors in SCID mice.

Optimization of UV3 therapy in this model was investigated by investigating the dose, injection frequency, and tumor size at the initiation of therapy. The previously tested dose of 0.3 mg UV3 was compared with two higher doses, 0.75 and 1.5 mg, injected i.p. once every 10 days. All three doses of UV3 significantly slowed tumor growth as compared to the control ($p < 0.05$). When injected into mice with 50 mm^3 tumors, UV3 slowed growth in a dose-dependent manner (**Figure 9**). When therapy was initiated in mice with 200 mm^3 tumors, 0.75 and 1.5 mg UV3 were

both more effective than 0.3 mg UV3, but the two doses were not different from each other (data not shown). Since increasing the dose of UV3 did improve the outcome, this suggested that even larger doses might be advantageous.

The frequency of UV3 administration to SCID/BxPC-3 mice was also investigated. UV3 was administered either as a single i.p. injection of 0.3, 0.75, or 1.5 mg once every 10 days, or in three i.p. injections of 0.1, 0.25, or 0.5 once every three days. For both schedules the total amount of UV3 over each 10-day period was 0.3, 0.75, or 1.5 mg. When mice with 50 mm^3 tumors were injected with UV3, therapy was significantly more effective when administered once every 10 days at all three doses investigated ($p < 0.05$; **Figure 10**). When mice with 200 mm^3 tumors were treated with 0.3 mg UV3, therapy was more effective given once every 10 days, but no difference in efficacy was observed between the schedules for the 0.75 or 1.5 mg doses (data not shown). These data indicate that for smaller tumors UV3 was more effective when injected in larger doses and less often.

The efficacy of UV3 when administered to mice with two different tumor sizes was also investigated. SCID mice with 50 or 200 mm^3 BxPC-3 pancreatic tumors were injected i.p. with 0.3, 0.75, or 1.5 mg UV3 or control antibody. UV3 was more effective when therapy was initiated in

mice with 50 mm^3 versus 200 mm^3 tumors at all three doses (**Figure 11** and data not shown). Together, the data demonstrate that elevated doses of UV3 further slowed tumor growth, and that therapy was more effective when it was initiated in mice with 50 mm^3 tumors and injected at higher doses and less frequently.

Uveal Melanomas.

The uveal melanoma studies were carried out in collaboration with Dr. Jerry Niederkorn's laboratory at UTSWMC. The efficacy of UV3 in uveal melanoma was investigated using SCID mice with either subcutaneous or intraocular tumors. Mice were injected s.c. with OCM-3 human uveal melanoma cells and then treated i.p. with 20 μg of UV3 or an isotype-matched control antibody on days 0, 2, 4, and 6. As shown in **Figure 12**, administration of UV3 immediately following tumor inoculation significantly delayed the formation of palpable tumors from 18 days to 50 days as compared to the control ($p < 0.001$). UV3 also continued to slow the growth of the tumors such that, as compared to the control, the time required for palpable tumors to reach 2000 mm^3 increased from 49 days to 79 days ($p < 0.001$).

SCID/beige mice with intraocular OCM-3 uveal melanoma tumors were injected subconjunctivally with 20 μg of UV3 or control antibody on

days 0, 2, 4, and 6. UV3 slowed the tumor growth of OCM-3 uveal melanoma tumors and eventually resulted in an 80% reduction in tumor size, as shown in **Figure 13**. UV3 injected i.p. also slowed the growth of intraocular tumors, but did not reduce tumor size (data not shown)[211]. Together these data showed that UV3 was effective in slowing the growth of uveal melanoma tumors grown either subcutaneously or orthotopically.

Some Tumor Cells Remaining After UV3 Therapy Showed Reduced Expression of CD54.

Since *in vivo* therapy with UV3 became less effective after multiple injections, it was possible that the remaining cells were $CD54^-$ or $CD54^{lo}$. To address this issue, the surface expression of CD54 on human tumors grown in mice injected with either UV3 or an isotype-matched control was determined. SCID/NCI-H157 or SCID/BxPC-3 mice with 100 mm^3 tumors were injected i.p. with 1.5 mg of UV3 or an isotype-matched control antibody once every 7 days for NCI-H157 tumors or once every 10 days for BxPC-3 tumors for a total of 4 injections. When tumors reached 1500 to 2000 mm^3, the mice were euthanized and the tumors were excised. Single cell suspensions were incubated with UV3 or RPC-5.4 control antibody, stained with FITC-goat anti-mouse IgG, and analyzed by flow cytometry. Live cells were identified either as PI^+ cells or as a distinct

population within a forward scatter versus side scatter plot; data shown were generated using the later, although similar data were obtained using the two methods (data not shown). Although mouse cells present in the cell suspensions can express murine CD54, UV3 recognized only human CD54 on tumor cells[96]. Both NCI-H157 and BxPC-3 tumors expressed CD54 regardless of which *in vivo* therapy the mice had received (**Table 3**). However, UV3 therapy did cause a significant decrease in the percentage of CD54+ cells in NCI-H157 tumors from mice treated with UV3 as compared to the control antibody. In contrast, UV3 therapy did not affect CD54 expression on BxPC-3 cells. Although it is not possible to determine the actual percentage of tumor cells expressing CD54 from these data, it is clear that UV3 does not lose its *in vivo* efficacy due to a lack of CD54 expression on the tumor cells. These data also suggest that larger doses of UV3 should be even more effective.

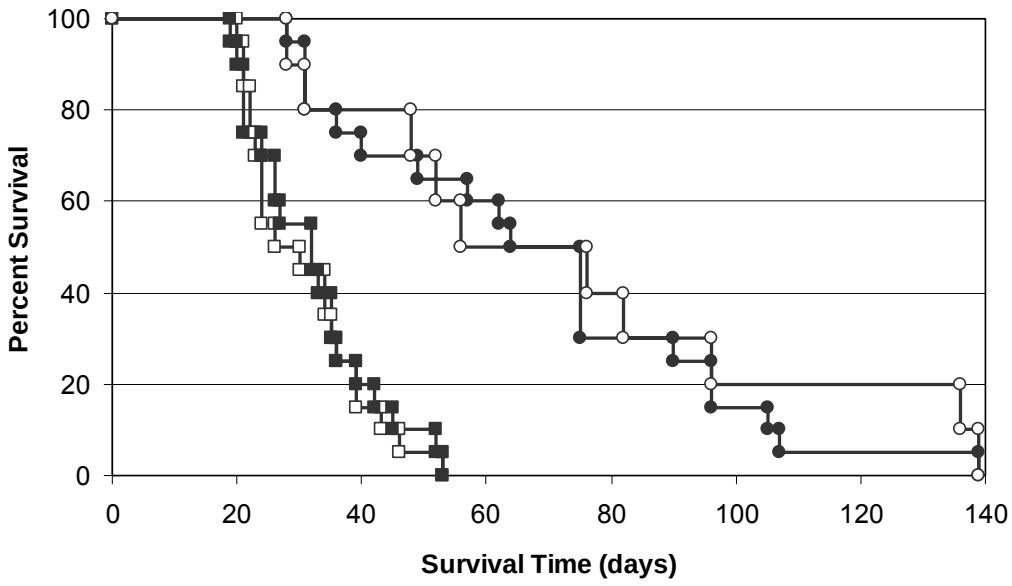

Figure 1. UV3 Prolonged the Survival of SCID/Human B Cell Non-Hodgkin's Lymphoma Mice.

Female SCID mice, 6-8 weeks of age, were injected i.v. with 1 x 10^7 Daudi NHL cells The mice were either left untreated (□) or were injected i.v. with UV3 (●), cUV3 (○), or an isotype-matched control antibody (■) at 0.8 mg/kg mouse on each of four consecutive days beginning one day after tumor cell inoculation. The mice were sacrificed when they developed hind-leg paralysis or were in ill health. Treatment with either UV3 or cUV3 significantly prolonged the survival of SCID mice with Daudi NHL cells as compared to the isotype control ($p < 0.005$ for both). There was no significant difference in efficacy between UV3 versus cUV3 ($p = 0.64$). This figure depicts the average of four experiments, with 5 mice per group in each experiment.

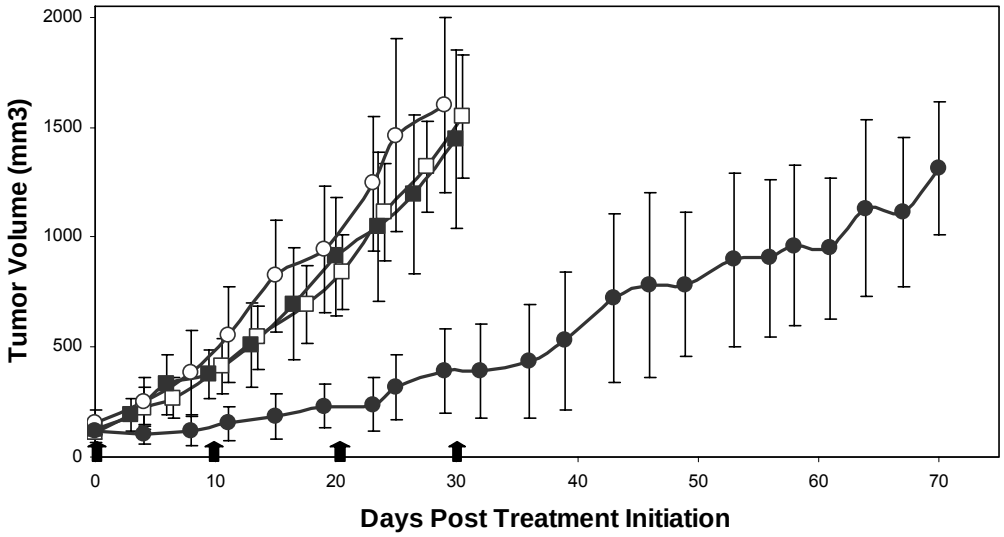

Figure 2. UV3 Slowed the Growth of CD54$^+$ Human Breast Tumors but Not CD54$^-$ Breast Tumors in SCID Mice.

Female SCID mice, 6-8 weeks of age, were irradiated with 150 rads and injected s.c. 24 hours later with 5 x 10^6 BT-474 or MDA-MB-435 human breast tumor cells mixed 1:1 with ice-cold matrigel. Tumor volumes were measured using calipers and calculated as Volume = W^2 x L ÷ 2. When the tumors reached 100 mm^3, mice were injected i.p. with 1.5 mg UV3 (● BT-474; ■ MDA-MB-435) or an isotype-matched control antibody (○ BT-474; □ MDA-MB-435) every 10 days, as indicated on the figure (arrows). The mice were sacrificed when the tumors reached 2000 mm^3. As compared to the isotype control, injection with UV3 significantly prolonged the survival of SCID mice with CD54$^+$ MDA-MB-435 ($p < 0.005$) but not CD54$^-$ BT-474 tumors ($p > 0.25$). This figure depicts a single experiment with 8 mice per group, but the BT-474 data are similar to those obtained in four separate experiments.

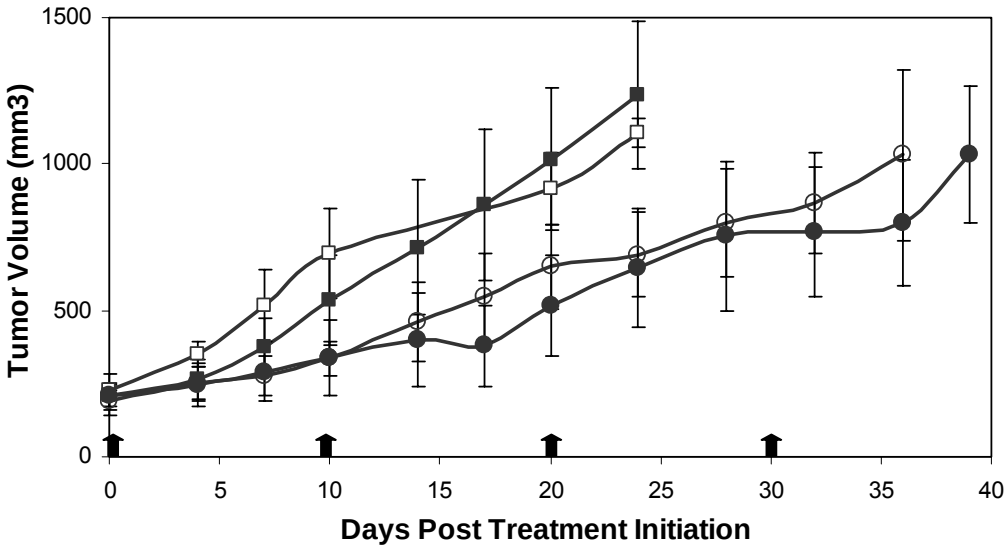

Figure 3. UV3 Slowed Tumor Growth in SCID/Human Prostate Cancer Mice.

Male SCID mice, 6-8 weeks of age, were irradiated with 150 rads, then injected s.c. 24 hours later with 5 x 10^6 PC-3 human prostate tumor cells. Tumor volumes were measured using calipers and calculated as Volume = W^2 x L ÷ 2. When the tumors reached 200 mm^3, the mice were either left untreated (□) or were injected i.p. with 0.3 mg UV3 (●), cUV3 (○), or an isotype-matched control antibody (■) once every 10 days, as indicated on the figure (arrows). The mice were sacrificed when the tumors reached 2000 mm^3. As compared to the isotype control, both UV3 and cUV3 significantly prolonged the survival of the mice ($p < 0.005$ for both). This figure depicts the average of three experiments, with 5-10 mice per group in each experiment.

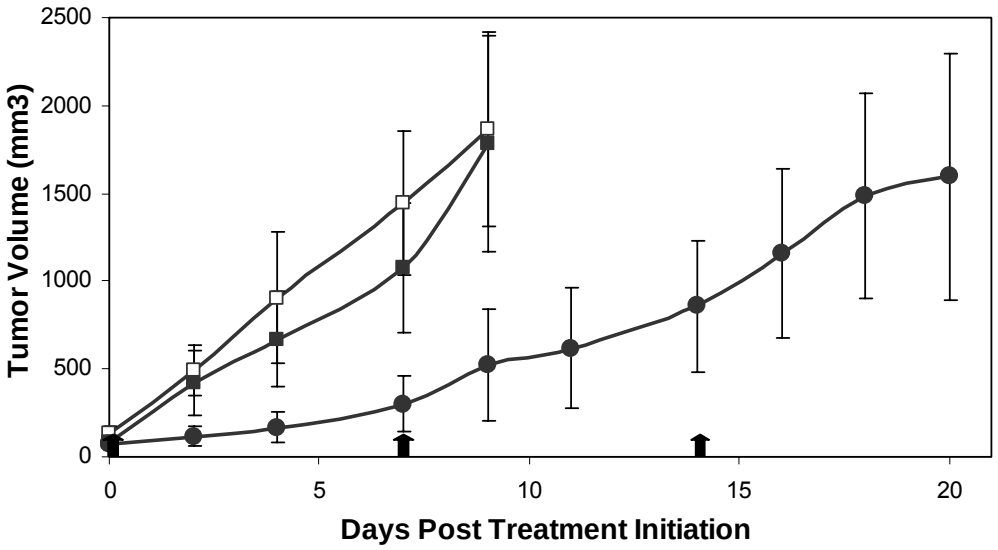

Figure 4. UV3 Slowed Tumor Growth in SCID/Human Non-Small Cell Lung Cancer Mice.

Female SCID mice, 6-8 weeks of age, were injected s.c. with 1 x 10^6 NCI-H157 human NCS lung cancer cells. Tumor volumes were measured using calipers and calculated as Volume = W^2 x L ÷ 2. When the tumors reached 100 mm^3, the mice were either left untreated (□) or were injected i.p. with 0.3 mg UV3 (●) or an isotype-matched control antibody (■) once every 7 days, as indicated on the figure (arrows). The mice were sacrificed when the tumors reached 2000 mm^3. As compared to the isotype control, injection with UV3 significantly prolonged the survival of the mice ($p < 0.05$). This figure depicts the average of three experiments, with 5-10 mice per group in each experiment.

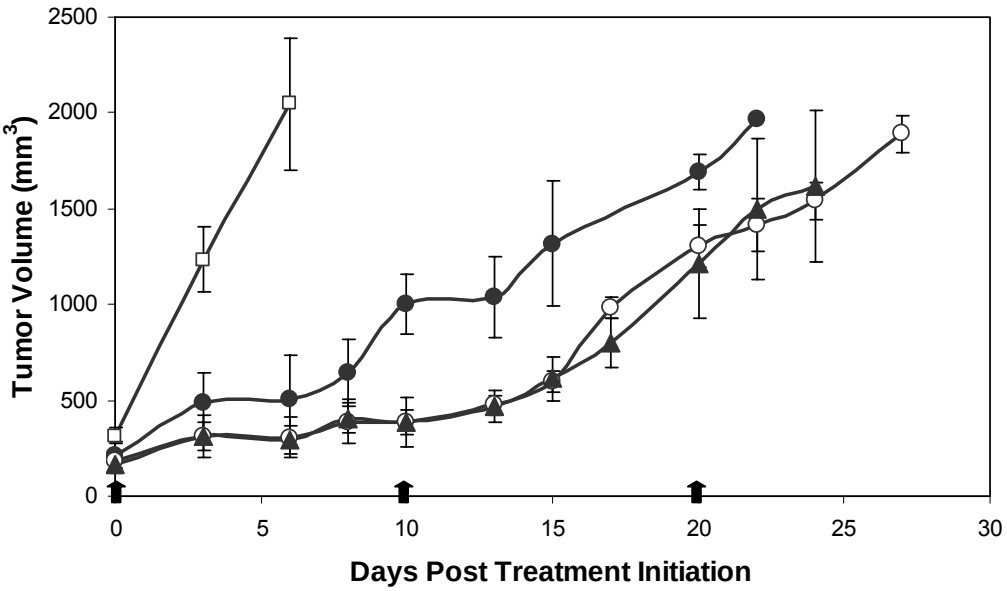

Figure 5. Elevated Doses of UV3 Increased Its Anti-Tumor Efficacy in SCID/Human Non-Small Cell Lung Cancer Mice.

Female SCID mice, 6-8 weeks of age, were injected s.c. with 1 x 10^6 NCI-H157 cells. Tumor volumes were measured using calipers and calculated as Volume = W^2 x L ÷ 2. Mice with 200 mm^3 tumors were injected i.p. with 1.5 mg of isotype-matched control antibody (■), 0.3 mg UV3 (●), 0.75 mg UV3 (○), or 1.5 mg UV3 (▲) once every 10 days as indicated on the figure (arrows). The mice were sacrificed when tumors reached 2000 mm^3. As compared to the isotype control, all three doses of UV3 significantly prolonged the survival of the mice ($p < 0.05$ for all). There was no difference in efficacy in mice treated with 0.75 mg versus 1.5 mg UV3. The 0.3 mg dose of UV3 was significantly less effective than the other two ($p < 0.05$). When mice with 50 mm^3 tumors were treated with UV3, or the antibody dose was administered by a different schedule, similar results were observed. This figure depicts a single experiment with 6 mice per group; Figures 5, 6, and 7 depict different data series from the same single experiment.

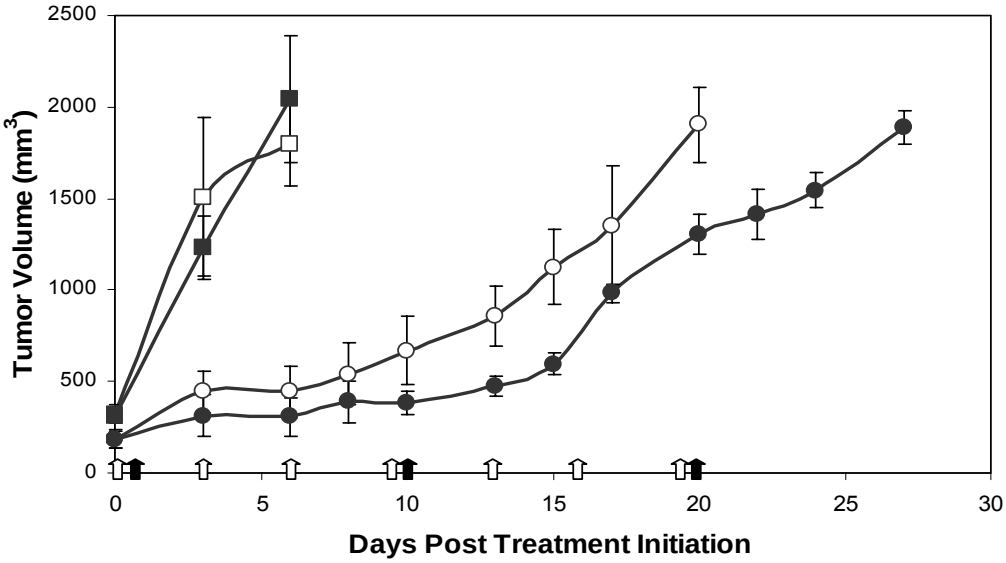

Figure 6. More Frequent Injection of UV3 Did Not Further Slow Tumor Growth in SCID/Human Non-Small Cell Lung Cancer Mice.

Female SCID mice, 6-8 weeks of age, were injected s.c. with 1 x 10^6 NCI-H157 cells. Tumor volumes were measured using calipers and calculated as Volume = W^2 x L ÷ 2. Mice with 200 mm^3 tumors were injected i.p. with 0.75 mg of isotype-matched control antibody (■) or UV3 (●) every 10 days, or 0.25 mg of isotype control (□) or UV3 (○) once every 3 days (0.75 mg total over each 10 day period) as shown on the figure (closed arrows—once every 10 days; open arrows—once every 3 days). The mice were sacrificed when tumors reached 2000 mm^3. Compared to the control, UV3 significantly prolonged survival of the mice ($p < 0.05$). At the 0.75 mg (shown) and 0.3 mg doses, UV3 given once every 10 days was significantly more effective than once every 3 days ($p < 0.05$ for both). There was no difference between the dose schedules at the 1.5 mg dose or at any dose when therapy was initiated in mice with 50 mm^3 tumors. This figure depicts a single experiment with 6 mice per group; Figures 5, 6, and 7 depict different data series from the same single experiment.

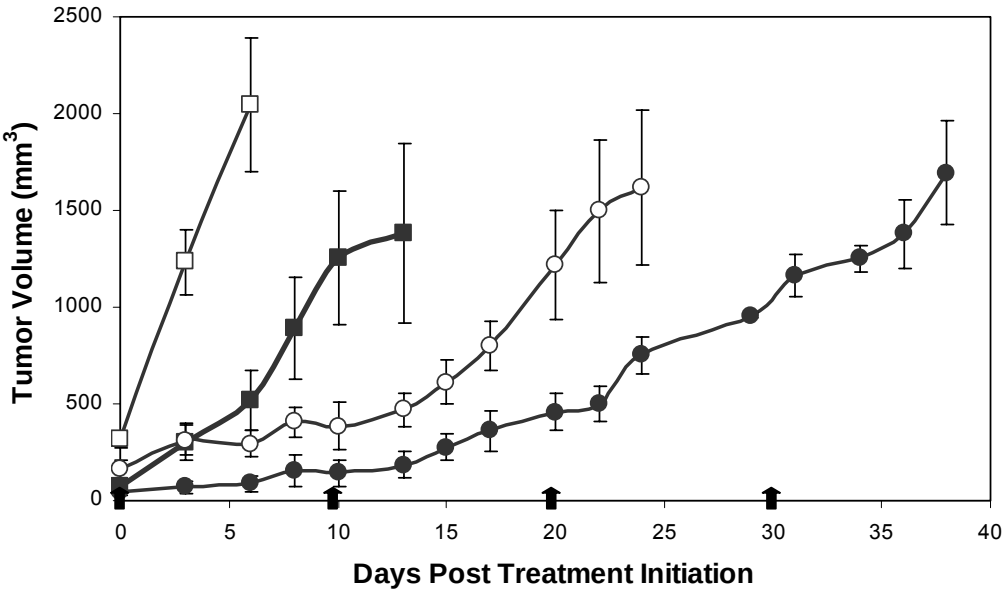

Figure 7. UV3 was More Effective When Initiated in SCID/Human Non-Small Cell Lung Cancer Mice with Small Tumors.

Female SCID mice, 6-8 weeks of age, were injected s.c. with 1 x 10^6 NCI-H157 human NSC lung tumor cells. Tumor volumes were measured using calipers and calculated as Volume = W^2 x L ÷ 2. When tumors reached 50 or 200 mm^3, mice were injected i.p. with 1.5 mg of an isotype-matched control antibody (■, □ respectively) or UV3 (●, ○ respectively) once every 10 days as indicated on the figure (arrows). The mice were sacrificed when the tumors reached 2000 mm^3. As compared to the isotype control, all three doses of UV3 significantly prolonged the survival of the mice ($p < 0.0l$). Therapy with UV3 was significantly more effective when initiated in mice with 50 mm^3 versus 200 mm^3 tumors ($p < 0.05$ for all). This figure depicts a single experiment with 6 mice per group; Figures 5, 6, and 7 depict different data series from the same single experiment.

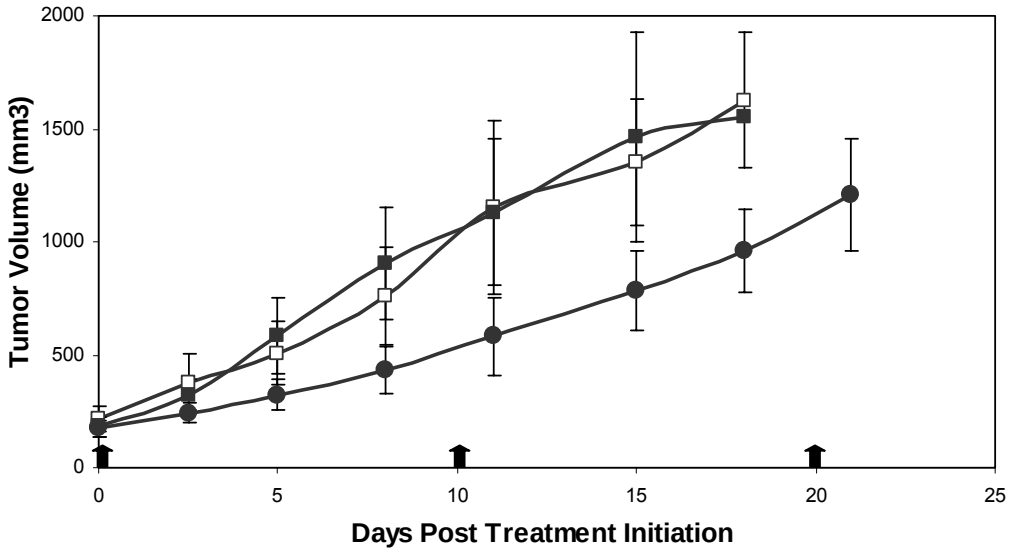

Figure 8. UV3 Slowed Tumor Growth in SCID/Human Pancreatic Cancer Mice.

Female SCID mice, 6-8 weeks of age, were irradiated with 150 rads and injected s.c. 24 hours later with 1 x 10^6 BxPC-3 human pancreatic tumor cells. Tumor volumes were measured using calipers and calculated as Volume = W^2 x L ÷ 2. When the tumors reached 200 mm^3, the mice were either left untreated (□) or were injected i.p. with 0.3 mg of UV3 (●) or isotype-matched control antibody (■) once every 10 days, as indicated on the figure (arrows). The mice were sacrificed when the tumors reached 2000 mm^3. As compared to the isotype control, UV3 therapy significantly prolonged the survival of the mice ($p < 0.01$). This figure depicts the average of two experiments, with 5-10 mice per group in each experiment.

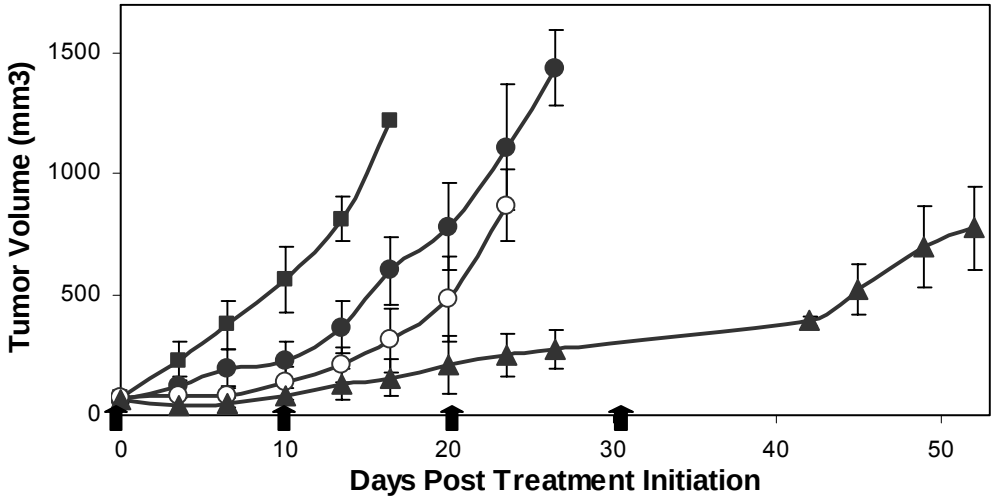

Figure 9. Elevated Doses of UV3 Increased Its Anti-Tumor Efficacy in SCID/Human Pancreatic Cancer Mice.

Female SCID mice, 6-8 weeks of age, were irradiated with 150 rads and injected s.c. 24 hours later with 1 x 10^6 BxPC-3 cells. Tumor volumes were measured using calipers and calculated as Volume = W^2 x L ÷ 2. Mice with 50 mm^3 tumors were injected i.p. with 1.5 mg isotype-matched control antibody (■), 0.3 mg UV3 (●), 0.75 mg UV3 (○), or 1.5 mg UV3 (▲) once every 10 days as indicated on the figure (arrows). The mice were sacrificed when the tumors reached 2000 mm^3. All three doses of UV3 significantly prolonged the survival as compared to the control ($p < 0.05$), but all three UV3 doses were significantly different from each other in a dose-responsive manner ($p < 0.05$). When UV3 was administered on a different schedule, the 0.75 mg and 1.5 mg doses were not different from each other; the 0.3 mg dose remained significantly less effective than the other two ($p < 0.05$). This figure depicts a single experiment with 5 mice per group; Figures 9, 10, and 11 depict different data series from the same single experiment.

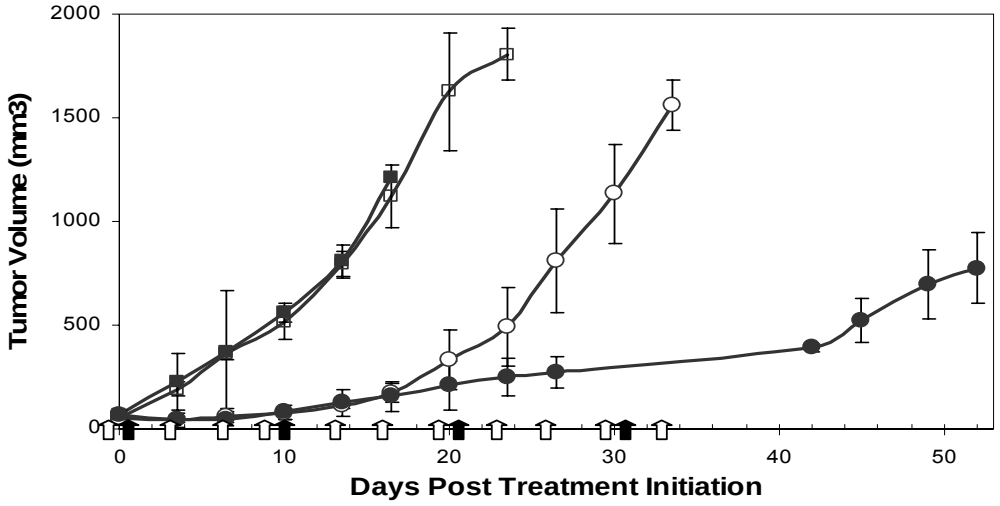

Figure 10. More Frequent Injection of UV3 Did Not Further Slow Tumor Growth in SCID/Human Pancreatic Cancer Mice.

Female SCID mice, 6-8 weeks of age, were irradiated with 150 rads and injected s.c. 24 hours later with 1 x 10^6 BxPC-3 cells. Tumor volumes were measured using calipers and calculated as Volume = W^2 x L ÷ 2. Mice with 50 mm^3 tumors were injected i.p. with 1.5 mg of isotype-matched control antibody (■) or UV3 (●) every 10 days, or 0.5 mg isotype control (□) or UV3 (○) once every 3 days (1.5 mg total over each 10 day period) as indicated on the figure (closed arrows—once every 10 days; open arrows—once every 3 days). The mice were sacrificed when the tumors reached 2000 mm^3. All of the UV3 therapy regimens significantly prolonged the survival of the mice as compared to the isotype control ($p < 0.05$), but administration of UV3 once every 10 days was more effective than the more frequent dose schedule for the 0.3 mg, 0.75 mg, and 1.5 mg doses (shown) ($p < 0.05$). When therapy was initiated in mice with 200 mm^3 tumors, the only significant difference between dosing schedules occurred with the 0.3 mg dose ($p < 0.05$). This figure depicts a single experiment with 5 mice per group; Figures 9, 10, and 11 depict different data series from the same single experiment.

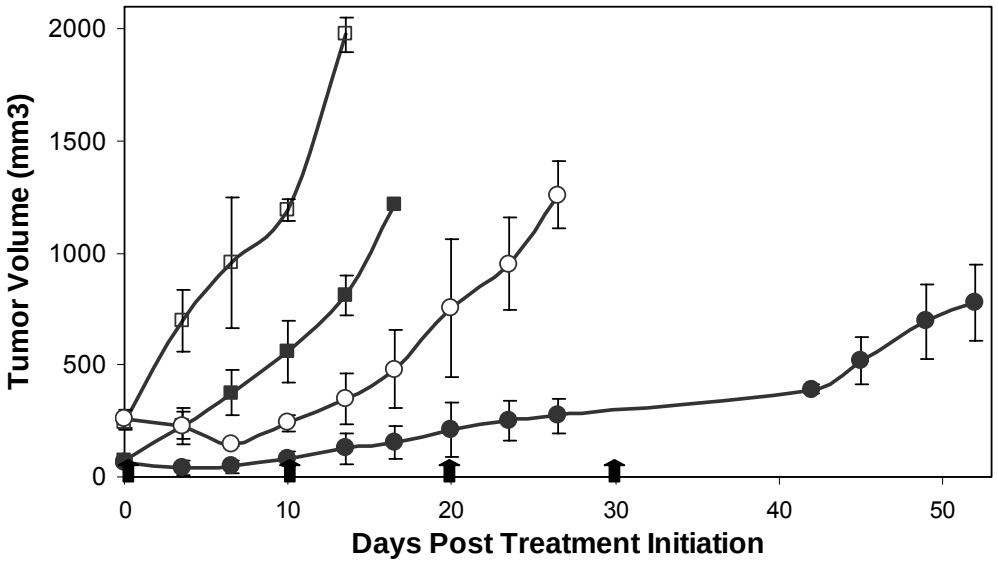

Figure 11. UV3 was More Effective When Initiated in SCID/Human Pancreatic Cancer Mice with Small Tumors.

Female SCID mice, 6-8 weeks of age, were irradiated with 150 rads and injected s.c. 24 hours later with 1 x 10^6 BxPC-3 human pancreatic tumor cells. Tumor volumes were measured using calipers and calculated as Volume = W^2 x L ÷ 2. When tumors reached 50 or 200 mm^3, mice were injected i.p. with 1.5 mg of isotype-matched control antibody (■, □ respectively) or UV3 (●, ○ respectively) once every 10 days as indicated on the figure (arrows). The mice were sacrificed when the tumors reached 2000 mm^3. As compared to the isotype control, all three doses of UV3 significantly prolonged survival ($p < 0.05$). All three UV3 doses were significantly more effective when therapy was initiated in mice with 50 mm^3 versus 200 mm^3 tumors ($p < 0.05$ for all). This figure depicts a single experiment with 5 mice per group; Figures 9, 10, and 11 depict different data series from the same single experiment.

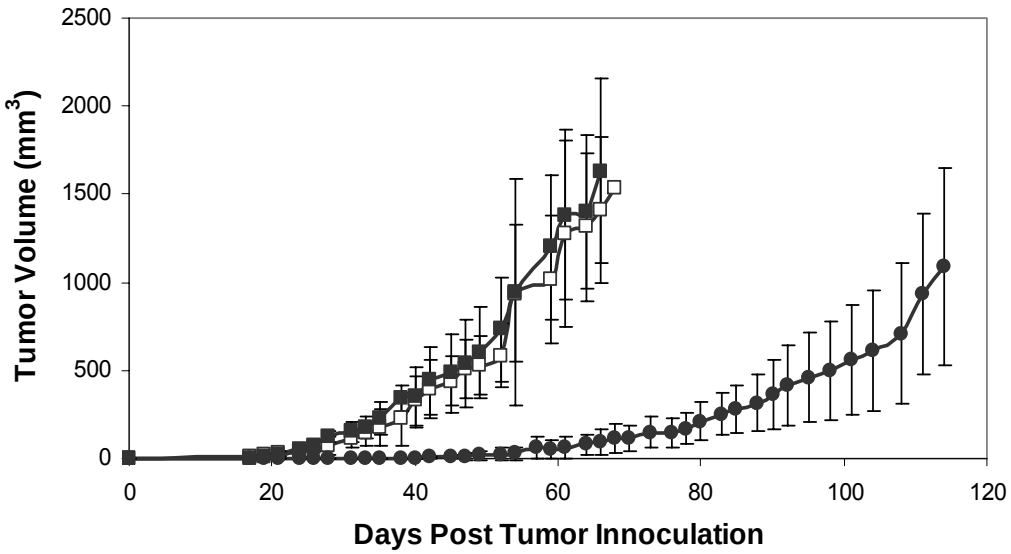

Figure 12. UV3 Slowed Tumor Growth in SCID/Human Uveal Melanoma Mice with Subcutaneous Tumors.

Female SCID/beige mice, 6-8 weeks of age, were injected s.c. with 1 x 10^7 OCM-3 human uveal melanoma cells. Tumor volumes were measured using calipers and calculated as Volume = W^2 x L ÷ 2. The mice were either left untreated (□) or were injected i.p. with 20 µg of isotype-matched control antibody (■) or UV3 (●) on days 0, 2, 4, and 6 following tumor inoculation for a total of four injections, as indicated on the figure (arrows). The mice were sacrificed when the tumors reached 2000 mm^3. Injection with UV3 significantly slowed tumor growth as compared to the control ($p < 0.001$). This figure is of a single experiment with 6 mice per group, but the data were similar in two other experiments[211].

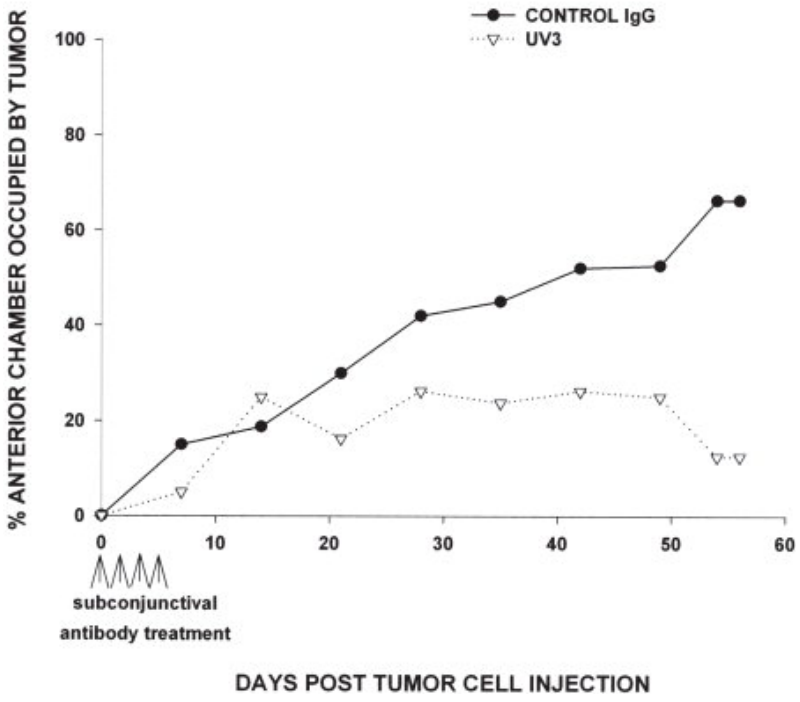

Figure 13. UV3 Reduced Tumor Size in SCID/Human Uveal Melanoma Mice with Intraocular Tumors.

Female SCID/beige mice, 6-8 weeks of age, were injected with 3 x 10^5 OCM-3 human uveal melanoma cells in the anterior chamber of the eye. Tumor volumes were determined as the percentage of the anterior chamber occupied by tumor. The mice were injected subconjunctivally with 20 µg of isotype-matched control antibody (■) or UV3 (●) on days 0, 2, 4, and 6 following tumor inoculation for a total of four injections, as indicated on the figure (arrows). As compared to the isotype control, UV3 slowed tumor growth and eventually reduced the size of the intraocular tumors. This figure is representative of two separate experiments each with 5 mice per group[211].

This figure is reprinted from S. Wang, et al. (2006) Int J Cancer 118:932-941 with the permission of Wiley-Liss, Inc., a subsidiary of John Wiley & Sons, Inc.

Table 3. Tumors Recovered After UV3 Therapy Can Show Reduced Expression of CD54.

Cancer Type	Cell Line	UV3 *in vivo* Therapy*	FACS MAb**	% $CD54^+$ Cells	Mean Fluorescence Intensity
Lung Cancer (Non-Small Cell)	NCI-H157	-	Control	15.08 ± 2.67	100.43 ± 21.6
		-	UV3	37.01 ± 12.37 †	145.81 ± 58.29
		+	Control	10.50 ± 2.19	84.27 ± 27.53
		+	UV3	24.63 ± 5.34 † ‡	104.72 ± 35.53
Pancreatic Cancer	BxPC-3	-	Control	11.06 ± 5.32	77.88 ± 27.01
		-	UV3	35.98 ± 11.39 †	80.60 ± 20.02
		+	Control	12.45 ± 5.61	67.16 ± 22.90
		+	UV3	33.02 ± 4.62 †	67.32 ± 15.76

SCID mice were injected s.c. with either NCI-H157 or BxPC-3 human tumor cells. Mice were injected with UV3 at 1.5 mg i.p. every 10 days once solid tumors were established. 1500-2000 mm^3 tumors were removed from the mice, stained as a single cell suspension with UV3 or an isotype control antibody (RPC-5.4), and analyzed by flow cytometry. N = 5 and 4 for BxPC-3 tumors treated with and without UV3 therapy, respectively. N = 9 for both NCI-H157 therapy groups.

* SCID mice bearing the tumor cell lines indicated either received no UV3 at any time (-) or received 1.5 mg UV3 i.p. every 10 days (+).

** Tumor cells were stained with UV3 or control mAb and analyzed by FACS.

† Indicates a significant percentage of CD54+ tumor cells ($p<0.01$).

‡ Indicates a significant decrease in CD54+ cells with UV3 *in vivo* therapy ($p<0.01$).

C. Combination Therapy of UV3 and Gemcitabine Further Slowed Tumor Growth in SCID Mice.

Since the mechanisms of action of UV3 are not yet well understood and synergistic interactions could therefore not be accurately predicted, effective standard therapies were chosen for the two tumor models investigated. The chemotherapeutic drug gemcitabine was chosen for *in vivo* combination therapy with UV3 because it is now the standard therapy for pancreatic cancers and is also commonly used for the treatment of non-small cell lung cancers due to its improved tolerability profile compared with traditional chemotherapy drugs[7, 10, 16]. Combination therapies could not be tested on all tumors due to cost and time.

The LD_{50} of Gemcitabine in SCID Mice.

It was necessary to first determine the largest dose that could be safely administered to SCID mice. SCID mice were injected i.p. with 100 to 1000 mg/kg mouse gemcitabine and monitored daily for weight loss. If a mouse lost 20% of its baseline weight or appeared in ill health it was euthanized. The LD_{50}, the dose at which gemcitabine was lethal to about half the mice, was determined to be 500 mg/kg mouse (data not shown), which is roughly similar to doses reported in the literature[36, 87, 123].

The LD_{50} was high enough to safely inject the mice with therapeutically relevant doses.

Gemcitabine Inhibited the Proliferation of Non-Small Cell Lung Cancer Cells.

It was necessary to determine whether NCI-H157 NSC lung cancer cells were sensitive to gemcitabine in order to determine whether or not this cell line was a candidate for *in vivo* combination therapy. The cells were incubated with 0.001 to 1000 µg/mL gemcitabine for 72 hours and cytotoxicity was determined by measuring the ability of metabolically active cells able to convert a tetrazolium compound into a formazan product. The formazan product was measured using a plate reader. As shown in **Figure 14**, the NCI-H157 cell line was sensitive to gemcitabine-mediated cytotoxicity, and the IC_{50} was approximately 0.23 µg/mL. When 1 mg/mL UV3 plus 0.001 to 10 µg/mL gemcitabine were incubated with the cells for 72 hours, the combination had no further affect on gemcitabine-mediated cytotoxicity (**Figure 15**). This result was not unexpected since UV3 alone had no effect on tumor cells *in vitro*. These data indicate that the NCI-H157 cell line was a good candidate for combination therapy studies because it is sensitive to gemcitabine *in vitro*

and because UV3 has anti-tumor activity *in vivo*, despite the lack of an additive or synergistic affect on *in vitro* cellular proliferation.

Combination Therapy with UV3 and Gemcitabine Further Slowed Tumor Growth in SCID/Human Non-Small Cell Lung Cancer Mice.

To compare UV3 and gemcitabine on tumor growth *in vivo*, SCID mice bearing 100 mm^3 NCI-H157 NSC lung tumors were injected i.p. with 50, 100, 150, or 300 mg/kg mouse gemcitabine once every 7 days. All four doses of gemcitabine were more effective than the control ($p < 0.05$). UV3 at 1.5 mg once every 7 days was statistically similar to 150 mg/kg (**Figure 16**) and 300 mg/kg (data not shown) gemcitabine and more effective than 50 or 100 mg/kg gemcitabine ($p < 0.05$; data not shown). Therefore, in this model UV3 is as effective as another anti-tumor agent already FDA-approved for the treatment of NSC lung cancer.

When gemcitabine and UV3 were administered concurrently at the given doses, the combination was significantly more effective at slowing tumor growth than either UV3 or gemcitabine alone ($p < 0.05$). Although the combination did not cure the mice, these data demonstrate that UV3 therapy can be improved through combination with a chemotherapeutic drug. It is possible that even more effective combinations involving UV3 can be identified for NSC lung cancer.

Gemcitabine Inhibited the Proliferation of Pancreatic Cancer Cells.

The sensitivity of BxPC-3 cells to gemcitabine was also determined. The cells were incubated with 0.001 to 1000 µg/mL gemcitabine for 72 hours and cytotoxicity was determined by measuring the relative number of metabolically active cells as described above. The BxPC-3 cell line was sensitive to gemcitabine in a concentration-dependent manner, with an IC_{50} of approximately 0.25 µg/mL (**Figure 17**). When 1 mg/mL UV3 was added to cells incubated with 0.001 to 10 µg/mL gemcitabine for 72 hours, the combination had no further affect on gemcitabine-mediated cytotoxicity (**Figure 18**). Despite the lack of a combinatorial effect on tumor cell proliferation, these data indicate that the BxPC-3 pancreatic tumor cell line was also a good candidate for *in vivo* combination therapy due to its sensitivity to gemcitabine *in vitro* and to UV3 *in vivo*.

Combination Therapy with UV3 and Gemcitabine Further Slowed Tumor Growth in SCID/Human Pancreatic Cancer Mice.

Gemcitabine was administered i.p. to SCID mice with 100 mm^3 BxPC-3 pancreatic tumors at doses of 50, 100, 150, and 300 mg/kg mouse once weekly. All doses of gemcitabine investigated demonstrated anti-tumor activity in a dose-dependent manner, as compared with the control ($p < 0.01$). UV3 therapy was also administered i.p at 1.5 mg once

every 10 days and was therapeutically similar to the 150 mg/kg (**Figure 19**) and 300 mg/kg (data not shown) doses of gemcitabine and more effective than gemcitabine given at 50 and 100 mg/kg ($p < 0.05$; data not shown). UV3 was shown to be as effective as a currently FDA-approved chemotherapeutic agent in SCID/pancreatic cancer mice.

UV3 and gemcitabine were also administered together to SCID/pancreatic cancer mice at the does described for single agent therapy. This combination was significantly more effective at slowing pancreatic tumor growth than either UV3 or gemcitabine alone ($p < 0.01$). These data demonstrate that combination therapies involving UV3 have increased therapeutic activity and are worth pursuing into the clinic.

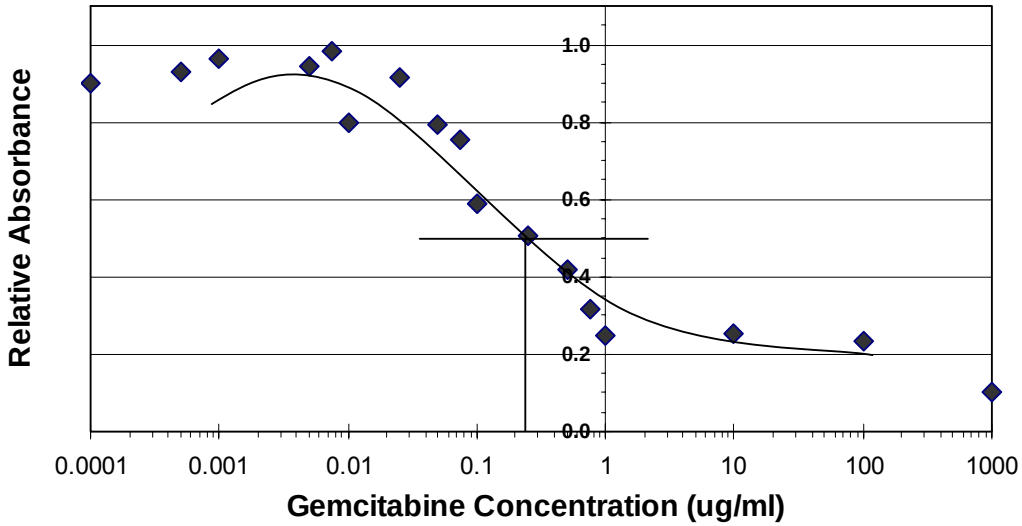

Figure 14. Gemcitabine Inhibited the Proliferation of NCI-H157 Non-Small Cell Lung Cancer Cells.

NCI-H157 cells were incubated for 72 hours with various concentrations of gemcitabine. Cellular proliferation was determined by measuring the metabolism of a tetrazolium compound into a formazan product detected using a plate reader. The absorbance readings of quadruplicate wells for each gemcitabine concentration were averaged and presented as values relative to untreated cells. The IC_{50} of gemcitabine for the NCI-H157 cells was 0.23 µg/mL. This figure depicts the values from three separate experiments.

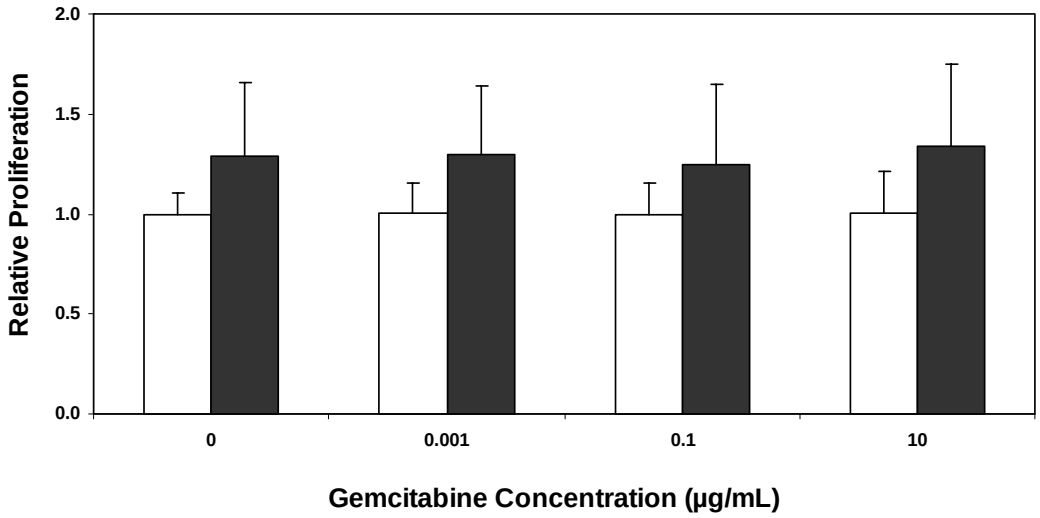

Figure 15. UV3 Does Not Affect the Gemcitabine-Mediated Inhibition of Proliferation of NCI-H157 Non-Small Cell Lung Cancer Cells *In Vitro*.

NCI-H157 cells were incubated for 72 hours with 0, 0.001, 0.1, or 10 µg/mL gemcitabine and 1 mg/mL of either UV3 (■) or control antibody (□). Cellular proliferation was determined by measuring the metabolism of a tetrazolium compound. Replicate wells were averaged and the values were presented as relative to gemcitabine plus the isotype-matched control antibody for each gemcitabine concentration. Instead of further inhibiting tumor cell proliferation, UV3 significantly reduced the gemcitabine-induced inhibition of NCI-H157 proliferation at each of the gemcitabine concentrations investigated ($p < 0.05$). The data shown depict the average values of five experiments with their corresponding standard deviations. The values shown are relative to the proliferation of cells treated with gemcitabine alone at each concentration.

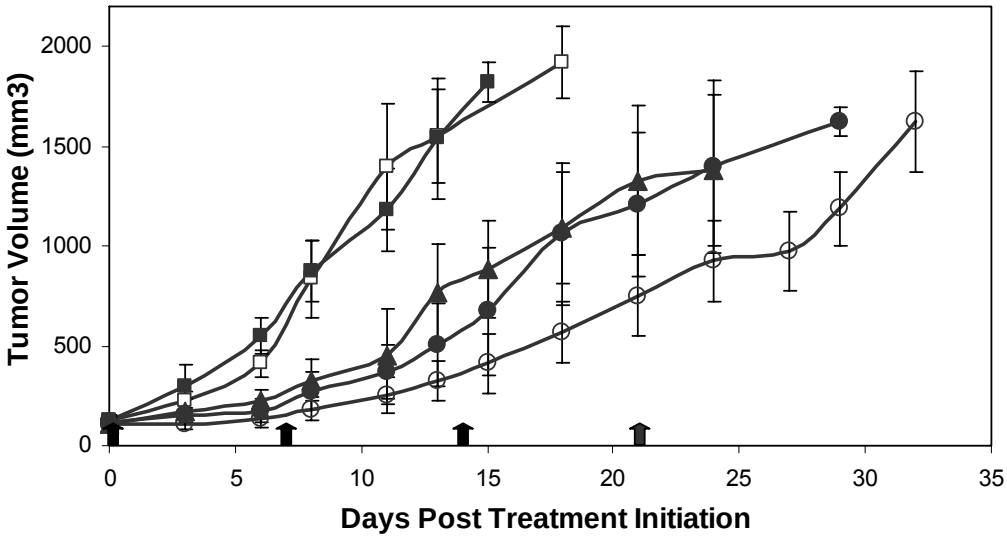

Figure 16. Combination Therapy with UV3 and Gemcitabine Further Slowed Tumor Growth in SCID/Human Non-Small Cell Lung Cancer Mice.

Female SCID mice, 6-8 weeks of age, were injected s.c. with 1 x 10^6 NCI-H157 cells. Tumor volumes were measured using calipers and calculated as Volume = W^2 x L ÷ 2. Mice with 100 mm^3 tumors were either left untreated (□) or were injected i.p. with 1.5 mg of UV3 (●), 1.5 mg isotype-matched control (■), 150 mg/kg mouse gemcitabine (▲), or 150 mg/kg mouse gemcitabine plus 1.5 mg UV3 (○) every 7 days, as indicated on the figure (arrows). The mice were sacrificed when the tumors reached 2000 mm^3. Compared to the control, UV3, gemcitabine, and combination therapy all significantly prolonged the survival of the mice ($p < 0.05$ for all). According to the Wilcoxon test UV3 was more effective than gemcitabine ($p < 0.05$), but tumors differed in size only on days 6, 13, and 15 post treatment initiation ($p < 0.05$). Combination therapy was more effective than either UV3 or gemcitabine alone ($p < 0.005$ for both). This figure depicts the average of two experiments, with 8-10 mice per group in each experiment.

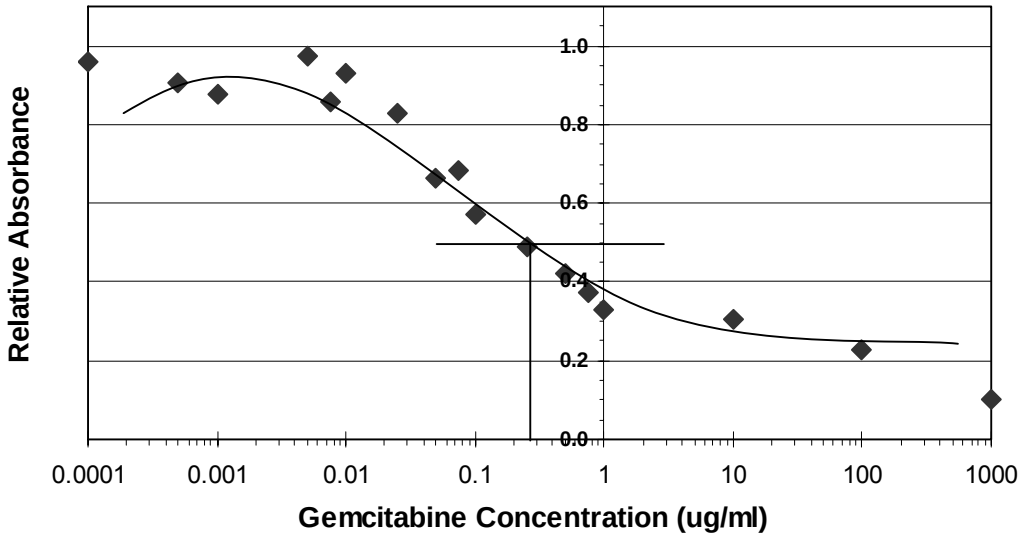

Figure 17. Gemcitabine Inhibited the Proliferation of BxPC-3 Pancreatic Cancer Cells.

BxPC-3 cells were incubated for 72 hours with various concentrations of gemcitabine (shown below). Cellular proliferation was determined by measuring the metabolism of a tetrazolium compound into a formazan product detected using a plate reader. The absorbance readings of quadruplicate wells for each gemcitabine concentration were averaged and presented as values relative to untreated cells. The IC_{50} of gemcitabine for the BxPC-3 cells was determined to be 0.25 µg/mL. This figure depicts values from four separate experiments.

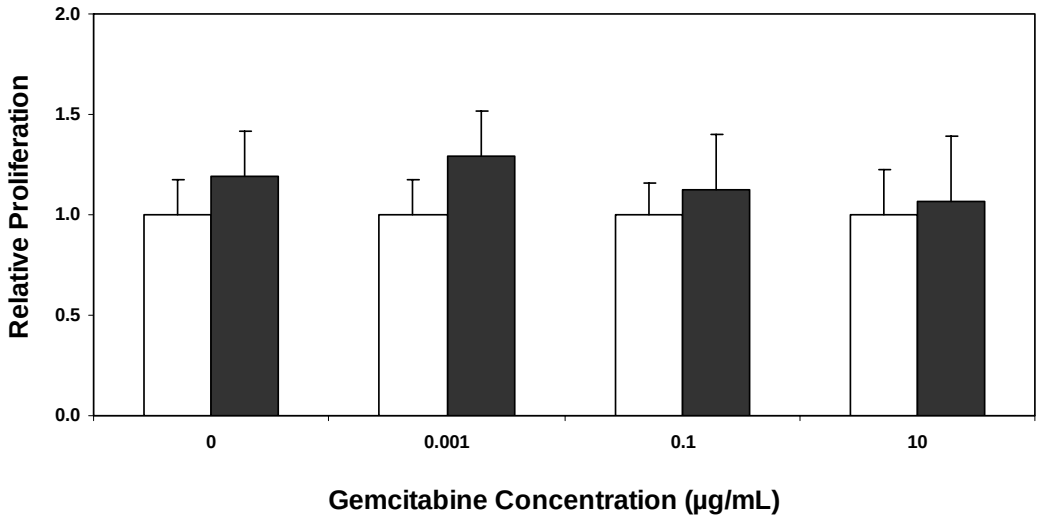

Figure 18. UV3 Does Not Affect the Gemcitabine-Mediated Inhibition of Proliferation of BxPC-3 Pancreatic Cancer Cells *In Vitro*.

BxPC-3 cells were incubated for 72 hours with 0, 0.001, 0.1, or 10 µg/mL gemcitabine and 1 mg/mL of either UV3 (■) or control antibody (□). Cellular proliferation was determined by measuring the metabolism of a tetrazolium compound. Replicate wells were averaged and the values were presented as relative to gemcitabine plus the isotype-matched control antibody for each gemcitabine concentration. UV3 had no effect on gemcitabine-mediated inhibition of BxPC-3 proliferation in the presence of 0.1 and 10 µg/mL gemcitabine, and UV3 induced increased proliferation in the absence of gemcitabine and at 0.001 µg/mL gemcitabine ($p < 0.05$). The data shown depict the average values of five experiments with their corresponding standard deviations. The values shown are relative to the proliferation of cells treated with gemcitabine alone at each concentration.

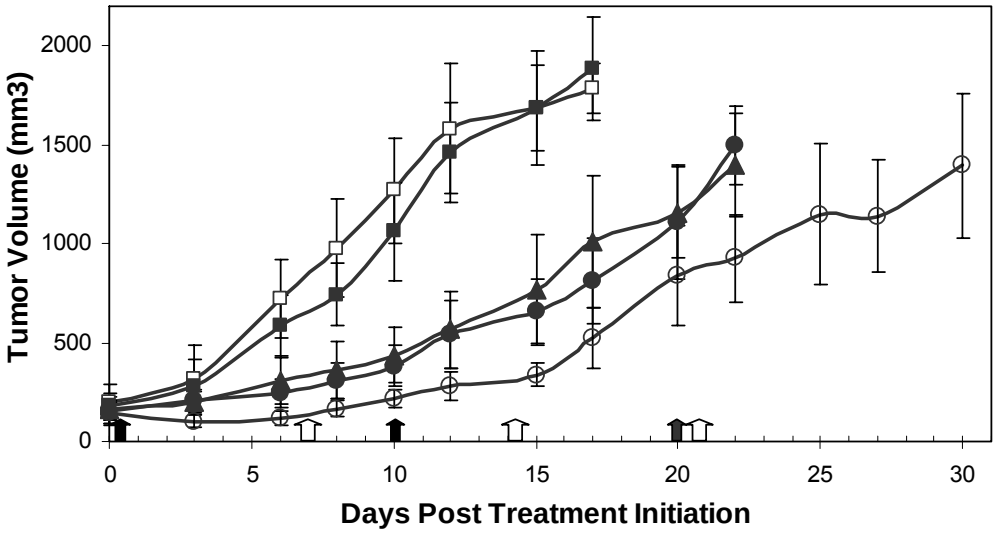

Figure 19. Combination Therapy with UV3 and Gemcitabine Further Slowed Tumor Growth in SCID/Human Pancreatic Cancer Mice.

Female SCID mice, 6-8 weeks of age, were irradiated with 150 rads and injected s.c. 24 hours later with 1 x 10^6 BxPC-3 cells. Tumor volumes were measured using calipers and calculated as Volume = W^2 x L ÷ 2. Mice with 200 mm^3 tumors were either left untreated (□) or injected i.p. with 1.5 mg of UV3 (●) or isotype-matched control antibody (■) every 10 days, 150 mg/kg mouse gemcitabine (▲) every 7 days, or a combination of 1.5 mg UV3 plus 150 mg/kg gemcitabine (○), as indicated on the figure (closed arrows = antibody; open arrows = gemcitabine). The mice were sacrificed when the tumors reached 2000 mm^3. As compared to the isotype control, UV3, gemcitabine, and combination therapy all prolonged survival ($p < 0.01$ for all). There was no difference between the UV3 and gemcitabine therapies ($p > 0.25$). Combination therapy was more effective than either UV3 or gemcitabine ($p < 0.001$ for both). This figure depicts the average of two experiments, with 8-10 mice per group in each experiment.

D. UV3 Does Not Inhibit the Proliferation of Tumor Cell Lines *In Vitro.*

It is currently unclear how UV3 mediates its anti-tumor activity. To investigate this, human tumor cell lines were incubated with UV3 *in vitro* to determine whether UV3 directly inhibits proliferation or induces apoptosis of tumor cells. Cultured tumor cell lines were incubated with 1 mg/mL of UV3 or an isotype-matched control antibody, or 5 mg/mL sodium azide (positive control) for 72 hours at 37°C in 5% CO_2/95% air, and proliferation was determined either by incorporation of ^{3}H-thymidine or cellular metabolism of a tetrazolium compound. The data were represented as proliferation relative to untreated cells. There was no difference in the data generated with the two methods (data not shown). UV3 did not inhibit the proliferation of any of the tumor cell lines investigated, and the data for $CD54^+$ cell lines were similar to those for two $CD54^-$ cell lines (**Table 4**). In contrast, treatment with sodium azide (positive control) significantly inhibited proliferation or induced apoptosis in the cell lines ($p < 0.001$; data not shown). These data indicate that UV3 does not inhibit tumor cell proliferation, even at concentrations as high as 1 mg/mL.

Table 4. UV3 Does Not Inhibit the Proliferation of Tumor Cell Lines *In Vitro*.

		Relative Proliferation **	
Cancer Type	**Cell Line**	**Control Antibody**	**UV3 Antibody**
Breast Cancer	BT-474	1.1 ± 0.37	0.7 ± 0.34
	MDA-MB-435	1.1 ± 0.32	1.1 ± 0.26
Lung Cancer (NSC)	NCI-H157	1.0 ± 0.28	0.8 ± 0.09
Lymphoma (NHL)	Daudi	0.7 ± N/A*	1.0 ± 0.05*
Melanoma	397	0.9 ± 0.33	1.2 ± 0.53
Melanoma (Uveal)	OCM-3	1.1 ± 0.25	0.9 ± 0.22
Multiple Myeloma	KM-3	1.1 ± 0.39	1.1 ± 0.32
Pancreatic Cancer	BxPC-3	0.8 ± 0.26	0.8 ± 0.15
Prostate Cancer	LNCaP	0.8 ± 0.15	0.8 ± 0.21
	PC-3	0.9 ± 0.42	0.8 ± 0.31

Tumor cell lines were incubated for 72 hours with 1 mg/mL of isotype control or UV3 antibody. Proliferation was determined either by incorporation of ^{3}H-thymidine or cellular metabolism of a tetrazolium compound. The data shown are the average values of at least three experiments with their corresponding standard deviations. UV3 did not significantly inhibit proliferation of any of the tumor cell lines.

* Data included from Coleman, et al. [52]

** Data are expressed relative to untreated tumor cells.

N/A Indicates data not available.

E. The Importance of the Fc Portion of UV3 to its Anti-Tumor Activity Varies Among Individual Tumor Cell Lines.

B Cell Non-Hodgkin's Lymphomas.

In order to investigate the importance of the Fc portion of UV3 for its anti-tumor activity, $F(ab')_2$ fragments of UV3 were compared with IgG *in vivo* in several xenograft tumor models. SCID mice with disseminated Daudi NHL tumors were injected i.v. with 0.8 mg/kg of mouse UV3 or isotype-matched control antibody, or with 4 mg/kg of UV3 $F(ab')_2$ fragments on days 1-4 following tumor inoculation. The $F(ab')_2$ fragments were given at a five-fold higher dose than the IgG in order to compensate for the fragments' faster clearance rate. As shown in **Figure 20**, the $F(ab')_2$ fragments had significant anti-tumor activity, but they were not as effective as IgG. Mice treated with the control antibody had an average survival time of 32 days, mice treated with $F(ab')_2$ fragments had an average survival time of 47 days, and mice treated with IgG had an average survival time of 68 days.

UV3 and its $F(ab')_2$ fragments were also compared in a subcutaneous model of Daudi NHL in SCID mice in order to better compare the in vivo efficacy of $F(ab')_2$ fragments between this model and the other subcutaneous tumor models. SCID mice with s.c. Daudi NHL

tumors were injected i.p. with 0.8 mg/kg mouse UV3 or isotype-matched control antibody or 4 mg/kg mouse UV3 $F(ab')_2$ fragments on days 1-4 following tumor inoculation. As before, the $F(ab')_2$ fragments demonstrated an intermediate therapeutic activity (**Figure 21**). The intermediate activity was observed both with regard to the time it took for palpable tumors to develop (16 days for control, 21 days for $F(ab')_2$, and 27 days for UV3) and the time it took for the tumors to reach 2000 mm^3 (28 days for control, 34 days for $F(ab')_2$, and 46 days for UV3). Together, the data for both Daudi lymphoma models show that the Fc was important to the activity of UV3, regardless of how the tumors were grown, since the intact IgG was more effective than its $F(ab')_2$ fragments.

Prostate Tumors.

The efficacy of UV3 and its $F(ab')_2$ fragments were compared in mice with human prostate tumors to investigate the importance of the Fc for anti-tumor activity. Male SCID mice with 200 mm^3 PC-3 tumors were injected i.p. with 0.3 mg UV3 or an isotype-matched control antibody, or with 1.5 mg of $F(ab')_2$ fragments. Therapy was repeated once every 10 days for a total of four injections. UV3 IgG and $F(ab')_2$ fragments both slowed tumor growth as compared to the isotype control (**Figure 22**). Statistically, the $F(ab')_2$ fragments were not quite as effective as UV3 in

this model, though the growth curves for the two treatment groups were very similar, with tumor measurements that were significantly different for only three measurements. Although the Fc was likely involved in the activity of UV3, these data indicate that UV3 can mediate its anti-tumor activity through Fc-independent mechanisms in these cells.

Non-Small Cell Lung Tumors.

The importance of the Fc of UV3 to its anti-tumor activity was investigated by comparing the efficacy of UV3 and its $F(ab')_2$ fragments in a xenograft model of NSC lung cancer. SCID mice with 100 mm^3 NCI-H157 NSC lung tumors were injected i.p. with 0.3 mg UV3 or an isotype-matched control antibody or 1.5 mg of $F(ab')_2$ fragments once every 7 days for a total of three injections. The $F(ab')_2$ fragments had no therapeutic effect, and tumors grew similarly to those in the control mice (**Figure 23**). These data demonstrate that the anti-tumor efficacy of UV3 in this model is Fc-dependent.

Pancreatic Tumors.

UV3 and its $F(ab')_2$ fragments were compared *in vivo* in a model of pancreatic cancer to investigate the importance of the Fc for the anti-tumor activity of UV3. SCID mice with 200 mm^3 BxPC-3 pancreatic tumors

were injected i.p. with 0.3 mg UV3 or an isotype-matched control antibody or 1.5 mg of $F(ab')_2$ fragments once every 10 days for a total of three injections. UV3 and its $F(ab')_2$ fragments were equally effective at slowing tumor growth as compared to the control (**Figure 24**). Therefore, the Fc of UV3 was not essential for UV3 anti-tumor activity *in vivo* in this pancreatic tumor model.

Uveal Melanomas.

The *in vivo* efficacy of $F(ab')_2$ fragments was investigated in two models of uveal melanoma in mice through collaboration with Dr. Jerry Niederkorn's laboratory at UTSW. SCID/beige mice with barely palpable subcutaneous OCM-3 uveal melanoma tumors were injected i.p. with 100 μg of UV3, $F(ab')_2$, or an isotype-matched control antibody on each of four consecutive days. As compared to the control, UV3 and its $F(ab')_2$ fragments both slowed tumor growth for 80 days following tumor cell inoculation (**Figure 25**). However, in the later stages of the experiment the tumors treated with $F(ab')_2$ fragments progressed more rapidly than those treated with the IgG. Still, the tumors treated with $F(ab')_2$ fragments were only about half the size of control-treated tumors at day 100 following tumor inoculation.

SCID/beige mice with barely detectable intraocular OCM-3 uveal melanoma tumors were injected subconjuctivally with 100 µg of UV3 $F(ab')_2$ fragments or control antibody on days 0, 2, 4, and 6 following tumor inoculation. As compared with the control, the F(ab')2 fragments dramatically slowed tumor growth, resulting in a 60% inhibition (**Figure 26**)[211]. Together these data show that the $F(ab')_2$ fragments of UV3 did slow the growth of uveal melanoma tumors, typically with an efficacy similar to that of IgG.

UV3 Mediates ADCC in Some Human Tumor Cell Lines *In Vitro*.

In some tumors, $F(ab')_2$ fragments of UV3 lacked the full efficacy of IgG, indicating that the Fc may be required to mediate effector functions. Therefore, *in vitro* assays were utilized to differentiate between the ADCC and CDC effector mechanisms in several human tumor cell lines. Tumor cells were labeled with ^{51}Chromium and then incubated with effector cells at various ratios in the presence of UV3 or an isotype-matched control antibody for 4 hours. ADCC was determined by measuring the amount of ^{51}Chromium released by lysed tumor cells. The values were represented as specific lysis relative to tumor cells incubated with effector cells in the presence of the isotype control. UV3 mediated ADCC in five out of eight $CD54^+$ cell lines investigated (**Figure 27**), including the BxPC-3 pancreatic

cancer, Daudi B cell NHL, KM-3 multiple myeloma, NCI-H157 NSC lung cancer, and OCM3 uveal melanoma cell lines. UV3 did not mediate ADCC in the $CD54^+$ 397 melanoma, MDA-MB-435 breast cancer, and PC-3 prostate cancer cell lines or in the $CD54^-$ BT-474 breast cancer and LNCaP prostate cancer cell lines (data not shown). These data indicate that UV3 does mediate ADCC in at least some $CD54^+$ cell lines *in vitro*, but that there is variation among the cell lines.

UV3 Mediates CDC in Some Human Tumor Cell Lines *In Vitro*.

In addition to ADCC, UV3-mediated CDC was also investigated. Tumor cells were labeled with ^{51}Chromium and then incubated with rabbit serum in the presence of UV3 or an isotype-matched control antibody for 4 hours. CDC was determined by measuring the amount of ^{51}Chromium released by lysed tumor cells. The values were represented as specific lysis relative to tumor cells incubated with rabbit serum in the presence of the isotype control. UV3 mediated CDC in four out of eight $CD54^+$ cell lines investigated (**Figure 28**), including the BxPC-3 pancreatic cancer, KM-3 multiple myeloma, NCI-H157 NSC lung cancer, and OCM3 uveal melanoma cell lines. UV3 did not mediate CDC in the $CD54^+$ 397 melanoma, Daudi B cell NHL, MDA-MB-435 breast cancer, and PC-3 prostate cancer cell lines or in the $CD54^-$ BT-474 breast cancer and

LNCaP prostate cancer cell lines (data not shown). These data indicate that UV3 does mediate CDC *in vitro*, but only in some $CD54^+$ cell lines.

These *in vitro* and *in vivo* data concerning the importance of the Fc portion of UV3 are summarized together in **Table 5**. $F(ab')_2$ fragments lacked anti-tumor activity only in SCID mice with NCI-H157 NSC lung tumors, a cell line that was susceptible to both ADCC and CDC *in vitro* in the presence of UV3. $F(ab')_2$ fragments demonstrated intermediate anti-tumor efficacy in SCID mice with disseminated and solid Daudi NHL tumors, and the Daudi cell line was lysed by ADCC but not CDC in the presence of UV3. The $F(ab')_2$ fragments had strong anti-tumor activity *in vivo* in pancreatic cancer and uveal melanoma, though both the BxPC-3 and OCM3 cell lines were susceptible to the ADCC and CDC *in vitro*, possibly because other mechanisms were able to compensate for the lack of Fc effector functions *in vivo*. Together the *in vivo* and *in vitro* data indicate that UV3 does mediate its effect at least in part through Fc effector mechanisms, but that the importance of these mechanisms to *in vivo* therapy varied among the cell lines tested.

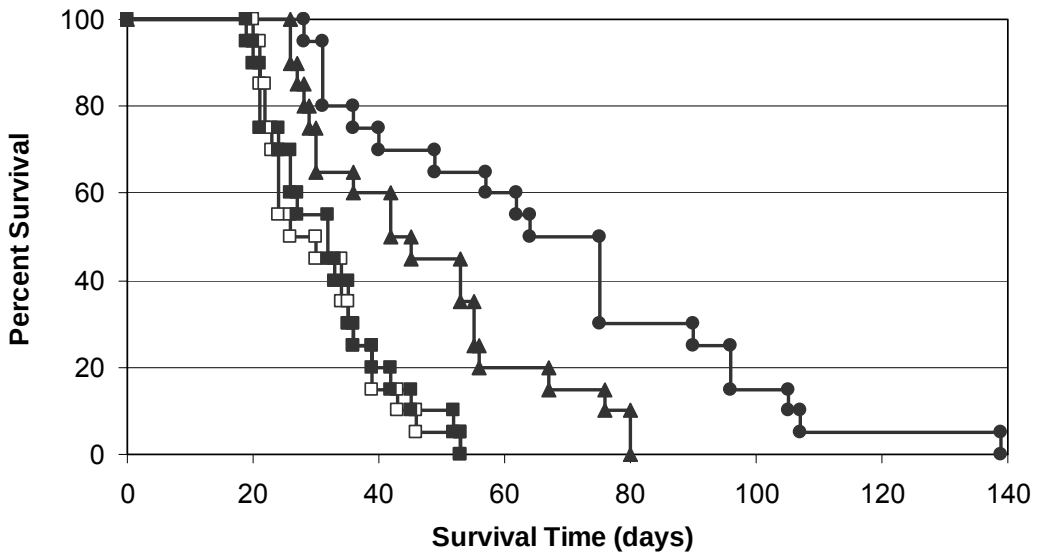

Figure 20. Therapy of SCID/Disseminated Human B Cell Non-Hodgkin's Lymphoma Mice with UV3 IgG Versus Its F(ab')$_2$ Fragments.

Female SCID mice, 6-8 weeks of age, were injected with 1 x 10^7 Daudi NHL cells i.v. The mice were either left untreated (□) or were injected i.v. with UV3 (●) or isotype-matched control antibody (■) at 0.8 mg/kg mouse or UV3 F(ab')$_2$ (▲) at 4.0 mg/kg mouse on each of four consecutive days beginning one day after tumor cell inoculation. The mice were sacrificed when the mice developed hind-leg paralysis or were in ill health. F(ab')$_2$ fragments of UV3 significantly prolonged survival as compared to the isotype control ($p < 0.005$), but were not as effective as the IgG ($p < 0.005$). This figure depicts the average of four experiments, with 5 mice per group in each experiment.

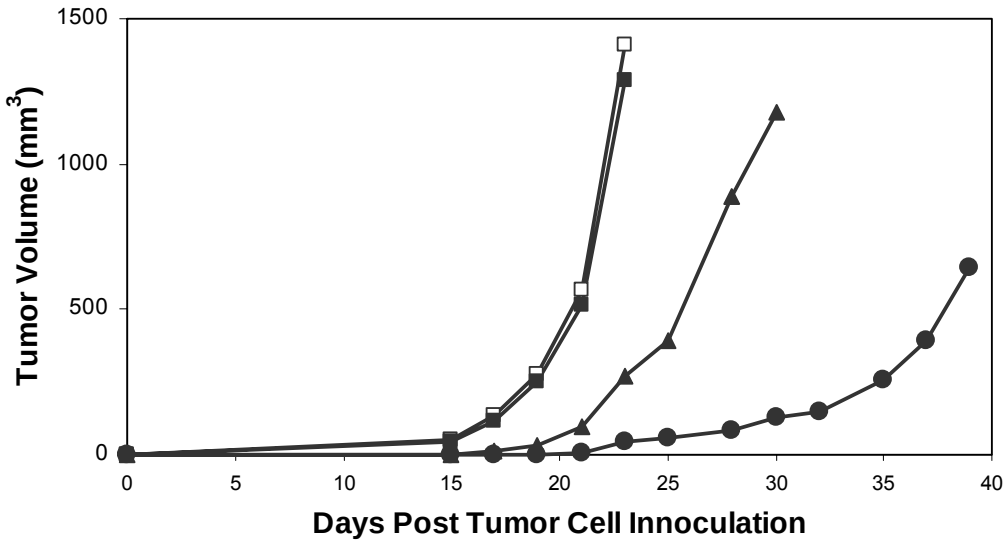

Figure 21. Therapy of SCID/Subcutaneous Human B Cell Non-Hodgkin's Lymphoma Mice with UV3 IgG Versus Its F(ab')$_2$ Fragments.

Female SCID mice, 6-8 weeks of age, were injected with 1 x 10^7 Daudi NHL cells s.c. The mice were either left untreated (□) or injected i.p. with UV3 (●) or isotype-matched control antibody (■) at 0.8 mg/kg mouse or UV3 F(ab')$_2$ (▲) at 4.0 mg/kg mouse on each of four consecutive days beginning one day after tumor cell inoculation. The mice were sacrificed when the solid tumors reached 2000 mm^3. Both IgG UV3 and its F(ab')$_2$ fragments significantly slowed solid tumor growth as compared to the isotype control ($p < 0.05$ for both), but the F(ab')$_2$ fragments were not as effective as IgG ($p < 0.05$).This figure depicts a single experiment with 6 mice per group.

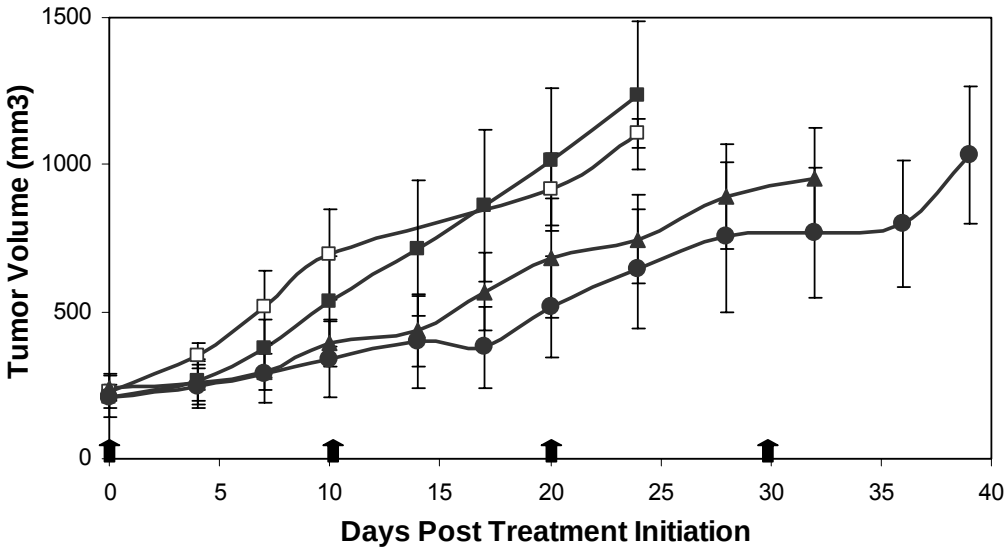

Figure 22. Therapy of SCID/Human Prostate Cancer Mice with UV3 IgG Versus Its F(ab')$_2$ Fragments.

Male SCID mice, 6-8 weeks of age, were irradiated with 150 rads and injected s.c. 24 hours later with 5 x 10^6 PC-3 human prostate cancer cells. Tumor volumes were measured using calipers and calculated as Volume = W^2 x L ÷ 2. When the tumors reached 200 mm^3, the mice were either untreated (□) or injected i.p. with 0.3 mg UV3 (●), 0.3 mg isotype control antibody (■), or 1.5 mg UV3 F(ab')$_2$ fragments (▲) once every 10 days, as indicated on the figure (arrows). The mice were sacrificed when the solid tumors reached 2000 mm^3. Both IgG UV3 and its F(ab')$_2$ fragments significantly slowed tumor growth as compared to the isotype control ($p < 0.01$ for both). The efficacy of therapy with UV3 versus its F(ab')$_2$ fragments was different by the Wilcoxon test ($p < 0.05$), but tumor measurements were different only on days 17, 20, and 32 following the initiation of treatment ($p < 0.05$). This figure depicts the average of three experiments, with 5-10 mice per group in each experiment.

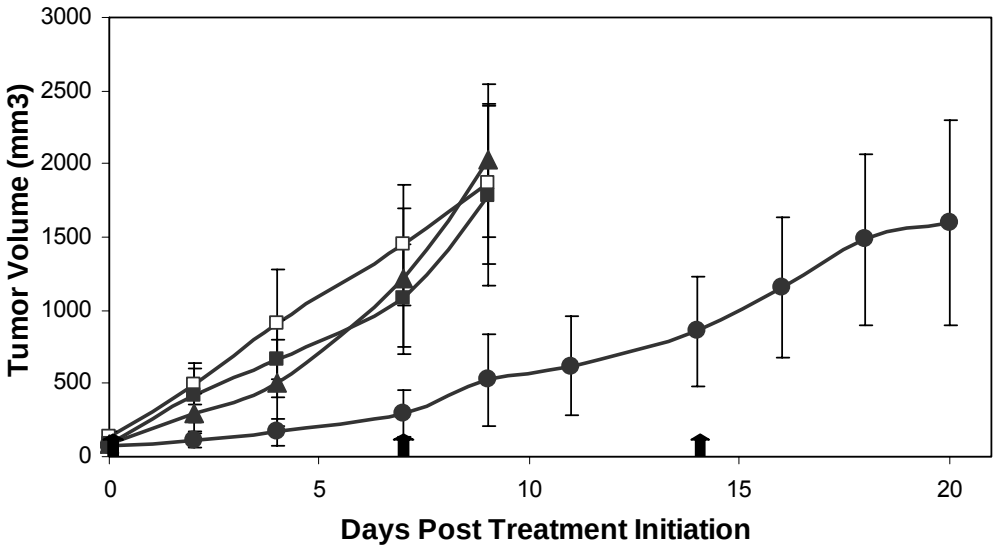

Figure 23. Therapy of SCID/Human Non-Small Cell Lung Cancer Mice with UV3 IgG Versus Its F(ab')$_2$ Fragments.

Female SCID mice, 6-8 weeks of age, were injected s.c. with 1 x 10^6 NCI-H157 human NSC lung cancer cells. Tumor volumes were measured using calipers and calculated as Volume = W^2 x L ÷ 2. When the tumors reached 100 mm^3, the mice were either untreated (□) or injected i.p. with 0.3 mg UV3 (●), 0.3 mg isotype-matched control antibody (■), or 1.5 mg UV3 F(ab')$_2$ fragments (▲) once every 7 days, as indicated on the figure (arrows). The mice were sacrificed when the solid tumors reached 2000 mm^3. Treatment with UV3 F(ab')$_2$ fragments had no effect on solid tumor growth as compared to the isotype control ($p > 0.80$). F(ab')$_2$ fragments of UV3 were significantly less effective than the IgG ($p < 0.05$). This figure depicts the average of three experiments, with 5-10 mice per group in each experiment.

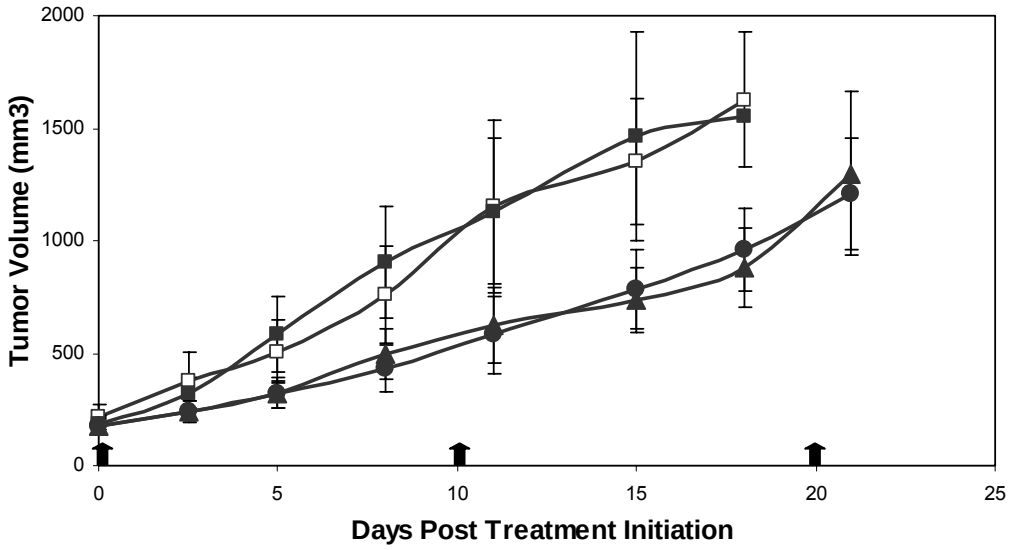

Figure 24. Therapy of SCID/Human Pancreatic Cancer Mice with UV3 IgG Versus Its F(ab')$_2$ Fragments.

Female SCID mice, 6-8 weeks of age, were irradiated with 150 rads and injected s.c. 24 hours later with 1 x 10^6 BxPC-3 cells. Tumor volumes were measured using calipers and calculated as Volume = W^2 x L ÷ 2. When the tumors reached 200 mm^3, the mice were either untreated (□) or injected i.p. with 0.3 mg UV3 (●), 0.3 mg isotype-matched control antibody (■), or 1.5 mg UV3 F(ab')$_2$ fragments (▲) once every 10 days, as indicated on the figure (arrows). The mice were sacrificed when the solid tumors reached 2000 mm^3. Both IgG UV3 and its F(ab')$_2$ fragments significantly slowed tumor growth as compared to the isotype control ($p < 0.01$). The efficacy of therapy with UV3 versus its F(ab')$_2$ fragments was not different at any time point ($p > 0.50$). This figure depicts the average of two experiments, with 5-10 mice per group in each experiment.

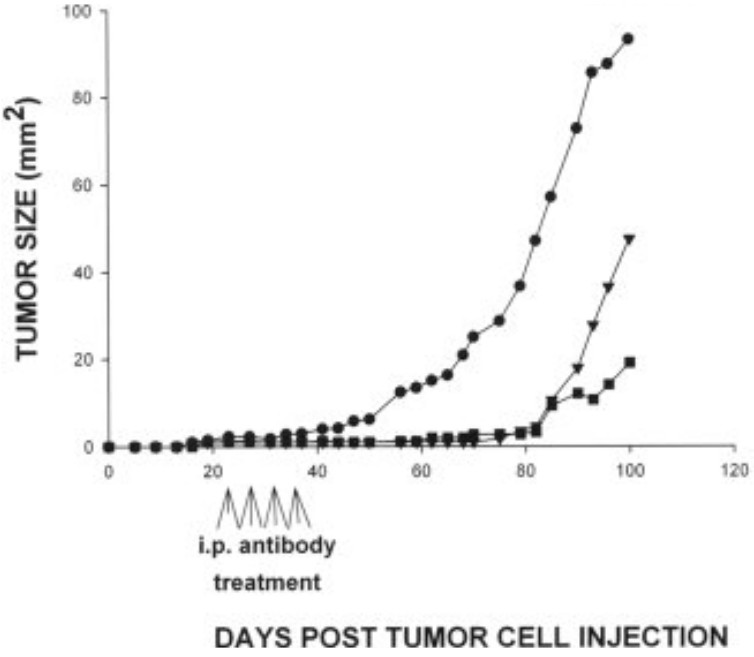

Figure 25. Therapy of SCID/Subcutaneous Human Uveal Melanoma Mice with UV3 IgG Versus Its F(ab')$_2$ Fragments.

Female SCID/beige mice, 6-8 weeks of age, were injected s.c. with 1 x 10^7 OCM-3 cells. Tumors were measured using calipers and calculated as W x L for the two largest tumor diameters. When tumors became palpable, the mice were injected i.p. with 100 µg of isotype-matched control antibody (●), UV3 (■), or F(ab')$_2$ fragments (▲) for 4 consecutive days, as indicated on the figure (arrows). The mice were sacrificed when the solid tumors reached 100 mm^2. Injection with UV3 or its F(ab')$_2$ fragments significantly slowed tumor growth as compared to the control, and appeared to have roughly similar anti-tumor efficacy. This figure is representative of two separate experiments each with 5 mice per group [211].

This figure is reprinted from S. Wang, et al. (2006) Int J Cancer 118:932-941 with the permission of Wiley-Liss, Inc., a subsidiary of John Wiley & Sons, Inc.

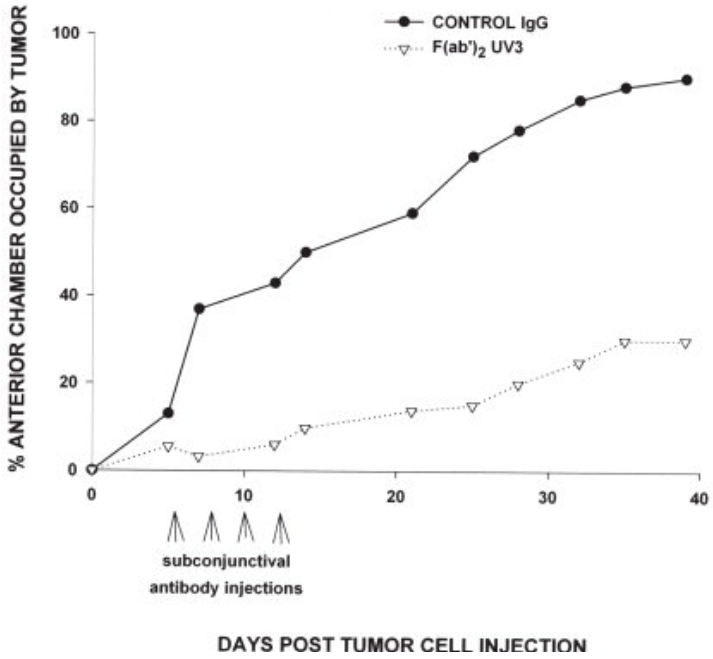

Figure 26. Therapy of SCID/Intraocular Human Uveal Melanoma Mice with UV3 IgG Versus Its F(ab')$_2$ Fragments.

Female SCID/beige mice, 6-8 weeks of age, were injected with 3 x 10^5 OCM-3 cells in the anterior chamber of the eye. Tumor size was described as the percentage of the anterior chamber occupied by tumor. The mice were injected subconjunctivally with 20 µg of isotype-matched control antibody (●) or 100 µg of F(ab')$_2$ fragments of UV3 (∆) on days 0, 2, 4, and 6 following tumor inoculation for a total of four injections, as indicated on the figure (arrows). As compared to the isotype control, F(ab')$_2$ fragments of UV3 slowed the growth of the intraocular tumors. This figure is representative of two separate experiments each with 5 mice per group[211].

This figure is reprinted from S. Wang, et al. (2006) Int J Cancer 118:932-941 with the permission of Wiley-Liss, Inc., a subsidiary of John Wiley & Sons, Inc.

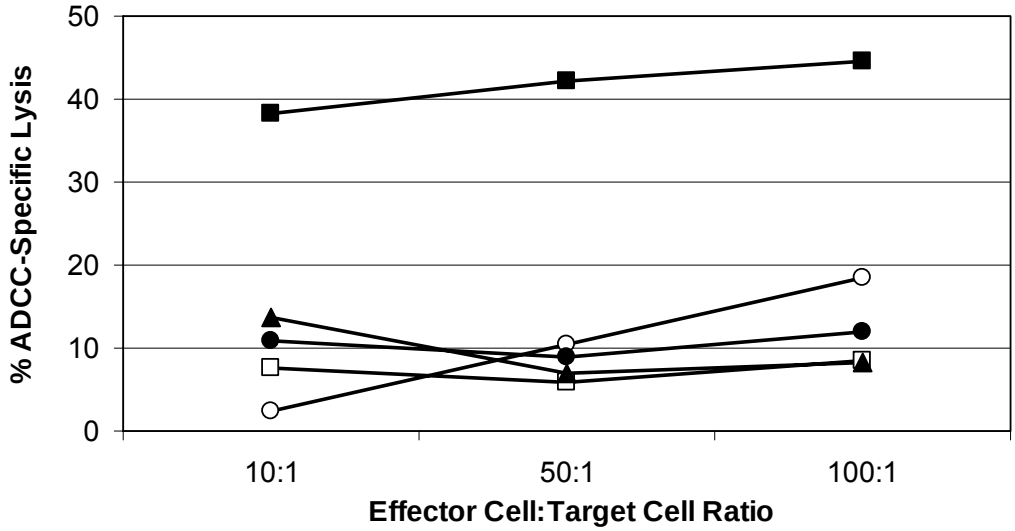

Figure 27. UV3 Mediated ADCC of Human Tumor Cell Lines *In Vitro*.

Tumor cells labeled with ^{51}Chromium were incubated for 4 hours with activated mouse splenocytes (effector cells) at the Effector Cell:Target Cell (E:T) ratios indicated in the presence of UV3 or control antibody. ^{51}Chromium released from lysed target cells was measured using a gamma counter. Cell lines with significant UV3-mediated ADCC are shown: BxPC-3 (□; $p < 0.05$), Daudi (○; $p < 0.05$), KM-3 (■; $p < 0.001$), NCI-H157 (●; $p < 0.005$), and OCM-3 (▲; $p < 0.001$) for all three E:T ratios. UV3 did not mediate ADCC of the CD54$^-$ BT-474 ($p > 0.1$) and LNCaP cell lines ($p > 0.1$) or the CD54$^+$ 397 ($p > 0.1$), MDA-MB-435 ($p > 0.1$), and PC-3 cell lines ($p > 0.05$). Significance was determined by comparing values from tumor cells incubated with effector cells in the presence of an isotype control. The data shown represent the average values of at least three experiments.

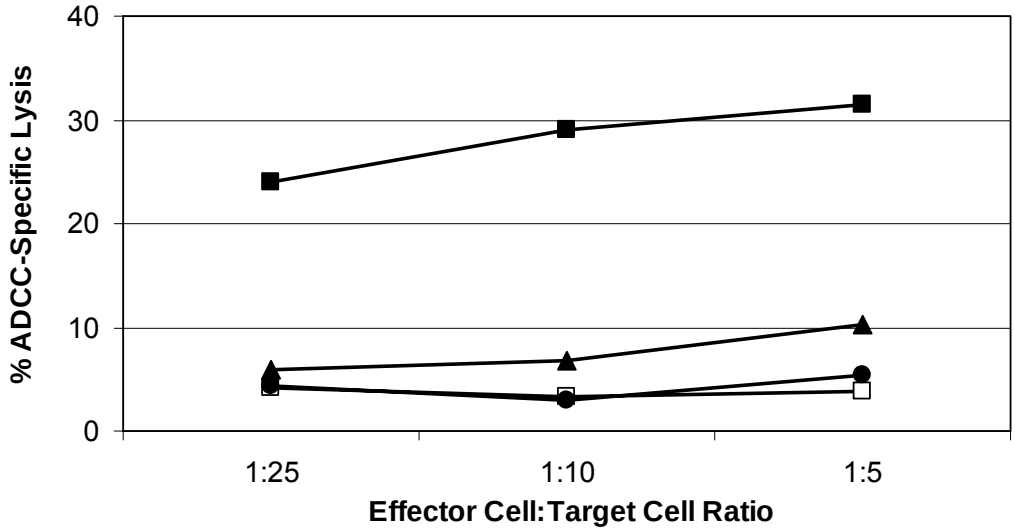

Figure 28. UV3 Mediated CDC of Human Tumor Cell Lines *In Vitro*.

Tumor cells labeled with ^{51}Chromium were incubated for 4 hours with rabbit serum at the dilutions indicated in the presence of UV3 or control antibody. ^{51}Chromium released from lysed target cells was measured using a gamma counter. Cell lines with significant UV3-mediated CDC are shown: BxPC-3 (□; $p < 0.01$), KM-3 (■; $p < 0.001$), NCI-H157 (●; $p < 0.001$), and OCM-3 (▲; $p < 0.001$) at all three serum dilutions. UV3 did not mediate CDC of the CD54$^-$ BT-474 ($p > 0.05$) and LNCaP ($p > 0.8$) cell lines or the CD54$^+$ 397 ($p > 0.05$), Daudi ($p > 0.05$), MDA-MB-435 ($p > 0.6$), and PC-3 ($p > 0.06$) cell lines. Significance was determined by comparing values from tumor cells incubated with rabbit serum in the presence of an isotype control. The data shown represent the average values of at least three experiments.

Table 5. Comparison of the Fc Portion of UV3 Among Several Human Tumor Cell Lines.

		In Vitro		*In Vivo*
Cancer Type	**Cell Line**	**ADCC**	**CDC**	**F(ab')$_2$ Activity**
Breast Cancer	BT-474 (CD54$^-$)	-	-	N/A
	MDA-MB-435	-	-	N/A
Lung Cancer (NSC)	NCI-H157	++	+	Not Effective
Lymphoma (NHL)	Daudi (disseminated)	++	-	Intermediate
	Daudi (s.c.)			Intermediate
Melanoma	397	-	-	N/A
Melanoma (Uveal)	OCM-3 (s.c.)	+	++	Similar to UV3
	OCM-3 (intraocular)			Similar to UV3
Multiple Myeloma	KM-3	+++	+++	N/A
Pancreatic Cancer	BxPC-3	+	+	Similar to UV3
Prostate Cancer	LNCaP (CD54$^-$)	-	-	N/A
	PC-3	-	-	Similar to UV3

These data for the cell lines and tumor models listed are summarized from Figures 20-28. For ADCC data, an E:T of 100:1 was used; for CDC data, a serum dilution of 1:5 was used.

- Indicates that no lysis was observed.

+ Indicates the values remain under 10% lysis as compared to the control.

++ Indicates the values are between 10-20% lysis as compared to the control.

+++ Indicates the values are over 20% lysis as compared to the control.

N/A Indicates data not available.

Chapter 4: Discussion

A. Study Objectives and Major Findings.

The anti-CD54 MAb UV3 was developed as a novel therapy for multiple myeloma[94]. When administered to SCID/human multiple myeloma mice with advanced disease, UV3 was curative[96]. UV3 specifically recognizes human CD54[94], an adhesion molecule that is up-regulated in some cancers, including multiple myeloma[102, 130, 133, 181]. Since UV3 was highly effective in SCID/multiple myeloma mice, it was hypothesized that UV3 might have anti-tumor activity against other human tumors that express CD54.

The purpose of this study was to investigate the anti-tumor activity of UV3 in a variety of tumor types, with the goal of using these data to move UV3 forward into clinical trials. Several objectives were outlined for this study: 1) to examine the CD54 expression of a panel of human tumor cell lines, 2) to investigate the anti-tumor activity of UV3 in SCID mice with human tumors, 3) to determine whether the *in vivo* anti-tumor activity of UV3 was CD54-specific, 4) to compare the *in vivo* anti-tumor activity of murine UV3 and cUV3 in several tumor models, 5) to examine therapy optimization in two tumor models, 6) to determine whether combination

with a chemotherapeutic drug further enhances the anti-tumor activity of UV3 in SCID mice, and 7) to investigate some of the mechanisms underlying the anti-tumor activity of UV3.

The major findings to emerge from this study are that UV3 does have anti-tumor activity in several $CD54^{+}$ human tumors grown in SCID mice, and that tumor growth is further slowed when UV3 is injected in combination with the chemotherapeutic drug gemcitabine. In addition, it is suggested that UV3 may mediate its activity through multiple mechanisms, including Fc effector functions, and that the roles of these mechanisms are tumor-specific.

B. UV3 Has Anti-Tumor Activity in SCID Mice with Human Tumor Cell Lines.

UV3 is CD54-Specific *In Vivo*.

Since UV3 has demonstrated anti-tumor activity *in vivo* in this and previous studies[96], it was important to determine whether its activity was CD54-specific. To this end, UV3 was administered in parallel to SCID mice with subcutaneous $CD54^+$ or $CD54^-$ human breast tumors. As expected, UV3 had anti-tumor activity against the $CD54^+$ tumors but not the $CD54^-$ tumors. This result indicates the *in vivo* activity of UV3 is dependent upon the binding of UV3 to CD54 on the surface of the human tumor cells.

B Cell Non-Hodgkin's Lymphomas.

B cell non-Hodgkin's lymphoma is a group of fairly heterogeneous cancers of B cell origin, and the treatment options thus vary according to NHL type and stage but traditionally involved some combination of chemotherapy, radiation therapy, and hematopoietic stem cell transplant[127]. In the last decade several antibody therapies targeted to CD22 or CD20, such as Rituxan™ and the radioimmunoconjugates Bexxar™ and Zevalin™, have demonstrated activity with comparatively

reduced systemic toxicity in patients with B cell NHLs[50, 66, 122]. CD54 has also been consistently shown to be up-regulated in both NHLs in patients and in human lymphoma cell lines, although its relationhsip to disease progression is debated[56, 89, 91, 130, 204]. Therefore it is not surprising that all four lymphoma cell lines investigated in this study were $CD54^{+}$.

UV3 was then evaluated in SCID mice with human NHL tumors, and it was found to prolong survival in mice with disseminated disease and to delay the formation of palpable tumors and slow subsequent tumor growth in mice with subcutaneous lymphoma. In these experiments, UV3 was administered at a dose of 0.8 mg/kg mouse (2.4 mg/m^2 human equivalent) on each of four consecutive days (9.6 mg/m^2 total), which is much lower that the doses of either Rituxan™ (375 mg/m^2 weekly)[18] or epratuzumab (360 mg/m^2 weekly), an anti-CD22 MAb currently under evaluation in in patients with NHL both alone and in combination with Rituxan™[122]. These data indicate that higher doses of UV3 might be safe and more effective in treating NHL than the dose used in this study.

Breast Tumors.

In addition to advances in the traditional options of surgery, chemotherapy, radiation, and hormonal therapy for the treatment of

patients with breast cancer, the development of several targeted biologic therapies, most notably the anti-Her-2 MAb Herceptin™, have demonstrated efficacy in subsets of patients with tumors that overexpress Her-2. These targeted therapies have demonstrated activity with reduced toxicity, but not all breast cancers express the targeted antigens, suggesting a need for therapies targeting additional antigens[80, 141, 142]. CD54 is expressed on some breast cancer cell lines and patient specimens, but its expression is variable and has not been related to disease progression[21, 38, 147, 165]. In this study we investigated the reactivity of UV3 with four human breast cancer cell lines and found that over 98% of cells were $CD54^+$ in two human breast cancer cell lines and 64% of the cells were $CD54^+$ in a third cell line; one cell line did not express CD54.

UV3 was further investigated for its anti-tumor activity in SCID mice with $CD54^+$ human breast tumors. In this model administration of UV3 significantly slowed the growth of established tumors, with UV3-treated tumors requiring over twice as long to reach maximal size. Additionally, the dose used in this model was approximately 112.5 mg/m^2, over three-fold lower than the dose of Herceptin™ recommended for patients with breast cancer (375 mg/m^2)[14]. Therefore, UV3 may demonstrate further therapeutic potential at higher doses. Although the expression of

membrane-bound CD54 on breast cancer cells is variable, the presence of soluble CD54 is more consistent[23, 114]. The effect of UV3 on the secretion of sCD54 by cancer cells has not yet been determined, but UV3 might have therapeutic activity in breast cancers that express either the membrane-bound or the soluble forms.

Prostate Tumors.

Several prostate cancer cell lines have previously been characterized as $CD54^+$, although the relationship between the expression of CD54 and cancer progression or metastasis is not well understood in prostate cancer[40, 163, 217]. In this study, over 85% of cells stained with UV3 were $CD54^+$ in four of five cell lines; the one $CD54^-$ cell line, LNCaP, had previously been shown to be negative[40, 163, 217].

When UV3 was tested in SCID mice with established PC-3 tumors it significantly slowed tumor growth, even though it was used at a dose lower than that recommended for any FDA-approved anti-cancer MAb (1.2 mg/kg UV3 vs. 1.5 mg/kg Campath™ per 10-day period)[3]. The PC-3 cell line is androgen-independent[103], and this model thus represents therapy of advanced hormone-refractory disease. While early prostate cancer may be effectively treated with currently available therapies, hormone-refractory disease exhibits a reduced response to traditional

chemotherapy, and newer, more effective treatments are needed[83, 84]. Based on these results, anti-CD54 therapy in the form of UV3 MAb may represent an effective therapy for prostate cancer.

Non-Small Cell Lung Tumors.

Despite ongoing research to identify more effective treatment options, lung cancer remains the second leading cancer in estimated incidence and the leading cancer in estimated deaths for both men and women in the U.S.[4, 101]. Among the advances for treatment of patients with NSC lung cancer are the identification of EGFR and VEGF as therapeutic targets and the demonstration that immunotherapy can be effective in this cancer[43, 82, 129]. Although not all lung cancer types express CD54, the literature has consistently demonstrated up-regulated expression of CD54 on NSC lung tumor cell lines and on NSC lung tumor cells and tumor-associated cells from patient specimens[125, 133, 153, 171, 191]. Some studies have even demonstrated a correlation between CD54 expression and a greater risk for advanced cancer[125]. In this study, over 90% of cells in 4 of the 5 NSC lung tumor lines investigated expressed CD54, further indicating that NSC lung cancer is an appropriate target for UV3 therapy.

Initial experiments investigating UV3 therapy in SCID/NSC lung cancer mice showed that UV3 had anti-tumor activity, slowing the growth of established subcutaneous tumors. Optimization experiments raised the dose to 1.5 mg every 10 days and demonstrated improved anti-tumor efficacy; however this dose was still not curative. A dose of 1.5 mg UV3 in SCID mice (about 20 g) corresponds to approximately 225 mg/m^2 in patients, and is lower than the suggested dose for some other MAbs (Rituxan™ at 375 mg/m^2 weekly, Avastin™ at 370 mg/m^2 every 14 days, Erbitux™ at 400 mg/m^2 initially then 250 mg/m^2 weekly)[1, 13, 18]. Based on these antibody doses, it may be possible to further increase the dose of UV3 in patients.

One possibility for the decrease in UV3 activity in the later stages of disease progression is that UV3 caused a reduction in expression of CD54 on tumor cells. To investigate this possibility, tumors were excised from UV3- or control-treated mice and analyzed for surface expression of CD54 by flow cytometry. Only live cells were analyzed, and the percentage of $CD54^+$ tumor cells was determined. A significant percentage of tumor cells expressed CD54, regardless of *in vivo* treatment, but UV3 therapy did decrease the percentage of $CD54^+$ tumor cells. There was also a slight decrease in the density of CD54 expressed on UV3-treated tumor cells, but this change was not significant due to variations in MFI among

different tumor specimens. Additionally, among tumor cells stained *in vitro* with the control antibody, the percentage of positive cells was similar regardless of what therapy the mice had previously received. Therefore, it was concluded that UV3 from prior *in vivo* therapy was no longer bound to the tumor cells at the time of this assay. It should also be noted that the tumor suspensions contained both human tumor cells and mouse tumor-associated cells, such as mouse endothelial cells, stromal cells, and infiltrating lymphocytes[27]. However, all of the $CD54^+$ cells identified were human tumor cells because UV3 only recognizes human CD54 (and not mouse CD54)[94]. This may explain why only 37% of the cells in the untreated tumor preparation were $CD54^+$. So, while the exact percentage of $CD54^+$ human tumor cells could not be determined, the relative percentages of UV3 and control-treated tumor cells stained with anti-CD54 could be compared with each other and against isotype control-stained cells. Since UV3 was still expressed on the tumor cells, higher doses of antibody may have further improved anti-tumor activity.

Pancreatic Tumors.

Pancreatic cancer remains difficult to treat due to a lack of early diagnostic procedures and the limited efficacy of chemotherapy and radiation. Immunotherapy is now being considered as a source of more

effective treatment options, and some agents have already demonstrated modest activity in clinical trials and pre-clinical studies, including MAbs against EGFR, VEGF, and other targets[117]. The over-expression of CD54 on pancreatic tumor cell lines and patient specimens has previously been described, indicating anti-CD54 therapy might demonstrate activity[158, 178, 180, 181]. In this study two pancreatic tumor cell lines were examined for CD54 expression using UV3, and both were found to consist of greater than 85% $CD54^+$ cells.

To examine the activity of anti-CD54 therapy, SCID/pancreatic tumor mice were treated with UV3, and the growth of solid tumors was monitored. Experiments designed to optimize therapy were then carried out with 1.5 mg of UV3 every 10 days. This dose increased the anti-tumor activity of UV3, but was still not curative. Higher doses of UV3 have not yet been investigated, but may have even stronger anti-tumor activity. Since the current recommended doses for some other MAbs are higher than 1.5 mg, it may be possible to further raise the dose of UV3 without an increase in adverse reactions.

The expression of surface CD54 was examined by flow cytometry on pancreatic tumors excised from mice treated with UV3 or an isotype-matched control. There was a significant percentage of $CD54^+$ cells in tumors removed from mice in both treatment groups, and there was no

difference between the groups. There was a slight, but non-significant, drop in the density of CD54 on the tumor cells. CD54 was still expressed on a large percentage of the tumor cells, indicating that higher doses of UV3 may demonstrate further improved anti-tumor efficacy.

In summary, *in vivo* therapy with UV3 did not affect the expression of CD54 on tumors in SCID/pancreatic mice and only moderately affected the expression of CD54 on tumors in SCID/NSC lung cancer mice. Therefore, if the expression of CD54 is reduced during tumor progression, it is unlikely to be due to therapy with UV3. Unfortunately, CD54 expression on the suspensions of cells from excised tumors could not be reliably compared with that on the original tumor cell lines in this assay.

Other possible explanations for the loss of efficacy of UV3 over time include reduced penetration due to an increase in tumor bulk[104, 138] and the escape of tumor stem cells. Cancer stem cells are a relatively recently recognized type of cell found in most tumors, and they could represent a source of self-renewing tumor cells, although their role remains to be further investigated in tumor cell lines. Such stem cells are not as differentiated and divide more slowly than other tumor cells. They are therefore not targeted well by most traditional therapies, leading to relapse[137, 149].

Cutaneous and Uveal Melanomas.

Melanomas of both ocular and skin origin were investigated in this study. Cutaneous melanoma is successfully treated through surgery for a majority of patients with early, localized disease, but the mortality rates for patients with metastatic disease remains high due to its resistance to systemic chemotherapy. Therefore, current research is focused on the evaluation of a wide spectrum of immunotherapy strategies, including therapies targeting B-RAF, $\alpha_5\beta_1$ integrin, and CTLA-4[203, 213]. For cutaneous melanomas, CD54 expression has been shown to correlate with metastatic potential[102]. In this study a panel of six melanoma cell lines was examined for CD54 expression, and all six were found to contain a high percentage of $CD54^+$ cells. Based on these data, UV3 is being perused as a potential anti-tumor therapy in a mouse xenograft model of cutaneous melanoma.

Localized uveal melanomas are typically treated with a combination of radiation therapy and surgery, but approximately 50% eventually become metastatic even with initial therapy. For metastatic uveal melanoma, the prognosis remains poor despite improvements in systemic chemotherapy regimens because this cancer metastasizes to the liver. Therefore, various immunotherapeutic and anti-angiogenic options are now being explored for metastatic disease[58, 184]. Although uveal

melanomas are biologically quite different from cutaneous melanomas, CD54 expression has been demonstrated on both patient specimens and tumor cell lines[24, 33]. Seven human uveal melanoma cell lines and three metastatic cell lines have been evaluated for reactivity with UV3 in this and previous studies, and 7 of the 10 cell lines were found to contain greater than 70% of $CD54^+$ cells, with an eighth cell line containing approximately 25% $CD54^+$ cells[211]. These results indicated that UV3 might be beneficial for some patients with uveal melanoma.

To test the efficacy of anti-CD54 therapy, SCID/beige mice were treated with UV3 or an isotype-matched control antibody either immediately following intraocular or subcutaneous inoculation with uveal melanoma cells or after the tumors were established. In mice with subcutaneous tumors, therapy delayed the formation of palpable tumors and slowed the growth of established tumors. When given to mice with intraocular tumors, UV3 slowed tumor growth and, in some experiments, caused a decrease in tumor size[211]. These results suggest UV3 may provide a therapeutic benefit for patients with $CD54^+$ ocular tumors.

Not surprisingly, the different human tumor cell lines grew at different rates in SCID mice; some tumor types are naturally more aggressive. In the case of the NSC lung tumor cells, the most aggressively-growing tumor, UV3 therapy was increased from once every

10 days to once every 7 days to compensate for the growth rate. However, there was no obvious relationship between the rate of tumor growth and the efficacy of UV3, although the different rates of tumor growth made it difficult to statistically compare the efficacy of UV3 therapy among tumor models. UV3 had statistically significant activity in all of the tumors studied, but was not curative.

UV3 and cUV3 Have Equivalent Anti-Tumor Activity.

UV3 and cUV3 were previously shown to have identical binding affinities to the ARH-77 and KM-3 human multiple myeloma cell lines and similar anti-tumor activity in SCID/ARH-77 mice[187]. In this study UV3 and cUV3 were further compared and shown to have equivalent anti-tumor activity in SCID mice with either disseminated Daudi lymphoma tumors or subcutaneous PC-3 prostate tumors. Therefore, cUV3 and murine UV3 have similar activity in all three xenograft models of tested, suggesting that its activity will be similar to UV3 in a variety of other tumor types as well. This is an important point, since chimerized UV3 will be used in clinical trials. As compared to mouse MAbs, chimeric MAbs, which contain human constant regions and murine variable regions, are less immunogenic in humans[42, 104]. Further testing on cUV3 is currently underway, with plans to move cUV3 into clinical trials.

C. Combination Therapy of UV3 and Gemcitabine Further Slowed Tumor Growth in SCID Mice.

Years ago it was recognized that combination therapies had the potential to be more beneficial than single anti-tumor agents because of subtle variations between patients and the heterologous nature of the cells within tumors. In addition, cancer stem cells that escape therapy can re-grow, and cancer cells can become drug resistant, no longer responding to therapy[27, 137, 146, 149, 199]. Together, multiple agents can attack tumor cells through different mechanisms, killing tumor cells that might be resistant to a single therapy and therefore making it more likely that all the cells are killed. In some cases anti-tumor agents can even work in a synergistic manner. Another potential benefit in using a combination therapy is the decrease in dosage of the individual agents and thus the severity of their associated adverse effects.

The anti-tumor activity of MAbs in combination with many other therapies has been investigated in numerous pre-clinical experiments and clinical trials. The specific chemotherapy drugs chosen for evaluation of combination therapies depend upon previously demonstrated anti-tumor activity in the cancer type investigated and the potential for interacting mechanisms of action. Clinical trials demonstrated an improved anti-

cancer activity for Avastin™ in combination with chemotherapeutic drugs as compared to the administration of either Avastin™ or chemotherapy alone[97, 98, 100, 169, 196]. Based on these results, Avastin™ is now indicated for the therapy of colorectal cancer in combination with 5-FU-based chemotherapy and for the therapy of NSC lung cancer in combination with carboplatin and paclitaxel[1]. Although Campath™ is currently FDA-approved as a single agent therapy, initial clinical trials show improved anti-tumor activity in combination with fludarabine and clyclophosphamide[22, 109]. Erbitux™ is FDA-approved for patients with metastatic colorectal cancer in combination with irinotecan based on clinical studies indicating the combination was significantly more effective than either monotherapy, even in irinotecan-refractory patients[34, 57, 207]. Although it is traditionally combined with radiation therapy in head and neck cancers[13], Erbitux™ in combination with 5-FU and platinum-based chemotherapy has also shown improved activity in these cancers, and other combinations are currently being evaluated[150]. Although Vectibix™ has not been as well studied as other approved MAbs since it is a newer therapy, it is likely that effective combination therapies for it will be similar to those of Erbitux™, as they are both anti-EGFR MAbs. Herceptin™ was FDA-approved for the treatment of breast cancer patients when given in combination with cyclophosphamide, docetaxel, and

paclitaxel after clinical studies demonstrated the synergistic activity of these chemotherapy drugs with Herceptin™[67, 131, 142, 179, 186]. Rituxan™ is often combined with several chemotherapeutic agents depending upon the sub-type and stage of NHL, and it has shown synergistic activity in combination with a variety of different drugs[18, 50, 68]. In addition to the traditional combination therapy regimens involving MAbs with chemotherapy agents, some MAbs have also demonstrated improved activity when combined with small molecule targeted agents (such as the EGFR tyrosine kinase inhibitor erlotinib), other MAbs, immunoconjugates, radiation therapy, and even hormonal therapy, depending upon the cancer type investigated[22, 61, 75, 80, 170].

For this study the investigation of combination therapies was limited to two xenograft tumor models, SCID/pancreatic cancer and SCID/NSC lung cancer. Since the mechanisms of action of UV3 are not yet well understood and synergistic activities could not be predicted, standard chemotherapy was used for the initial combination studies. The chemotherapy drug gemcitabine was chosen because it is one of the few agents approved by the FDA for the treatment of either NSC lung cancer or pancreatic cancer[16]. Gemcitabine is now considered standard therapy for pancreatic cancer and is becoming a common treatment for NSC lung

cancer because it is better tolerated than other chemotherapeutic drugs[7, 10, 16].

In this study, UV3 therapy was therapeutically similar to 150 and 300 mg/kg of gemcitabine in SCID mice with established NSC lung or pancreatic tumors. When UV3 and gemcitabine were administered together, they significantly slowed tumor growth in the mice as compared with either agent alone. The observed effect was additive, not synergistic, which is not surprising since UV3 and gemcitabine work via different pathways. Hence, while UV3 does not directly inhibit tumor cell proliferation, gemcitabine induces cell cycle arrest due to the inhibition of DNA replication and repair. Both the pancreatic and NSC lung cancer cell lines evaluated are highly aggressive, growing quickly in SCID mice, and the tumor outgrowth in mice receiving combination therapy indicates either that doses were too low or that some tumor cells were resistant to both UV3 and chemotherapy.

Other combination therapies might be more rationally designed once the mechanisms of action of UV3 are better understood. In addition, current studies are aimed at investigating potential combination therapies in SCID/lymphoma mice (L. Pop, unpublished data), and combination therapies are planned in other xenograft tumor models.

D. Mechanisms of Action of UV3.

It is important not only to examine the anti-tumor activity of new MAb therapies, but also, if possible, how they mediate their activity. This information may help to predict potential side effects, identify patients for whom therapy would be most effective, aid in selecting appropriate combination therapies, and even predict its therapeutic activity in other diseases. MAbs mediate their activity through a variety of mechanisms[198]. Although other anti-cancer MAbs primarily mediate their activity through Fc effector functions[49], some Fc-independent mechanisms are likely still involved.

Potential mechanisms of action of UV3 were previously investigated in multiple myeloma. UV3 did not induce tumor cell apoptosis or cell cycle arrest, nor did it interfere with *in vitro* adhesion of tumor cells to one another or to the bone marrow stroma[96], although other studies have since implicated CD54 in the mediation of post-homing events in metastatic lymphoma[25, 118]. UV3 may have reduced the expression and secretion of pro-angiogenic factors by myeloma cells, but these data were not conclusive[51]. The Fc of UV3 was required for activity in multiple myeloma, as $F(ab')_2$ fragments of UV3 were not effective in SCID/multiple myeloma mice and UV3 mediated both ADCC and CDC of

myeloma cells *in vitro*[51, 96]. Investigations into the mechanisms of UV3 become more complicated when considering other possibilities suggested in the literature and other tumor types, since UV3 may mediate its effect differently in each tumor.

UV3 Does Not Inhibit Tumor Cell Proliferation.

UV3 did not inhibit proliferation or induce apoptosis in any of the human tumor cell lines tested, regardless of CD54 expression, even at concentrations as high as 1 mg/mL. These data suggest that UV3 does not directly cause the death of the tumor cells, but mediates its activity through other mechanisms. However, one recent paper comparing the effect of different protocols on the proliferation of lymphocytes in the presence of the anti-CD28 MAb TGN1412 found that even though cellular proliferation was not affected by soluble antibody, proliferation was increased when a cross-linking anti-Fc antibody was dried on the culture plate prior to incubation with TGN1412[194]. In another recent publication, the authors found that cross-linking of an anti-CD54 MAb (not UV3) induced apoptosis of two human Burkitt's lymphoma cell lines[111]. Preliminary experiments in our laboratory have not shown similar results with UV3 and these cell lines (L. Pop, unpublished data). Still, it is possible that UV3 may induce apoptosis or cell cycle arrest under cross-linking

conditions in some tumor cell lines, even though aqueous UV3 does not, and this is a possibility that will be examined in the future. It has also been shown with other MAbs that a lack of direct *in vitro* tumor cell inhibition does not necessarily predict *in vivo* anti-tumor activity[71], as appears to be the case with UV3.

Importance of the Fc to the Activity of UV3.

The most widely recognized mechanisms of action of MAbs are ADCC and CDC. Some MAbs currently approved for cancer therapy, such as Herceptin™ and Rituxan™, are thought to work primarily through effector functions[49]. To address this issue with UV3, the anti-tumor activity of $F(ab')_2$ fragments of UV3, which lack the Fc portion of the antibody, were examined *in vitro* in SCID mice xenografted with human tumor cell lines and the ability to mediate ADCC and CDC was examined *in vitro* in the presence of effector cells or complement.

Fc-Independent Activity.

UV3 $F(ab')_2$ fragments were as effective as the IgG in SCID/prostate cancer mice, and the PC-3 prostate cancer cell line was not lysed by ADCC or CDC in the presence of UV3. These results suggest that Fc effector mechanisms are either not important to the anti-tumor

activity of UV3 in this model or that other, Fc-independent mechanisms are able to compensate in the absence of an Fc. Although they are likely still be involved *in vivo*, Fc-dependent mechanisms are not essential to the anti-tumor activity of UV3 in this model of prostate cancer.

Tumor growth in SCID/pancreatic mice treated with $F(ab')_2$ fragments of UV3 was similar to treatment with the IgG, indicating that Fc-independent mechanisms of action must be involved. However, the BxPC-3 pancreatic tumor cell line was lysed by both ADCC and CDC in the presence of UV3 *in vitro*, suggesting that UV3 does mediate Fc effector mechanisms. Therefore, both Fc-dependent and Fc-independent mechanisms are present in this model. While the Fc effector mechanisms may be important for the activity of UV3, Fc-independent mechanisms are able to compensate *in vivo* when the Fc is absent.

The anti-tumor activity of $F(ab')_2$ fragments of UV3 were investigated in both a subcutaneous and an intraocular model of uveal melanoma in SCID/beige mice. In both xenograft models $F(ab')_2$ fragments had an activity similar to UV3 IgG. However, the OCM-3 uveal melanoma cell line was lysed *in vitro* by both ADCC and CDC in the presence of UV3. These data indicate that while UV3 does mediate Fc effector mechanisms in uveal melanoma, based on the *in vitro* data, Fc-independent mechanisms must also be important to the activity of UV3 in

uveal melanoma since the F(ab')$_2$ fragments were able to slow tumor growth in the absence of an Fc.

Although the Fc portion of UV3 does not appear to be required for activity against some tumors in SCID mice, it should be noted that SCID mice are capable of lysing cells via both ADCC and CDC in the presence of intact MAbs. While SCID mice develop few T cells and B cells, they do have normal levels of complement protein and active NK effector cells [30, 62]. Complement from normal rabbit sera was used in the CDC in vitro assays for cost and convenience. Spleens from non-immunocompromized mice were used as the source of activated effector cells in the in vitro ADCC assays because higher ratios of effector cells to target cells are required when using SCID mice [62].

Fc-"Intermediate" Activity.

In SCID/Daudi lymphoma mice F(ab')$_2$ fragments of UV3 demonstrated anti-tumor activity, but were not as effective as intact UV3. This intermediate activity was observed in both a disseminated and a subcutaneous model of Daudi lymphoma. In addition, UV3 mediated ADCC, but not CDC, of the Daudi cell line *in vitro*. Together these data indicate important roles for both Fc-dependent and Fc-independent mechanisms of UV3 activity in lymphoma.

Fc-Dependent Activity.

SCID/NSC lung cancer mice injected with $F(ab')_2$ fragments of UV3 had tumor growth curves similar to mice treated with control antibody, indicating a lack of UV3 activity in the absence of Fc effector mechanisms. Additionally, NCI-H157 cells were lysed by ADCC and CDC in the presence of UV3 *in vitro*, again indicating an important role for Fc-dependent mechanisms in this tumor model.

Alternately, the observed lack of activity of the $F(ab')_2$ fragments could be due to their faster clearance rate as compared to intact IgG. The faster clearance rate may have been responsible, at least in part, for the reduced efficacy of $F(ab')_2$ fragments observed in the NSC lung cancer, lymphoma, and multiple myeloma xenograft models, despite the higher dose of fragments administered. It is possible that a combination of factors are involved, including more rapid clearance, the absence of available Fc effector mechanisms, and a lack of compensation from other anti-tumor mechanisms.

Conclusions.

In addition to results from the tumor models discussed above, two $CD54^+$ cell lines, the 397 melanoma and MDA-MB-435 breast cancer cell lines, demonstrated no ADCC or CDC lysis *in vitro*. These two cell lines

have not been examined *in vivo* for $F(ab')_2$ activity, however, so a complete picture of Fc effector mechanisms is not available. $F(ab')_2$ fragments of UV3 demonstrated no *in vivo* activity in SCID/ARH-77 multiple myeloma mice, but UV3 mediated ADCC and CDC lysis of both the ARH-77 and KM3 myeloma cell lines *in vitro*[96, 187].

Overall, the Fc portion of UV3 was demonstrated to be important to its activity in almost all of the $CD54^+$ tumor cell lines investigated, either by a lack of full $F(ab')_2$ fragment efficacy *in vivo* or by significant ADCC and CDC lysis *in vitro*. However, most of the tumor xenograft models also demonstrated a role for Fc-independent mechanisms of action *in vivo*.

Investigations into the mechanisms of UV3 suggest a role for both Fc-dependent and Fc-independent mechanisms in most of the tumor xenograft models investigated. However, the dependence on the Fc varied greatly according to tumor type, and Fc-independent mechanisms have yet to be identified with certainty. While different tumor types share many characteristics, their complex tumor microenvironments are also unique, so certain mechanisms may be tumor-specific or have variable degrees of importance *in vivo*.

The fact that UV3 mediates ADCC and CDC is not surprising, since studies have demonstrated that murine IgG_{2a} antibodies, such as UV3, often have enhanced effector mechanism capabilities in mice as

compared to other IgG subclasses. IgG_{2a} antibodies also have a greater ability to prevent tumor metastases[145]. Although the strength of effector mechanisms of murine MAb isotypes does not directly translate to human isotypes, cUV3 (which has a human IgG_{1k} Fc) mediates ADCC and CDC *in vitro* and has anti-tumor activity in SCID mice that is similar to that of UV3[187]. In addition, other humanized or chimeric antibodies are thought to mediate their anti-tumor activity by Fc-dependent mechanisms, despite their ability to mediate Fc-independent mechanisms *in vitro*[49].

E. The Future of UV3 Immunotherapy.

UV3 was shown to be curative in SCID mice with human myeloma tumors[96], and will now be evaluated in clinical trials for multiple myeloma as a chimerized antibody[187]. It is expected that cUV3 will also enter clinical trials for other cancer types based on the data presented here. Although CD54 is involved in multiple immunologic processes, it is unlikely that cUV3 therapy will be associated with dangerous adverse effects in clinical trials since phase I/II studies in patients with rheumatoid arthritis have already demonstrated the safety of another anti-CD54 MAb, BIRR1. Patients in the clinical trials experienced only minor adverse effects, and the symptoms typically abated after the second day of therapy[106, 107].

However, the BIRR1 MAb used in these trials mediated its activity through immunosuppressive mechanisms, although no therapy-related infectious complications arose during the studies[106, 107]. Therefore, it is likely that cUV3 therapy will also be immunosuppressive. While immunosuppression is always a concern when treating patients, it is of particular concern in patients with immunosuppressive cancers, such as multiple myeloma or lymphoma, or in patients receiving other immunosuppressive therapies, including chemotherapy. Further immunosuppression of these patients could lead to opportunistic illnesses

that become life-threatening, interfere with the continuation of anti-cancer therapy, or prevent necessary palliative surgeries. At this time the suspected immunosuppressive activity of UV3 does not preclude it from being considered as a viable anti-cancer therapy, but the actual degree of immunosuppression in patients will have to be determined in clinical trials.

In addition to the planned clinical studies, there are still a number of pre-clinical studies to be completed. In the current studies, UV3 did not induce tumor cell apoptosis or cell cycle arrest *in vitro* in any of the human tumor cell lines investigated. On-going experiments include examination of Fc cross-linking on the ability of UV3 to induce apoptosis or cell cycle arrest in human tumor cells, which is currently underway (L. Pop, unpublished data). Experiments investigating the importance of the Fc to the activity of UV3 demonstrated that UV3 does mediate the effector mechanisms ADCC and CDC, but that UV3 also mediates Fc-independent mechanisms. Further work to elucidate the mechanisms of action is warranted. Additional signaling pathways might be identified through changes in the transcription of tumor cell proteins following UV3 treatment via gene arrays.

In addition, the therapeutic benefit of combining UV3 with chemotherapy agents is of interest, and to this end UV3 was combined with gemcitabine in the SCID/NSC lung cancer and SCID/pancreatic

cancer models. Combination therapy slowed tumor growth more effectively than either UV3 or gemcitabine alone. The investigation of UV3 in combination with chemotherapeutic drugs is currently underway in SCID/lymphoma mice (L. Pop, unpublished data). It is hoped that a better understanding of how UV3 mediates its activity will give us insights into the rational design of other combination therapies. However, in the absence of this information UV3 should be combined with current effective, standard therapies. Suggestions include different approved MAbs[5, 7, 9] or the chemotherapeutic drugs cyclophosphamide, doxorubicin, or vincristine for NHL[9]; cyclophosphamide for breast cancer[5]; docetaxel for prostate cancer[11]; the platinum drugs cisplatin or carboplatin for NSC lung cancer[7]; and dacarbazine or INF-α therapy for ocular and cutaneous melanomas[6, 12].

F. Conclusions.

MAbs targeted at tumor antigens have proven anti-cancer activity and have become important therapeutic options, either alone or in combination with other treatment modalities. Several MAbs have already been FDA-approved for the treatment of certain cancers, and their scope is rapidly expanding. MAbs are a valuable treatment option due to their ability to target antigens specifically expressed or up-regulated on tumor cells, reducing toxicity and adverse effects.

The objective of this study was to investigate the anti-tumor activity of a novel anti-CD54 MAb, UV3, in a variety of different tumor types. Since UV3 had previously been shown to be curative in SCID/multiple myeloma mice, it was important to evaluate its activity in other $CD54^+$ cancers. UV3 was tested in SCID xenograft models of an additional six tumors: lymphoma, breast cancer, prostate cancer, NSC lung cancer, pancreatic cancer, and uveal melanoma. UV3 slowed tumor growth and prolonged life in all six tumor models, although it was not curative. Both the optimization of UV3 therapy and the combination of UV3 with the chemotherapeutic drug gemcitabine led to significantly improved anti-tumor activity in SCID mice with NSC lung tumors or pancreatic tumors. Work to elucidate potential mechanisms of action for UV3 indicated that

both Fc-dependent and Fc-independent mechanisms are involved, but the role of individual mechanisms is still unclear.

The development of new and better cancer therapies is of obvious importance. In particular, major goals of this field are to develop therapies that have activity against a larger proportion of tumors, greater efficacy in patients with advanced and metastatic cancers, and reduced adverse effects. Novel MAbs, such as UV3, are one important developing treatment modality. UV3 will soon enter clinical trials based on the anti-tumor activity observed in mice. It is expected that UV3 will be safe in patients, based on previous Phase I/II clinical trials reporting the safety of another anti-CD54 MAb, and that UV3 will prove to be a valuable new anti-cancer therapy.

References

1. "Avastin (bevacizumab): Reach beyond convention". *Genentech, Inc.* February 2008. http://www.Avastin.com
2. "Bexxar (tositumomab and Iodine 131 tositumomab)". *GlaxoSmithKline.* February 2008. http://www.Bexxar.com
3. "Campath (alemtuzumab)". *Bayer HealthCare Pharmaceuticals.* February 2008. http://www.Campath.com
4. *Cancer Facts and Figures 2007*. Atlanta: American Cancer Society.
5. "Detailed Guide: Breast Cancer". *American Cancer Society.* May 2008. http://www.cancer.org
6. "Detailed Guide: Eye Cancer". *American Cancer Society.* May 2008. http://www.cancer.org
7. "Detailed Guide: Lung Cancer - Non-Small Cell". *American Cancer Society.* May 2008. http://www.cancer.org
8. "Detailed Guide: Multiple Myeloma". *American Cancer Society.* February 2008. http://www.cancer.org
9. "Detailed Guide: Non-Hodgkin's Lymphoma". *American Cancer Society.* February 2008. http://www.cancer.org

10. "Detailed Guide: Pancreatic Cancer". *American Cancer Society.* May 2008. http://www.cancer.org

11. "Detailed Guide: Prostate Cancer". *American Cancer Society.* May 2008. http://www.cancer.org

12. "Detailed Guide: Skin Cancer". *American Cancer Society.* May 2008. http://www.cancer.org

13. "Erbitux (cetuximab)". *ImClone Systems, Inc., Bristol-Myers Squibb Co., and Merck KGaA.* February 2008. http://www.Erbitux.com

14. "Herceptin (trastuzumab)". *Genentech, Inc.* February 2008. http://www.Herceptin.com

15. "Mylotarg (gemtuzumab ozogamicin for injection)". *Wyeth.* February 2008. http://www.wyeth.com/content/ShowLabeling.asp?id=119

16. "Oncology Tools: Approved Oncology Drugs". *Food and Drug Administration/Center for Drug Evaluation and Research.* January 2008. http://www.fda.gov/cder/cancer/approved.htm

17. "Radiation Therapy Principles". *American Cancer Society.* May 2008. http://www.cancer.org

18. "Rituxan (rituximab): Targeted B-cell therapy". *Genentec, Inc. and Biogen IDEC, Inc.* February 2008. http://www.rituxan.com

19. "Vectibix (panitumumab)". *Amgen, Inc.* February 2008. http://www.Vectibix.com

20. "Zevalin (ibritumomab tiuxetan)". *Cell Therapeutics, Inc.* February 2008. http://www.Zevalin.com

21. Ali, S., J. Kaur, and K.D. Patel. 2000. Intercellular cell adhesion molecule-1, vascular cell adhesion molecule-1, and regulated on activation normal T cell expressed and secreted are expressed by human breast carcinoma cells and support eosinophil adhesion and activation. *Am J Pathol* 157:313-321.

22. Alinari, L., R. Lapalombella, L. Andritsos, R.A. Baiocchi, T.S. Lin, and J.C. Byrd. 2007. Alemtuzumab (Campath-1H) in the treatment of chronic lymphocytic leukemia. *Oncogene* 26:3644-3653.

23. Altomonte, M., E. Fonsatti, E. Lamaj, I. Cattarossi, A. Cattelan, and M. Maio. 1999. Differential levels of soluble intercellular adhesion molecule-1 (sICAM-1) in early breast cancer and benign breast lesions. *Breast Cancer Res Treat* 58:19-23.

24. Anastassiou, G., H. Schilling, A. Stang, S. Djakovic, A. Heiligenhaus, and N. Bornfeld. 2000. Expression of the cell adhesion molecules ICAM-1, VCAM-1 and NCAM in uveal melanoma: a clinicopathological study. *Oncology* 58:83-88.

25. Aoudjit, F., E.F. Potworowski, T.A. Springer, and Y. St-Pierre. 1998. Protection from lymphoma cell metastasis in ICAM-1 mutant mice: a posthoming event. *J Immunol* 161:2333-2338.

26. Avery, R.B., M.P. Mehta, R.M. Auchter, and D.M. Albert. 2005. Melanoma: Intraocular melanoma. In *Cancer: Principles and Practice of Oncology*. V.T. DeVita, S. Hellman, and S.A. Rosenberg, eds. Lippincott Williams and Wilkins: Philadelphia. 1809-1825.

27. Axelrod, R., D.E. Axelrod, and K.J. Pienta. 2006. Evolution of cooperation among tumor cells. *Proc Natl Acad Sci U S A* 103:13474-13479.

28. Baker, C.H., J. Banzon, J.M. Bollinger, J. Stubbe, V. Samano, M.J. Robins, B. Lippert, E. Jarvi, and R. Resvick. 1991. 2'-Deoxy-2'-methylenecytidine and 2'-deoxy-2',2'-difluorocytidine 5'-diphosphates: potent mechanism-based inhibitors of ribonucleotide reductase. *J Med Chem* 34:1879-1884.

29. Balch, C.M., M.B. Atkins, and A.J. Sober. 2005. Melanoma: Cutaneous melanoma. In *Cancer: Principles and Practice of Oncology*. V.T. DeVita, S. Hellman, and S.A. Rosenberg, eds. Lippincott Williams and Wilkins: Philadelphia. 1754-1809.

30. Bancroft, G.J., and J.P. Kelly. 1994. Macrophage activation and innate resistance to infection in SCID mice. *Immunobiology* 191:424-431.

31. Banks, R.E., A.J. Gearing, I.K. Hemingway, D.R. Norfolk, T.J. Perren, and P.J. Selby. 1993. Circulating intercellular adhesion molecule-1 (ICAM-1), E-selectin and vascular cell adhesion molecule-1 (VCAM-1) in human malignancies. *Br J Cancer* 68:122-124.

32. Bendjelloul, F., P. Maly, V. Mandys, M. Jirkovska, L. Prokesova, L. Tuckova, and H. Tlaskalova-Hogenova. 2000. Intercellular adhesion molecule-1 (ICAM-1) deficiency protects mice against severe forms of experimentally induced colitis. *Clin Exp Immunol* 119:57-63.

33. Bene, L., A. Bodnar, S. Damjanovich, G. Vamosi, Z. Bacso, J. Aradi, A. Berta, and J. Damjanovich. 2004. Membrane topography of HLA I, HLA II, and ICAM-1 is affected by IFN-gamma in lipid rafts of uveal melanomas. *Biochem Biophys Res Commun* 322:678-683.

34. Blick, S.K., and L.J. Scott. 2007. Cetuximab: a review of its use in squamous cell carcinoma of the head and neck and metastatic colorectal cancer. *Drugs* 67:2585-2607.

35. Boyd, A.W., S.O. Wawryk, G.F. Burns, and J.V. Fecondo. 1988. Intercellular adhesion molecule 1 (ICAM-1) has a central role in cell-cell contact-mediated immune mechanisms. *Proc Natl Acad Sci U S A* 85:3095-3099.

36. Braakhuis, B.J., G.A. van Dongen, J.B. Vermorken, and G.B. Snow. 1991. Preclinical in vivo activity of 2',2'-difluorodeoxycytidine (Gemcitabine) against human head and neck cancer. *Cancer Res* 51:211-214.

37. Bronte, V., D.B. Chappell, E. Apolloni, A. Cabrelle, M. Wang, P. Hwu, and N.P. Restifo. 1999. Unopposed production of granulocyte-macrophage colony-stimulating factor by tumors inhibits CD8+ T cell responses by dysregulating antigen-presenting cell maturation. *J Immunol* 162:5728-5737.

38. Budinsky, A.C., T. Brodowicz, C. Wiltschke, K. Czerwenka, I. Michl, M. Krainer, and C.C. Zielinski. 1997. Decreased expression of ICAM-1 and its induction by tumor necrosis factor on breast-cancer cells in vitro. *Int J Cancer* 71:1086-1090.

39. Cailleau, R., R. Young, M. Olive, and W.J. Reeves, Jr. 1974. Breast tumor cell lines from pleural effusions. *J Natl Cancer Inst* 53:661-674.

40. Carlsson, B., O. Forsberg, M. Bengtsson, T.H. Totterman, and M. Essand. 2007. Characterization of human prostate and breast cancer cell lines for experimental T cell-based immunotherapy. *Prostate* 67:389-395.

41. Carteni, G., R. Fiorentino, L. Vecchione, B. Chiurazzi, and C. Battista. 2007. Panitumumab a novel drug in cancer treatment. *Ann Oncol* 18 Suppl 6:vi16-21.

42. Carter, P. 2001. Improving the efficacy of antibody-based cancer therapies. *Nat Rev Cancer* 1:118-129.

43. Cascone, T., C. Gridelli, and F. Ciardiello. 2007. Combined targeted therapies in non-small cell lung cancer: a winner strategy? *Curr Opin Oncol* 19:98-102.

44. Casero, R.A., Jr., S.B. Baylin, B.D. Nelkin, and G.D. Luk. 1986. Human lung tumor sensitivity to difluoromethylornithine as related to ornithine decarboxylase messenger RNA levels. *Biochem Biophys Res Commun* 134:572-579.

45. Casero, R.A., Jr., P. Celano, S.J. Ervin, C.W. Porter, R.J. Bergeron, and P.R. Libby. 1989. Differential induction of spermidine/spermine N1-acetyltransferase in human lung cancer cells by the bis(ethyl)polyamine analogues. *Cancer Res* 49:3829-3833.

46. Chabner, B.A., and T.G. Roberts, Jr. 2005. Timeline: Chemotherapy and the war on cancer. *Nat Rev Cancer* 5:65-72.

47. Chu, E., and V.T.D. Jr. 2005. Principles of medical oncology. In *Cancer: Principles and Practice of Oncology*, 7th ed. V.T. DeVita, S. Hellman, and S.A. Rosenberg, eds. Lippincott Williams and Wilkins: Philadelphia. 295-306.

48. Clinchy, B., A. Gazdar, R. Rabinovsky, E. Yefenof, B. Gordon, and E.S. Vitetta. 2000. The growth and metastasis of human, HER-2/neu-overexpressing tumor cell lines in male SCID mice. *Breast Cancer Res Treat* 61:217-228.

49. Clynes, R.A., T.L. Towers, L.G. Presta, and J.V. Ravetch. 2000. Inhibitory Fc receptors modulate in vivo cytoxicity against tumor targets. *Nat Med* 6:443-446.

50. Coiffier, B. 2007. Rituximab therapy in malignant lymphoma. *Oncogene* 26:3603-3613.

51. Coleman, E.J. 2005. Understanding the mechanism of action of UV3, an anti-CD54 monoclonal antibody, in the therapy of multiple myeloma. In *Graduate School of Biomedical Sciences*. University of Texas Southwestern Medical Center, Dallas.

52. Coleman, E.J., K.J. Brooks, J.E. Smallshaw, and E.S. Vitetta. 2006. The Fc portion of UV3, an anti-CD54 monoclonal antibody, is critical for its antitumor activity in SCID mice with human multiple myeloma or lymphoma cell lines. *J Immunother (1997)* 29:489-498.

53. Connell, P.P., M.K. Martel, and S. Hellman. 2005. Princeples of radiation oncology. In *Cancer: Principles and Practice of Oncology*, 7th ed. V.T. DeVita, S. Hellman, and S.A. Rosenberg, eds. Lippincott Williams and Wilkins: Philadelphia. 267-293.

54. Copur, M.S., M.G. Rose, and E. Chu. 2005. Pharmacology of cancer chemotherapy: Miscellaneous chemotherapeutic agents. In *Cancer: Principles and Practice of Oncology*, 7th ed. V.T. DeVita, S. Hellman, and S.A. Rosenberg, eds. Lippincott Weilliams and Wilkins: Philadelphia. 416-422.

55. Crino, L., and F. Cappuzzo. 2002. Present and future treatment of advanced non-small cell lung cancer. *Semin Oncol* 29:9-16.

56. Csanaky, G., E. Matutes, J.A. Vass, R. Morilla, and D. Catovsky. 1997. Adhesion receptors on peripheral blood leukemic B cells. A comparative study on B cell chronic lymphocytic leukemia and related lymphoma/leukemias. *Leukemia* 11:408-415.

57. Cunningham, D., Y. Humblet, S. Siena, D. Khayat, H. Bleiberg, A. Santoro, D. Bets, M. Mueser, A. Harstrick, C. Verslype, I. Chau, and E. Van Cutsem. 2004. Cetuximab monotherapy and cetuximab plus irinotecan in irinotecan-refractory metastatic colorectal cancer. *N Engl J Med* 351:337-345.

58. Damato, B. 2004. Developments in the management of uveal melanoma. *Clin Experiment Ophthalmol* 32:639-647.

59. Dass, C.R., T.M. Tran, and P.F. Choong. 2007. Angiogenesis inhibitors and the need for anti-angiogenic therapeutics. *J Dent Res* 86:927-936.

60. Dearden, C. 2006. The role of alemtuzumab in the management of T-cell malignancies. *Semin Oncol* 33:S44-52.

61. DeNardo, G.L., E. Tobin, K. Chan, B.M. Bradt, and S.J. DeNardo. 2005. Direct antilymphoma effects on human lymphoma cells of monotherapy and combination therapy with CD20 and HLA-DR antibodies and 90Y-labeled HLA-DR antibodies. *Clin Cancer Res* 11:7075s-7079s.

62. Dorshkind, K., S.B. Pollack, M.J. Bosma, and R.A. Phillips. 1985. Natural killer (NK) cells are present in mice with severe combined immunodeficiency (scid). *J Immunol* 134:3798-3801.

63. Drudge-Coates, L. 2005. Prostate cancer and the principles of hormone therapy. *Br J Nurs* 14:368-375.

64. El Karak, F., and A. Flechon. 2007. Gemcitabine in bladder cancer. *Expert Opin Pharmacother* 8:3251-3256.

65. Elsner, J., M. Sach, H.P. Knopf, J. Norgauer, A. Kapp, P. Schollmeyer, and G.J. Dobos. 1995. Synthesis and surface expression of ICAM-1 in polymorphonuclear neutrophilic leukocytes in normal subjects and during inflammatory disease. *Immunobiology* 193:456-464.

66. Emmanouilides, C. 2007. Radioimmunotherapy for non-hodgkin lymphoma : historical perspective and current status. *J Clin Exp Hematop* 47:43-60.

67. Esteva, F.J., V. Valero, D. Booser, L.T. Guerra, J.L. Murray, L. Pusztai, M. Cristofanilli, B. Arun, B. Esmaeli, H.A. Fritsche, N. Sneige, T.L. Smith, and G.N. Hortobagyi. 2002. Phase II study of weekly docetaxel and trastuzumab for patients with HER-2-overexpressing metastatic breast cancer. *J Clin Oncol* 20:1800-1808.

68. Fanale, M.A., and A. Younes. 2007. Monoclonal antibodies in the treatment of non-Hodgkin's lymphoma. *Drugs* 67:333-350.

69. Farah, R.A., B. Clinchy, L. Herrera, and E.S. Vitetta. 1998. The development of monoclonal antibodies for the therapy of cancer. *Crit Rev Eukaryot Gene Expr* 8:321-356.

70. Folkman, J. 2002. Role of angiogenesis in tumor growth and metastasis. *Semin Oncol* 29:15-18.

71. Funakoshi, S., D.L. Longo, and W.J. Murphy. 1996. Differential in vitro and in vivo antitumor effects mediated by anti-CD40 and anti-CD20 monoclonal antibodies against human B-cell lymphomas. *J Immunother Emphasis Tumor Immunol* 19:93-101.

72. Galizia, G., E. Lieto, F. De Vita, M. Orditura, P. Castellano, T. Troiani, V. Imperatore, and F. Ciardiello. 2007. Cetuximab, a chimeric human mouse anti-epidermal growth factor receptor monoclonal antibody, in the treatment of human colorectal cancer. *Oncogene* 26:3654-3660.

73. Gandhi, V., J. Legha, F. Chen, L.W. Hertel, and W. Plunkett. 1996. Excision of 2',2'-difluorodeoxycytidine (gemcitabine) monophosphate residues from DNA. *Cancer Res* 56:4453-4459.

74. Gerbitz, A., P. Ewing, K. Olkiewicz, N.E. Willmarth, D. Williams, G. Hildebrandt, A. Wilke, C. Liu, G. Eissner, R. Andreesen, E. Holler, R. Guo, P.A. Ward, and K.R. Cooke. 2005. A role for CD54 (intercellular adhesion molecule-1) in leukocyte recruitment to the lung during the development of experimental idiopathic pneumonia syndrome. *Transplantation* 79:536-542.

75. Ghetie, M.A., H. Bright, and E.S. Vitetta. 2001. Homodimers but not monomers of Rituxan (chimeric anti-CD20) induce apoptosis in human B-lymphoma cells and synergize with a chemotherapeutic agent and an immunotoxin. *Blood* 97:1392-1398.

76. Ghetie, M.A., L.J. Picker, J.A. Richardson, K. Tucker, J.W. Uhr, and E.S. Vitetta. 1994. Anti-CD19 inhibits the growth of human B-cell tumor lines in vitro and of Daudi cells in SCID mice by inducing cell cycle arrest. *Blood* 83:1329-1336.

77. Ghetie, M.A., E.M. Podar, B.E. Gordon, P. Pantazis, J.W. Uhr, and E.S. Vitetta. 1996. Combination immunotoxin treatment and chemotherapy in SCID mice with advanced, disseminated Daudi lymphoma. *Int J Cancer* 68:93-96.

78. Ghetie, M.A., K. Tucker, J. Richardson, J.W. Uhr, and E.S. Vitetta. 1992. The antitumor activity of an anti-CD22 immunotoxin in SCID mice with disseminated Daudi lymphoma is enhanced by either an anti-CD19 antibody or an anti-CD19 immunotoxin. *Blood* 80:2315-2320.

79. Giralt, S. 2006. The role of alemtuzumab in nonmyeloablative hematopoietic transplantation. *Semin Oncol* 33:S36-43.

80. Gligorov, J., D. Azria, M. Namer, D. Khayat, and J.P. Spano. 2007. Novel therapeutic strategies combining antihormonal and biological targeted therapies in breast cancer: focus on clinical trials and perspectives. *Crit Rev Oncol Hematol* 64:115-128.

81. Green, M.R. 1996. Gemcitabine safety overview. *Semin Oncol* 23:32-35.

82. Gridelli, C., P. Maione, A. Rossi, and F. De Marinis. 2007. The role of bevacizumab in the treatment of non-small cell lung cancer: current indications and future developments. *Oncologist* 12:1183-1193.

83. Hadaschik, B.A., and M.E. Gleave. 2007. Therapeutic options for hormone-refractory prostate cancer in 2007. *Urol Oncol* 25:413-419.

84. Hadaschik, B.A., R.D. Sowery, and M.E. Gleave. 2007. Novel targets and approaches in advanced prostate cancer. *Curr Opin Urol* 17:182-187.

85. Heicappell, R., J. Podlinski, H. Buszello, and R. Ackermann. 1994. Cell surface expression and serum levels of intercellular adhesion molecule-1 in renal cell carcinoma. *Urol Res* 22:9-15.

86. Heinemann, V., Y.Z. Xu, S. Chubb, A. Sen, L.W. Hertel, G.B. Grindey, and W. Plunkett. 1990. Inhibition of ribonucleotide reduction in CCRF-CEM cells by 2',2'-difluorodeoxycytidine. *Mol Pharmacol* 38:567-572.

87. Hertel, L.W., G.B. Boder, J.S. Kroin, S.M. Rinzel, G.A. Poore, G.C. Todd, and G.B. Grindey. 1990. Evaluation of the antitumor activity of gemcitabine (2',2'-difluoro-2'-deoxycytidine). *Cancer Res* 50:4417-4422.

88. Hertel, L.W., J.S. Kroin, J.W. Misner, and J.M. Tustin. 1988. Synthesis of 2-Deoxy-2',2'-difluoro-D-ribose and 2-Deoxy-2',2'-difluoro-D-ribofuranosyl Nucleosides. *Journal of Organic Cehmistry* 53:2406-2409.

89. Holland, J., and T. Owens. 1997. Signaling through intercellular adhesion molecule 1 (ICAM-1) in a B cell lymphoma line. The activation of Lyn tyrosine kinase and the mitogen-activated protein kinase pathway. *J Biol Chem* 272:9108-9112.

90. Horoszewicz, J.S., S.S. Leong, E. Kawinski, J.P. Karr, H. Rosenthal, T.M. Chu, E.A. Mirand, and G.P. Murphy. 1983. LNCaP model of human prostatic carcinoma. *Cancer Res* 43:1809-1818.

91. Horst, E., T. Radaszkiewicz, A. Hooftman-den Otter, R. Pieters, J.J. van Dongen, C.J. Meijer, and S.T. Pals. 1991. Expression of the leucocyte integrin LFA-1 (CD11a/CD18) and its ligand ICAM-1 (CD54) in lymphoid malignancies is related to lineage derivation and stage of differentiation but not to tumor grade. *Leukemia* 5:848-853.

92. Huang, P., S. Chubb, L.W. Hertel, G.B. Grindey, and W. Plunkett. 1991. Action of 2',2'-difluorodeoxycytidine on DNA synthesis. *Cancer Res* 51:6110-6117.

93. Huang, X.Q., M.S. Mitchell, P.E. Liggett, A.L. Murphree, and J. Kan-Mitchell. 1994. Non-fastidious, melanoma-specific CD8+ cytotoxic T lymphocytes from choroidal melanoma patients. *Cancer Immunol Immunother* 38:399-405.

94. Huang, Y.W., F.J. Burrows, and E.S. Vitetta. 1993. Cytotoxicity of a novel anti-ICAM-1 immunotoxin on human myeloma cell lines. *Hybridoma* 12:661-675.

95. Huang, Y.W., J.A. Richardson, A.W. Tong, B.Q. Zhang, M.J. Stone, and E.S. Vitetta. 1993. Disseminated growth of a human multiple myeloma cell line in mice with severe combined immunodeficiency disease. *Cancer Res* 53:1392-1396.

96. Huang, Y.W., J.A. Richardson, and E.S. Vitetta. 1995. Anti-CD54 (ICAM-1) has antitumor activity in SCID mice with human myeloma cells. *Cancer Res* 55:610-616.

97. Hurwitz, H. 2004. Integrating the anti-VEGF-A humanized monoclonal antibody bevacizumab with chemotherapy in advanced colorectal cancer. *Clin Colorectal Cancer* 4 Suppl 2:S62-68.

98. Hurwitz, H., L. Fehrenbacher, W. Novotny, T. Cartwright, J. Hainsworth, W. Heim, J. Berlin, A. Baron, S. Griffing, E. Holmgren, N. Ferrara, G. Fyfe, B. Rogers, R. Ross, and F. Kabbinavar. 2004. Bevacizumab plus irinotecan, fluorouracil, and leucovorin for metastatic colorectal cancer. *N Engl J Med* 350:2335-2342.

99. Imai, K., and A. Takaoka. 2006. Comparing antibody and small-molecule therapies for cancer. *Nat Rev Cancer* 6:714-727.

100. Jain, R.K. 2001. Normalizing tumor vasculature with anti-angiogenic therapy: a new paradigm for combination therapy. *Nat Med* 7:987-989.

101. Jemal, A., R. Siegel, E. Ward, T. Murray, J. Xu, and M.J. Thun. 2007. Cancer statistics, 2007. *CA Cancer J Clin* 57:43-66.

102. Johnson, J.P., B.G. Stade, B. Holzmann, W. Schwable, and G. Riethmuller. 1989. De novo expression of intercellular-adhesion molecule 1 in melanoma correlates with increased risk of metastasis. *Proc Natl Acad Sci U S A* 86:641-644.

103. Kaighn, M.E., K.S. Narayan, Y. Ohnuki, J.F. Lechner, and L.W. Jones. 1979. Establishment and characterization of a human prostatic carcinoma cell line (PC-3). *Invest Urol* 17:16-23.

104. Kalofonos, H.P., and P.D. Grivas. 2006. Monoclonal antibodies in the management of solid tumors. *Curr Top Med Chem* 6:1687-1705.

105. Kanzawa, F., and N. Saijo. 1997. In vitro interaction between gemcitabine and other anticancer drugs using a novel three-dimensional model. *Semin Oncol* 24:S7-8-S7-16.

106. Kavanaugh, A.F., L.S. Davis, R.I. Jain, L.A. Nichols, S.H. Norris, and P.E. Lipsky. 1996. A phase I/II open label study of the safety and efficacy of an anti-ICAM-1 (intercellular adhesion molecule-1; CD54) monoclonal antibody in early rheumatoid arthritis. *J Rheumatol* 23:1338-1344.

107. Kavanaugh, A.F., L.S. Davis, L.A. Nichols, S.H. Norris, R. Rothlein, L.A. Scharschmidt, and P.E. Lipsky. 1994. Treatment of refractory rheumatoid arthritis with a monoclonal antibody to intercellular adhesion molecule 1. *Arthritis Rheum* 37:992-999.

108. Kavanaugh, A.F., H. Schulze-Koops, L.S. Davis, and P.E. Lipsky. 1997. Repeat treatment of rheumatoid arthritis patients with a murine anti-intercellular adhesion molecule 1 monoclonal antibody. *Arthritis Rheum* 40:849-853.

109. Kennedy, B., A. Rawstron, C. Carter, M. Ryan, K. Speed, G. Lucas, and P. Hillmen. 2002. Campath-1H and fludarabine in combination are highly active in refractory chronic lymphocytic leukemia. *Blood* 99:2245-2247.

110. Khosravi Shahi, P., and I. Fernandez Pineda. 2008. Tumoral angiogenesis: review of the literature. *Cancer Invest* 26:104-108.

111. Kim, Y.S., G.B. Park, H.K. Song, I. Hur, H.K. Lee, J.S. Kang, E. Hahm, W.J. Lee, and D.Y. Hur. 2007. Cross-linking of CD54 on Burkitt lymphoma cell line Raji and Ramos induces FasL expression by reactive oxygen species and apoptosis of adjacent cells in Fas/FasL interaction. *J Immunother (1997)* 30:727-739.

112. Klein, E., G. Klein, J.S. Nadkarni, J.J. Nadkarni, H. Wigzell, and P. Clifford. 1968. Surface IgM-kappa specificity on a Burkitt lymphoma cell in vivo and in derived culture lines. *Cancer Res* 28:1300-1310.

113. Kohler, G., and C. Milstein. 1975. Continuous cultures of fused cells secreting antibody of predefined specificity. *Nature* 256:495-497.

114. Kostler, W.J., S. Tomek, T. Brodowicz, A.C. Budinsky, M. Flamm, M. Hejna, M. Krainer, C. Wiltschke, and C.C. Zielinski. 2001. Soluble ICAM-1 in breast cancer: clinical significance and biological implications. *Cancer Immunol Immunother* 50:483-490.

115. Koyama, S., T. Ebihara, and K. Fukao. 1992. Expression of intercellular adhesion molecule 1 (ICAM-1) during the development of invasion and/or metastasis of gastric carcinoma. *J Cancer Res Clin Oncol* 118:609-614.

116. Labourey, J.L., D. Cupissol, G. Calais, J.M. Tourani, F. Kohser, C. Borel, J.C. Eymard, N. Germann, and N. Tubiana-Mathieu. 2007. Docetaxel plus gemcitabine in recurrent and/or metastatic squamous cell carcinoma of the head and neck: a phase II multicenter study. *Am J Clin Oncol* 30:278-282.

117. Laheru, D., and E.M. Jaffee. 2005. Immunotherapy for pancreatic cancer - science driving clinical progress. *Nat Rev Cancer* 5:459-467.

118. Lalancette, M., F. Aoudjit, E.F. Potworowski, and Y. St-Pierre. 2000. Resistance of ICAM-1-deficient mice to metastasis overcome by increased aggressiveness of lymphoma cells. *Blood* 95:314-319.

119. Lasfargues, E.Y., W.G. Coutinho, and E.S. Redfield. 1978. Isolation of two human tumor epithelial cell lines from solid breast carcinomas. *J Natl Cancer Inst* 61:967-978.

120. Lawrence, T.S., A. Eisbruch, and D.S. Shewach. 1997. Gemcitabine-mediated radiosensitization. *Semin Oncol* 24:S7-24-S27-28.

121. Lei, K.I., and P.J. Johnson. 2000. The prognostic significance of serum levels of soluble intercellular adhesion molecules-1 in patients with primary extranodal non-Hodgkin lymphomas. *Cancer* 89:1387-1395.

122. Leonard, J.P., and D.M. Goldenberg. 2007. Preclinical and clinical evaluation of epratuzumab (anti-CD22 IgG) in B-cell malignancies. *Oncogene* 26:3704-3713.

123. Li, X.M., K. Tanaka, J. Sun, E. Filipski, L. Kayitalire, C. Focan, and F. Levi. 2005. Preclinical relevance of dosing time for the therapeutic index of gemcitabine-cisplatin. *Br J Cancer* 92:1684-1689.

124. Lieber, M., J. Mazzetta, W. Nelson-Rees, M. Kaplan, and G. Todaro. 1975. Establishment of a continuous tumor-cell line (panc-1) from a human carcinoma of the exocrine pancreas. *Int J Cancer* 15:741-747.

125. Lin, Y.C., C.T. Shun, M.S. Wu, and C.C. Chen. 2006. A novel anticancer effect of thalidomide: inhibition of intercellular adhesion molecule-1-mediated cell invasion and metastasis through suppression of nuclear factor-kappaB. *Clin Cancer Res* 12:7165-7173.

126. Liu, X.Y., L.M. Pop, D.C. Roopenian, V. Ghetie, E.S. Vitetta, and J.E. Smallshaw. 2006. Generation and characterization of a novel tetravalent anti-CD22 antibody with improved antitumor activity and pharmacokinetics. *Int Immunopharmacol* 6:791-799.

127. Long, J.M. 2007. Treatment approaches and nursing applications for non-Hodgkin lymphoma. *Clin J Oncol Nurs* 11:13-21.

128. Lynch, D.F., Jr., W. Hassen, M.A. Clements, P.F. Schellhammer, and G.L. Wright, Jr. 1997. Serum levels of endothelial and neural cell adhesion molecules in prostate cancer. *Prostate* 32:214-220.

129. Lynch, T.J., P.D. Bonomi, C. Butts, A.M. Davies, J. Engelman, R. Govindan, R.S. Herbst, J.V. Heymach, B.E. Johnson, R.G. Martins, R. Perez-Soler, G.J. Riely, A.B. Sandler, L.V. Sequist, M.A. Socinski, K.K. Wong, and C.S. Hart. 2007. Novel agents in the treatment of lung cancer: Fourth Cambridge Conference. *Clin Cancer Res* 13:s4583-4588.

130. Maio, M., A. Pinto, A. Carbone, V. Zagonel, A. Gloghini, G. Marotta, D. Cirillo, A. Colombatti, F. Ferrara, L. Del Vecchio, and et al. 1990. Differential expression of CD54/intercellular adhesion molecule-1 in myeloid leukemias and in lymphoproliferative disorders. *Blood* 76:783-790.

131. Marty, M., F. Cognetti, D. Maraninchi, R. Snyder, L. Mauriac, M. Tubiana-Hulin, S. Chan, D. Grimes, A. Anton, A. Lluch, J. Kennedy, K. O'Byrne, P. Conte, M. Green, C. Ward, K. Mayne, and J.M. Extra. 2005. Randomized phase II trial of the efficacy and safety of trastuzumab combined with docetaxel in patients with human epidermal growth factor receptor 2-positive metastatic breast cancer administered as first-line treatment: the M77001 study group. *J Clin Oncol* 23:4265-4274.

132. Melero, I., S. Hervas-Stubbs, M. Glennie, D.M. Pardoll, and L. Chen. 2007. Immunostimulatory monoclonal antibodies for cancer therapy. *Nat Rev Cancer* 7:95-106.

133. Melis, M., M. Spatafora, A. Melodia, E. Pace, M. Gjomarkaj, A.M. Merendino, and G. Bonsignore. 1996. ICAM-1 expression by lung cancer cell lines: effects of upregulation by cytokines on the interaction with LAK cells. *Eur Respir J* 9:1831-1838.

134. Meng, R., J.E. Smallshaw, L.M. Pop, M. Yen, X. Liu, L. Le, M.A. Ghetie, E.S. Vitetta, and V. Ghetie. 2004. The evaluation of recombinant, chimeric, tetravalent antihuman CD22 antibodies. *Clin Cancer Res* 10:1274-1281.

135. Mertens, W.C., E.A. Eisenhauer, M. Moore, P. Venner, D. Stewart, A. Muldal, and D. Wong. 1993. Gemcitabine in advanced renal cell carcinoma. A phase II study of the National Cancer Institute of Canada Clinical Trials Group. *Ann Oncol* 4:331-332.

136. Miklossy, J., D.D. Doudet, C. Schwab, S. Yu, E.G. McGeer, and P.L. McGeer. 2006. Role of ICAM-1 in persisting inflammation in Parkinson disease and MPTP monkeys. *Exp Neurol* 197:275-283.

137. Mimeault, M., R. Hauke, P.P. Mehta, and S.K. Batra. 2007. Recent advances in cancer stem/progenitor cell research: therapeutic implications for overcoming resistance to the most aggressive cancers. *J Cell Mol Med* 11:981-1011.

138. Minchinton, A.I., and I.F. Tannock. 2006. Drug penetration in solid tumours. *Nat Rev Cancer* 6:583-592.

139. Mohit, B., and K. Fan. 1971. Hybrid cell line from a cloned immunoglobulin-producing mouse myeloma and a nonproducing mouse lymphoma. *Science* 171:75-77.

140. Morris, M.J., and H.I. Scher. 2000. Novel strategies and therapeutics for the treatment of prostate carcinoma. *Cancer* 89:1329-1348.

141. Moulder, S., and G.N. Hortobagyi. 2008. Advances in the treatment of breast cancer. *Clin Pharmacol Ther* 83:26-36.

142. Nahta, R., and F.J. Esteva. 2007. Trastuzumab: triumphs and tribulations. *Oncogene* 26:3637-3643.

143. Ng, S.S., G.R. MacPherson, M. Gutschow, K. Eger, and W.D. Figg. 2004. Antitumor effects of thalidomide analogs in human prostate cancer xenografts implanted in immunodeficient mice. *Clin Cancer Res* 10:4192-4197.

144. Nilsson, K., B.C. Giovanella, J.S. Stehlin, and G. Klein. 1977. Tumorigenicity of human hematopoietic cell lines in athymic nude mice. *Int J Cancer* 19:337-344.

145. Nimmerjahn, F., and J.V. Ravetch. 2005. Divergent immunoglobulin g subclass activity through selective Fc receptor binding. *Science* 310:1510-1512.

146. O'Connor, R., M. Clynes, P. Dowling, N. O'Donovan, and L. O'Driscoll. 2007. Drug resistance in cancer - searching for mechanisms, markers and therapeutic agents. *Expert Opin Drug Metab Toxicol* 3:805-817.

147. Ogawa, Y., K. Hirakawa, B. Nakata, T. Fujihara, T. Sawada, Y. Kato, K. Yoshikawa, and M. Sowa. 1998. Expression of intercellular adhesion molecule-1 in invasive breast cancer reflects low growth potential, negative lymph node involvement, and good prognosis. *Clin Cancer Res* 4:31-36.

148. Oie, H.K., E.K. Russell, D.N. Carney, and A.F. Gazdar. 1996. Cell culture methods for the establishment of the NCI series of lung cancer cell lines. *J Cell Biochem Suppl* 24:24-31.

149. Pan, C.X., W. Zhu, and L. Cheng. 2006. Implications of cancer stem cells in the treatment of cancer. *Future Oncol* 2:723-731.

150. Panikkar, R.P., I. Astsaturov, and C.J. Langer. 2008. The emerging role of cetuximab in head and neck cancer: a 2007 perspective. *Cancer Invest* 26:96-103.

151. Parham, P. 1983. On the fragmentation of monoclonal IgG1, IgG2a, and IgG2b from BALB/c mice. *J Immunol* 131:2895-2902.

152. Parmiani, G., C. Castelli, M. Santinami, and L. Rivoltini. 2007. Melanoma immunology: past, present and future. *Curr Opin Oncol* 19:121-127.

153. Passlick, B., J.R. Izbicki, S. Simmel, B. Kubuschok, O. Karg, M. Habekost, O. Thetter, L. Schweiberer, and K. Pantel. 1994. Expression of major histocompatibility class I and class II antigens and intercellular adhesion molecule-1 on operable non-small cell lung carcinomas: frequency and prognostic significance. *Eur J Cancer* 30A:376-381.

154. Phelps, R.M., B.E. Johnson, D.C. Ihde, A.F. Gazdar, D.P. Carbone, P.R. McClintock, R.I. Linnoila, M.J. Matthews, P.A. Bunn, Jr., D. Carney, J.D. Minna, and J.L. Mulshine. 1996. NCI-Navy Medical Oncology Branch cell line data base. *J Cell Biochem Suppl* 24:32-91.

155. Ramanathan, R.K., and C.P. Belani. 1997. Chemotherapy for advanced non-small cell lung cancer: past, present, and future. *Semin Oncol* 24:440-454.

156. Ravandi, F., and S. O'Brien. 2006. Alemtuzumab in CLL and other lymphoid neoplasms. *Cancer Invest* 24:718-725.

157. Repp, A.C., E.S. Mayhew, S. Apte, and J.Y. Niederkorn. 2000. Human uveal melanoma cells produce macrophage migration-inhibitory factor to prevent lysis by NK cells. *J Immunol* 165:710-715.

158. Ringel, J., R. Jesnowski, C. Schmidt, H.J. Kohler, J. Rychly, S.K. Batra, and M. Lohr. 2001. CD44 in normal human pancreas and pancreatic carcinoma cell lines. *Teratog Carcinog Mutagen* 21:97-106.

159. Risher, R.I., P.M. Mauch, N.L. Harris, and J.W. Friedberg. 2005. Lymphomas: Non-hodgkin's lymphomas. In *Cancer: Principles and Practice of Oncology*. V.T. DeVita, S. Hellman, and S.A. Rosenberg, eds. Lippincott Williams and Wilkins: Philadelphia. 1957-1997.

160. Robertson, S.M., J.R. Kettman, J.N. Miller, and M.V. Norgard. 1982. Murine monoclonal antibodies specific for virulent Treponema pallidum (Nichols). *Infect Immun* 36:1076-1085.

161. Roebuck, K.A., and A. Finnegan. 1999. Regulation of intercellular adhesion molecule-1 (CD54) gene expression. *J Leukoc Biol* 66:876-888.

162. Rogers, B.B. 2006. Overview of non-Hodgkin's lymphoma. *Semin Oncol Nurs* 22:67-72.

163. Rokhlin, O.W., and M.B. Cohen. 1995. Expression of cellular adhesion molecules on human prostate tumor cell lines. *Prostate* 26:205-212.

164. Rosenberg, S.A. 2005. Principles of surgical oncology: General issues. In *Cancer: Principles and Practice of Oncology*, 7th ed. V.T. DeVita, S. Hellman, and S.A. Rosenberg, eds. Lippincott Williams and Wilkins: Philadelphia. 243-252.

165. Rosette, C., R.B. Roth, P. Oeth, A. Braun, S. Kammerer, J. Ekblom, and M.F. Denissenko. 2005. Role of ICAM1 in invasion of human breast cancer cells. *Carcinogenesis* 26:943-950.

166. Ross, J.S., D.P. Schenkein, R. Pietrusko, M. Rolfe, G.P. Linette, J. Stec, N.E. Stagliano, G.S. Ginsburg, W.F. Symmans, L. Pusztai, and G.N. Hortobagyi. 2004. Targeted therapies for cancer 2004. *Am J Clin Pathol* 122:598-609.

167. Rothlein, R., M.L. Dustin, S.D. Marlin, and T.A. Springer. 1986. A human intercellular adhesion molecule (ICAM-1) distinct from LFA-1. *J Immunol* 137:1270-1274.

168. Salomon, B., and J.A. Bluestone. 1998. LFA-1 interaction with ICAM-1 and ICAM-2 regulates Th2 cytokine production. *J Immunol* 161:5138-5142.

169. Sandler, A., R. Gray, M.C. Perry, J. Brahmer, J.H. Schiller, A. Dowlati, R. Lilenbaum, and D.H. Johnson. 2006. Paclitaxel-carboplatin alone or with bevacizumab for non-small-cell lung cancer. *N Engl J Med* 355:2542-2550.

170. Sandler, A., and R. Herbst. 2006. Combining targeted agents: blocking the epidermal growth factor and vascular endothelial growth factor pathways. *Clin Cancer Res* 12:4421s-4425s.

171. Schardt, C., J. Heymanns, M. Rotsch, and K. Havemann. 1993. Differential expression of the intercellular adhesion molecule-1 (ICAM-1) in lung cancer cell lines of various histological types. *Eur J Cancer* 29A:2250-2255.

172. Scher, H.I., S.A. Leibel, Z. Fuks, C. Cordon-Cardo, and P.T. Scardino. 2005. Cancers of the genitourinary system: Cancer of the prostate. In *Cancer: Principles and Practice of Oncology*. V.T. DeVita, S. Hellman, and S.A. Rosenberg, eds. Lippincott Williams and Wilkins: Philadelphia. 1192-1259.

173. Schmittel, A., M. Schmidt-Hieber, P. Martus, N.E. Bechrakis, R. Schuster, J.M. Siehl, M.H. Foerster, E. Thiel, and U. Keilholz. 2006. A randomized phase II trial of gemcitabine plus treosulfan versus treosulfan alone in patients with metastatic uveal melanoma. *Ann Oncol* 17:1826-1829.

174. Schmittel, A., R. Schuster, N.E. Bechrakis, J.M. Siehl, M.H. Foerster, E. Thiel, and U. Keilholz. 2005. A two-cohort phase II clinical trial of gemcitabine plus treosulfan in patients with metastatic uveal melanoma. *Melanoma Res* 15:447-451.

175. Schneider, U., H.U. Schwenk, and G. Bornkamm. 1977. Characterization of EBV-genome negative "null" and "T" cell lines derived from children with acute lymphoblastic leukemia and leukemic transformed non-Hodgkin lymphoma. *Int J Cancer* 19:621-626.

176. Schrump, D.S., N.K. Altorki, C.L. Henschke, D. Carter, A.T. Turrisi, and M.E. Gutierrez. 2005. Cancer of the lung: Non-small cell lung cancer. In *Cancer: Principles and Practice of Oncology*. V.T. DeVita, S. Hellman, and S.A. Rosenberg, eds. Lippincott Williams and Wilkins: Philadelphia. 753-810.

177. Schulz, T.F., W. Vogetseder, M. Mitterer, G. Bock, J.P. Johnson, and M.P. Dierich. 1988. Individual epitopes of an 85,000 MW membrane adherence molecule are variably expressed on cells of different lineage. *Immunology* 64:581-586.

178. Schwaeble, W., M. Kerlin, K.H. Meyer zum Buschenfelde, and W. Dippold. 1993. De novo expression of intercellular adhesion molecule 1 (ICAM-1, CD54) in pancreas cancer. *Int J Cancer* 53:328-333.

179. Seidman, A.D., M.N. Fornier, F.J. Esteva, L. Tan, S. Kaptain, A. Bach, K.S. Panageas, C. Arroyo, V. Valero, V. Currie, T. Gilewski, M. Theodoulou, M.E. Moynahan, M. Moasser, N. Sklarin, M. Dickler, G. D'Andrea, M. Cristofanilli, E. Rivera, G.N. Hortobagyi, L. Norton, and C.A. Hudis. 2001. Weekly trastuzumab and paclitaxel therapy for metastatic breast cancer with analysis of efficacy by HER2 immunophenotype and gene amplification. *J Clin Oncol* 19:2587-2595.

180. Shimoyama, S., F. Gansauge, S. Gansauge, M. Kaminishi, and H.G. Beger. 1999. Basal expression and cytokine induction of intercellular adhesion molecule-1 in human pancreatic cancer cell lines. *J Exp Clin Cancer Res* 18:107-110.

181. Shimoyama, S., F. Gansauge, S. Gansauge, U. Widmaier, T. Oohara, and H.G. Beger. 1997. Overexpression of intercellular adhesion molecule-1 (ICAM-1) in pancreatic adenocarcinoma in comparison with normal pancreas. *Pancreas* 14:181-186.

182. Shore, S., M.G. Raraty, P. Ghaneh, and J.P. Neoptolemos. 2003. Review article: chemotherapy for pancreatic cancer. *Aliment Pharmacol Ther* 18:1049-1069.

183. Singh, A.D., L. Bergman, and S. Seregard. 2005. Uveal melanoma: epidemiologic aspects. *Ophthalmol Clin North Am* 18:75-84, viii.

184. Singh, A.D., and E.C. Borden. 2005. Metastatic uveal melanoma. *Ophthalmol Clin North Am* 18:143-150, ix.

185. Siu, G., S.M. Hedrick, and A.A. Brian. 1989. Isolation of the murine intercellular adhesion molecule 1 (ICAM-1) gene. ICAM-1 enhances antigen-specific T cell activation. *J Immunol* 143:3813-3820.

186. Slamon, D.J., B. Leyland-Jones, S. Shak, H. Fuchs, V. Paton, A. Bajamonde, T. Fleming, W. Eiermann, J. Wolter, M. Pegram, J. Baselga, and L. Norton. 2001. Use of chemotherapy plus a monoclonal antibody against HER2 for metastatic breast cancer that overexpresses HER2. *N Engl J Med* 344:783-792.

187. Smallshaw, J.E., E. Coleman, C. Spiridon, and E.S. Vitetta. 2004. The generation and anti-myeloma activity of a chimeric anti-CD54 antibody, cUV3. *J Immunother (1997)* 27:419-424.

188. Soule, H.D., J. Vazguez, A. Long, S. Albert, and M. Brennan. 1973. A human cell line from a pleural effusion derived from a breast carcinoma. *J Natl Cancer Inst* 51:1409-1416.

189. Spiridon, C.I., S. Guinn, and E.S. Vitetta. 2004. A comparison of the in vitro and in vivo activities of IgG and F(ab')2 fragments of a mixture of three monoclonal anti-Her-2 antibodies. *Clin Cancer Res* 10:3542-3551.

190. Sprenger, A., C. Schardt, M. Rotsch, M. Zehrer, M. Wolf, K. Havemann, and J. Heymanns. 1997. Soluble intercellular adhesion molecule-1 in patients with lung cancer and benign lung diseases. *J Cancer Res Clin Oncol* 123:632-638.

191. Staal-van den Brekel, A.J., F.B. Thunnissen, W.A. Buurman, and E.F. Wouters. 1996. Expression of E-selectin, intercellular adhesion molecule (ICAM)-1 and vascular cell adhesion molecule (VCAM)-1 in non-small-cell lung carcinoma. *Virchows Arch* 428:21-27.

192. Staunton, D.E., M.L. Dustin, H.P. Erickson, and T.A. Springer. 1990. The arrangement of the immunoglobulin-like domains of ICAM-1 and the binding sites for LFA-1 and rhinovirus. *Cell* 61:243-254.

193. Staunton, D.E., S.D. Marlin, C. Stratowa, M.L. Dustin, and T.A. Springer. 1988. Primary structure of ICAM-1 demonstrates interaction between members of the immunoglobulin and integrin supergene families. *Cell* 52:925-933.

194. Stebbings, R., L. Findlay, C. Edwards, D. Eastwood, C. Bird, D. North, Y. Mistry, P. Dilger, E. Liefooghe, I. Cludts, B. Fox, G. Tarrant, J. Robinson, T. Meager, C. Dolman, S.J. Thorpe, A. Bristow, M. Wadhwa, R. Thorpe, and S. Poole. 2007. "Cytokine storm" in the phase I trial of monoclonal antibody TGN1412: better understanding the causes to improve preclinical testing of immunotherapeutics. *J Immunol* 179:3325-3331.

195. Steingass, S.K. 2006. Hematopoietic cell transplantation in non-Hodgkin's lymphoma. *Semin Oncol Nurs* 22:107-116.

196. Stinchcombe, T.E., and M.A. Socinski. 2007. Bevacizumab in the treatment of non-small-cell lung cancer. *Oncogene* 26:3691-3698.

197. Stone, K.R., D.D. Mickey, H. Wunderli, G.H. Mickey, and D.F. Paulson. 1978. Isolation of a human prostate carcinoma cell line (DU 145). *Int J Cancer* 21:274-281.

198. Strome, S.E., E.A. Sausville, and D. Mann. 2007. A mechanistic perspective of monoclonal antibodies in cancer therapy beyond target-related effects. *Oncologist* 12:1084-1095.

199. Szakacs, G., J.K. Paterson, J.A. Ludwig, C. Booth-Genthe, and M.M. Gottesman. 2006. Targeting multidrug resistance in cancer. *Nat Rev Drug Discov* 5:219-234.

200. Tacyildiz, N., G. Yavuz, S. Gozdasoglu, E. Unal, U. Ertem, F. Duru, A. Ikinciogullari, E. Babacan, A. Ensari, and A. Okcuoglu-Cavdar. 1999. Serum levels and differential expression of intercellular adhesion molecule-1 in childhood leukemia and malignant lymphoma: prognostic importance and relationship with survival. *Pediatr Hematol Oncol* 16:149-158.

201. Tan, M.H., N.J. Nowak, R. Loor, H. Ochi, A.A. Sandberg, C. Lopez, J.W. Pickren, R. Berjian, H.O. Douglass, Jr., and T.M. Chu. 1986. Characterization of a new primary human pancreatic tumor line. *Cancer Invest* 4:15-23.

202. Tanabe, K., S.C. Campbell, J.P. Alexander, F. Steinbach, M.G. Edinger, R.R. Tubbs, A.C. Novick, and E.A. Klein. 1997. Molecular regulation of intercellular adhesion molecule 1 (ICAM-1) expression in renal cell carcinoma. *Urol Res* 25:231-238.

203. Tawbi, H.A., and J.M. Kirkwood. 2007. Management of metastatic melanoma. *Semin Oncol* 34:532-545.

204. Terol, M.J., A. Lopez-Guillermo, F. Bosch, N. Villamor, M.C. Cid, C. Rozman, E. Campo, and E. Montserrat. 1998. Expression of the adhesion molecule ICAM-1 in non-Hodgkin's lymphoma: relationship with tumor dissemination and prognostic importance. *J Clin Oncol* 16:35-40.

205. van de Stolpe, A., and P.T. van der Saag. 1996. Intercellular adhesion molecule-1. *J Mol Med* 74:13-33.

206. Van Seventer, G.A., Y. Shimizu, K.J. Horgan, and S. Shaw. 1990. The LFA-1 ligand ICAM-1 provides an important costimulatory signal for T cell receptor-mediated activation of resting T cells. *J Immunol* 144:4579-4586.

207. Veronese, M.L., and P.J. O'Dwyer. 2004. Monoclonal antibodies in the treatment of colorectal cancer. *Eur J Cancer* 40:1292-1301.

208. Vitetta, E.S., and J.W. Uhr. 1994. Monoclonal antibodies as agonists: an expanded role for their use in cancer therapy. *Cancer Res* 54:5301-5309.

209. Waldmann, T.A. 2003. Immunotherapy: past, present and future. *Nat Med* 9:269-277.

210. Wang, J., and T.A. Springer. 1998. Structural specializations of immunoglobulin superfamily members for adhesion to integrins and viruses. *Immunol Rev* 163:197-215.

211. Wang, S., E.J. Coleman, L.M. Pop, K.J. Brooks, E.S. Vitetta, and J.Y. Niederkorn. 2006. Effect of an anti-CD54 (ICAM-1) monoclonal antibody (UV3) on the growth of human uveal melanoma cells transplanted heterotopically and orthotopically in SCID mice. *Int J Cancer* 118:932-941.

212. Witkowska, A.M., and M.H. Borawska. 2004. Soluble intercellular adhesion molecule-1 (sICAM-1): an overview. *Eur Cytokine Netw* 15:91-98.

213. Wolchok, J.D., and Y.M. Saenger. 2007. Current topics in melanoma. *Curr Opin Oncol* 19:116-120.

214. Wood, W.C., H.B. Muss, L.J. Solin, and O.I. Olopade. 2005. Cancer of the breast: Malignant tumors of the breast. In *Cancer: Principles and Practice of Oncology*. V.T. DeVita, S. Hellman, and S.A. Rosenberg, eds. Lippincott Williams and Wilkins: Philadelphia. 1415-1477.

215. Xydakis, E., E. Repassos, M. Poulou, M. Papadakou, C. Boukis, and G. Panagos. 2006. Second line chemotherapy with methotrexate and gemcitabine in patients with relapsing head and neck cancer. *J BUON* 11:419-424.

216. Yeo, C.J., T.P. Yeo, R.H. Hruban, S.E. Kern, C.A. Iacobuzio-Donohue, A. Maitra, M. Goggins, M.I. Canto, W. Messersmith, R.A. Abrams, D.A. Laheru, M. Hidalgo, and E.M. Jaffee. 2005. Cancers of the gastrointestinal tract: Cancer of the pancreas. In *Cancer: Principles and Practice of Oncology*. V.T. DeVita, S. Hellman, and S.A. Rosenberg, eds. Lippincott Williams and Wilkins: Philadelphia. 945-986.

217. Yu, D.M., N. Tokuda, S. Naito, M. Yoshikawa, K. Takahashi, J. Uozumi, and J. Kumazawa. 1998. Antiproliferative effect of calcitriol on human prostatic cancer cell lines: unrelated to the expression of major histocompatibility complex antigens or intercellular adhesion molecule-1 (ICAM-1). *Int J Urol* 5:595-600.

218. Zafir-Lavie, I., Y. Michaeli, and Y. Reiter. 2007. Novel antibodies as anticancer agents. *Oncogene* 26:3714-3733.

219. Ziras, N., A. Potamianou, I. Varthalitis, K. Syrigos, S. Tsousis, I. Boukovinas, E. Tselepatiotis, C. Christofillakis, and V. Georgoulias. 2006. Multicenter phase II study of gemcitabine and oxaliplatin (GEMOX) as second-line chemotherapy in colorectal cancer patients pretreated with 5-fluorouracil plus irinotecan. *Oncology* 70:106-114.